

University of Windsor

Scholarship at UWindor

Electronic Theses and Dissertations

Theses, Dissertations, and Major Papers

1-1-1967

Linear and nonlinear analyses of skewed plates.

Simon S. F. Ng
University of Windsor

Follow this and additional works at: <https://scholar.uwindsor.ca/etd>

Recommended Citation

Ng, Simon S. F., "Linear and nonlinear analyses of skewed plates." (1967). *Electronic Theses and Dissertations*. 6049.

<https://scholar.uwindsor.ca/etd/6049>

This online database contains the full-text of PhD dissertations and Masters' theses of University of Windsor students from 1954 forward. These documents are made available for personal study and research purposes only, in accordance with the Canadian Copyright Act and the Creative Commons license—CC BY-NC-ND (Attribution, Non-Commercial, No Derivative Works). Under this license, works must always be attributed to the copyright holder (original author), cannot be used for any commercial purposes, and may not be altered. Any other use would require the permission of the copyright holder. Students may inquire about withdrawing their dissertation and/or thesis from this database. For additional inquiries, please contact the repository administrator via email (scholarship@uwindsor.ca) or by telephone at 519-253-3000ext. 3208.

LINEAR AND NONLINEAR ANALYSES OF SKEWED PLATES

A THESIS

Submitted to the Faculty of Graduate Studies through the
Department of Civil Engineering in Partial Fulfillment
of the Requirements for the Degree of
Doctor of Philosophy at The
University of Windsor.

by

Simon S.F. NG

B.A.Sc., The University of British Columbia, 1962

M.A.Sc., The University of Windsor, 1964

Windsor, Ontario, Canada.
1967

UMI Number: DC52612

UMI[®]

UMI Microform DC52612
Copyright 2007 by ProQuest Information and Learning Company.
All rights reserved. This microform edition is protected against
unauthorized copying under Title 17, United States Code.

ProQuest Information and Learning Company
789 East Eisenhower Parkway
P.O. Box 1346
Ann Arbor, MI 48106-1346

APX 6339

APPROVED BY:

J. J. Kennedy

W. M. Vinnie

Cameron Mac Innis

A. B. Smith

169928

ABSTRACT

The perturbation method is used to analyze the problem of small and large deflections of clamped skewed plates under uniform pressure. The results are improved by successive approximations to the three displacement components in the middle plane of the plate. Numerical and graphical results are presented. Comparisons are made with existing results for skewed plates with small deflections as well as with results for rectangular plates with small and large deflection behaviour; good agreement is shown. The effects of skew and aspect ratio on plates with large deflections are investigated. It is shown that the centre deflection decreases with increase in skew and aspect ratio, and that the maximum resultant stress occurs along the longer edges of the plates and is displaced towards the obtuse corners.

Four aluminum skewed panels of different skew angles and aspect ratios were tested to verify the theoretical predictions. Experimental results for deflections as well as maximum edge and centre stresses are compared with those obtained analytically. Close agreement is found. It was also revealed from these experiments that, at large lateral loads producing plastic permanent deformations in the plate models, the obtuse corners are not only regions of stress concentration but also of instability, exhibited by sudden reversal of stresses.

ACKNOWLEDGMENTS

The writer wishes to express his gratitude to Dr. J.B. Kennedy for his guidance and suggestions in the preparation of this work and for his generous aid and constructive criticism throughout its development.

The writer is also indebted to Mr. William James and Mr. David Wongsing who have helped in the checking of the theoretical analysis. Thanks are also due to Mr. George Michalczuk who has helped generously in the setting up of the experiments.

The financial assistance given by the Defence Research Board is greatly appreciated.

TABLE OF CONTENTS	Page
ABSTRACT	iii
ACKNOWLEDGMENTS	iv
CHAPTER	
I INTRODUCTION	1
II REVIEW OF LITERATURE	7
III THEORETICAL ANALYSIS	
(a) Assumptions	10
(b) Formulation of the Governing Partial Differential Equations	11
(c) The Oblique Co-ordinate System	17
(d) Method of Solution	20
(e) Displacement and Stress Relationships	28
(f) Observation and Discussion of Theoretical Results	31
(g) Convergence of the Results	43
(h) Plastic Analysis	44
IV EXPERIMENTAL ANALYSIS	
(a) Materials and Apparatus	50
(b) Procedures and Results	54
(c) Comparison and Discussion of Experimental and Theoretical Results	61
V CONCLUSIONS	78
APPENDIX A Fortran Programmes for Theoretical Analysis...	80
Fortran Program for Experimental Analysis.....	116
APPENDIX B Experimental Data for Lateral Deflections.....	124
Experimental Data for unit strains for all gauges at different intensities of loadings	139
REFERENCES	160
NOMENCLATURE	163
VITA AUCTORIS	166

LIST OF TABLES

PAGE

Table 1.	Maximum 'Small' Deflection at Centre for Various Skew Angles and Ratio of Sides	32
Table 2.	Geometries of Test Plates	51
Table 3.	Location of Rosette Gauges in inches	51
Table 4.	Location of Dial Indicators (in)	57
Table 5.	Lateral Deflection Results for Plate 1, Test 1	125
Table 6.	Lateral Deflection Results for Plate 1, Test 2	126
Table 7.	Lateral Deflection Results for Plate 1, Test 3	127
Table 8.	Lateral Deflection Results for Plate 2, Test 1	128
Table 9.	Lateral Deflection Results for Plate 2, Test 2.	129
Table 10.	Lateral Deflection Results for Plate 2, Test 3	130
Table 11.	Lateral Deflection Results for Plate 3, Test 1	131
Table 12.	Lateral Deflection Results for Plate 3, Test 2	132
Table 13.	Lateral Deflection Results for Plate 3, Test 3	133
Table 14.	Lateral Deflection Results for Plate 4, Test 1	134
Table 15.	Lateral Deflection Results for Plate 4, Test 2	135
Table 16.	Lateral Deflection Results for Plate 4, Test 3	136

LIST OF TABLES (Cont.)

Page

Table 17.	Lateral Deflection Results for Plate 3, Yield Test	137
Table 18.	Lateral Deflection Results for Plate 4, Yield Test	138

LIST OF FIGURES

	Page
Fig. 1 In-plane Forces on Plate Element	12
Fig. 2 Moments and Shear Forces on Plate Element	12
Fig. 3 The Rectangular and Skewed Co-ordinate Systems	16
Fig. 4 Variation of Centre Deflections with Skew for Aspect Ratio = 1/2	34
Fig. 5 Variation of Centre Deflections with Skew for Aspect Ratio = 2/3	34
Fig. 6 Variation of Centre Deflections with Skew for Aspect Ratio = 1	34
Fig. 7 Variations of Bending and Membrane Edge Stresses with Centre Deflection for Aspect Ratio $b/a = 1/2$	36
Fig. 8 Variations of Bending and Membrane Stresses at Centre of Plate with Centre Deflections for Aspect Ratio $b/a = 1/2$	37
Fig. 9 Variations of Bending and Membrane Edge Stresses with Centre Deflections for Aspect Ratio $b/a = 2/3$...	38
Fig. 10 Variations of Bending and Membrane Stresses at Centre of Plate with Centre Deflections for Aspect Ratio $b/a = 2/3$	39
Fig. 11 Variation of Bending and Membrane Edge Stresses with Centre Deflection for Aspect Ratio $b/a = 1$	40
Fig. 12 Variation of Bending and Membrane Stresses at Centre of Plate with Centre Deflection for Aspect Ratio $b/a = 1$	41
Fig. 13 Initiation of Yield at A for Various Skew Angles for Aspect Ratio $b/a = 1/2$	46
Fig. 14 Initiation of Yield at A for Various Skew Angles for Aspect Ratio $b/a = 2/3$	47
Fig. 15 Initiation of Yield at A for Various Skew Angles for Aspect Ratio $b/a = 1$	48

LIST OF FIGURES

		Page
Fig. 16	Comparison of Experimental Centre Deflections with Theory	62
Fig. 17	Comparison of Experimental Edge and Centre Stresses with Theory for Test Plates 1 and 2	64
Fig. 18	Comparison of Experimental Edge and Centre Stresses with Theory for Test Plates 3 and 4	65
Fig. 19	Experimental and Theoretical Results for Bending and Membrane Stresses	66
Fig. 20	Experimental Stresses at Various Locations on Test Plate 1	69
Fig. 21	Experimental Stresses at Various Locations on Test Plate 2	70
Fig. 22	Experimental Stresses at Various Locations on Test Plate 3	71
Fig. 23	Experimental Stresses at Various Locations on Test Plate 4	72
Fig. 24	Centre Stresses at Large Lateral Pressures	75
Fig. 25.	Obtuse Corner Stresses at Large Lateral Pressures	76
Fig. 26	Acute Corner and Maximum Edge Stresses at Large Lateral Pressures	77

CHAPTER I

INTRODUCTION

Skewed plates and slabs are often required as component parts of large scale structures such as triangular dams and building floor systems. In the field of reinforced concrete, such plates are also of considerable interest and practical importance, especially in the case of skewed slabs for highway bridges that cross rivers, railways or other highways at an oblique angle. In general, the deflections of skewed plates or slabs used in the aforementioned structures are usually rather small in comparison with the thickness of the plate so that for a proper design of such plates, only a linear (small deflection) analysis is required. In contrast, the requirements of skewed plates or panels for the aircraft industry are quite different. In the case of the design of swept wings and skin panels of aircrafts, for example, the weight is of primary importance; for this reason, when skewed plates are used as their component parts, they must be thin and, as a result, their deflections are usually quite large in comparison with plate thickness. Hence, in order to obtain design charts and formulas for stressing skewed plates used for swept wings, skin panels and other related components of the aircraft, the nonlinear (large deflection) analysis must be used.

Many diverse and indirect methods are now available for

the linear analysis of clamped square and rectangular plates subjected to uniform normal loadings. Some of these methods are cited by Timoshenko and Woinowsky-Krieger (1). For the solution of a clamped uniformly loaded rectangular plate, Timoshenko and Woinowsky-Krieger employ a double series which operates with two independent systems of infinite linear simultaneous equations. Approximate solutions for the nonlinear (large deflection) analysis of uniformly loaded rectangular plates under similar boundary conditions have also been examined by Way (2) using the Rayleigh-Ritz technique and by Levy (3) who substituted a double Fourier series solution into the differential equations and evaluated the coefficients. Invariably, all the methods employed are extremely laborious and require considerable computations.

In contrast to the square and rectangular plates, skewed plates have not received as much attention. This may perhaps be due to its relatively difficult mathematical model and its absence of orthogonal relationships. For the clamped skewed plate under consideration, Morley (4) has presented results for a very limited number of skew angles and aspect ratios. Recently, due to the work of Kennedy (5) (6), deflections as well as principal stresses for such plates have been determined for various skews and aspect ratios both analytically and experimentally. However, with regard to large deflection behaviour of uniformly loaded skewed plates, no general solutions are as yet available.

The work embodied in this thesis comprises:

(i) a theoretical linear (small deflection) analysis on the bending of clamped skewed plates subjected to a uniformly distributed load and a comparison of the results so obtained with those obtained earlier by the author and other investigators (4) (5) (6) and (7)

(ii) an extension of the theoretical analysis to include the investigation into the large deflection behaviour of uniformly loaded skewed plates under the same boundary conditions.

(iii) an experimental investigation into the effect of varying the skew angle, aspect ratio and plate thickness on the small as well as the large deflection behaviour of uniformly loaded clamped skewed plates and thereby verify the theoretical predictions. The experiments performed consisted of the following aluminum plate models:

- a) Test Panel 1 --- a skewed plate with aspect ratio $1/2$, skew angle 50° and plate thickness $1/8$ in.
- b) Test Panel 2 --- a skewed plate with aspect ratio $1/2$, skew angle 50° and plate thickness $1/16$ in.
- c) Test Panel 3 --- a skewed plate with aspect ratio $2/3$, skew angle 30° and plate thickness $1/16$ in.
- and d) Test Panel 4 --- a skewed plate with aspect ratio $2/3$, skew angle 30° and plate thickness $1/8$ in.

With reference to the theoretical work, the perturbation method (8) (9), based on the smallness of the central deflection was used to determine the lateral deflection, the in-plane displacements and hence the moments and stresses of clamped skewed plates. Throughout the theoretical analysis, the dimensionless ratio of the central deflection to the thickness of the plate is used as the perturbation parameter. Essentially, the perturbation technique is based on the principle that, if a well constructed asymptotic power series should satisfy the differential equation, then each parameter should also satisfy the governing differential equation independently. Following the perturbation procedure, asymptotic power series containing a number of undetermined coefficients are assumed relating first the dimensionless load to the central deflection perturbation parameter W_0 . Power series containing unknown functions of the oblique co-ordinate axes are also assumed relating each of the displacement components u , v , and w in the middle plane of the plate with the same perturbation parameter W_0 . In assuming these functions for displacements, care was taken to ensure that these assumed functions satisfy not only the boundary conditions of the plate but also the condition of polar symmetry ---- a necessary condition for a uniformly loaded skewed plate. The assumed displacement functions are next substituted in turn into the governing partial differential equations derived in each step in the successive approximation sequence. By equating equal powers of the oblique co-ordinates ξ and η , and by solving the set of simultaneous linear

equations thus obtained, all the unknown coefficients in the displacement functions are evaluated. Finally, these displacement functions with their determined parameters are differentiated to yield the required bending and membrane stresses anywhere within the plate boundary.

Also included in the theoretical analysis is a brief discussion of the initiation of yield along the edge of the plate if the plate material reaches its yield in a region where the Von Karman equations are valid ($w/h \leq 2$). In this connection, the Huber-von Mises yield theory is used.

The experimental investigation consisted of the testing of four plate models of different skew angles, aspect ratios and plate thicknesses. All test plates were made of 6061-T6 aluminum alloy. Metal foil strain rosette gauges were installed at selected points on the plate models and principal stresses were calculated from the strain measurements recorded for the different intensities of loadings. Dial indicators were also installed at the bottom of the plate to measure the lateral deflections. In order to verify the results of the nonlinear (large deflection) analysis, all four test panels were loaded so that the centre deflection of the plate approaches twice the plate thickness.

In order to study the behaviour and stress distribution of skewed plates loaded beyond the validity of the Von Karman equations, two of the above-mentioned test panels were subjected to large loads resulting in plastic permanent deformation of the plate models.

To facilitate the computation of deflections, principal bending and membrane stresses at specified points on the skewed plate, all computational work for both the theoretical and experimental investigations was programmed in Fortran for the IBM 1620 II. The programmes are included in Appendix A.

CHAPTER II

Review of Literature

(a) Linear Analysis of Skewed Plates

The linear small deflection behaviour of skewed plates and slabs has been investigated mainly by the method of finite difference. The first publication on skewed plates was probably due to Brigatti (10) who obtained limited results, by means of finite difference equations, for uniformly loaded rhombic plates simply supported and clamped.

In 1939, Anzelius (11) investigated into the small deflection behaviour of uniformly loaded skewed plates, simply supported on two opposite sides and free on the other two. His solution is in the form of a series involving hyperbolic and trigonometric functions which yield an infinite system of linear equations. Results were given qualitatively only for twisting moments for a 45° skewed slab.

Studies of skewed plates by means of finite difference techniques were also made by Jensen (12) in 1941. Uniformly loaded skewed plates simply supported on four sides and similarly loaded skewed plates simply supported on two opposite edges and free on the other two sides were analysed by use of difference equations developed in a form readily applicable to networks made up of lines parallel to the sides. Throughout his work, the aspect ratio of the plate was taken as $1/2$ and Poisson's ratio was taken to be 0.2 .

Since the work of Jensen in 1941, a great deal of work has been done on skewed plates and skewed structures. In 1953, Dorman (13) used the energy approach to investigate into the bending behaviour of a clamped skewed plate but the function he assumed for the lateral deflection has the restrictive character of satisfying not only the polar symmetry but also quadrant symmetry ----- a condition which is non-existent in a skewed plate. The outstanding researchers in skewed plates and related structures in the past decade include Morley (4), Mirsky (14) and Jones (15).

More recently, Kennedy and the author (5) (6) have solved the small deflection problem of uniformly loaded skewed plates by means of variational techniques and the results were verified by experiments.

In 1964, Kennedy and Huggins (16) presented an analytical solution for skewed stiffened plates under a uniformly distributed load. Stresses near the corners of skewed stiffened plates were also examined by Kennedy and Martens (17) who have observed experimentally that critical stresses often occur in obtuse corners of such skewed plates.

(b) Nonlinear Analysis of Skewed Plates

No general solution for the nonlinear (large deflection) analysis of skewed plates is as yet available in the literature. However, nonlinear analyses of rectangular, circular and elliptical plates are quite well known. Results for the nonlinear analyses

of such plates are largely due to the work of Way (2), Levy (3), Chien (18), Wang (19) and Weil and Newmark (20). Large deflections of simply supported rectangular plates on elastic foundations were examined by Sinha (21) in 1963 and more recently, approximate solutions for the small and large deflection behaviour of rectangular plates resting on elastic supports have also been obtained by Kennedy and the author (22):

CHAPTER III

THEORETICAL ANALYSIS

(a) Assumptions

Based on the small deflection theory of elastic thin plates, the problem of the clamped skewed plate subjected to uniform normal loading has recently been solved (4) (5) (6) by various theoretical methods. However, in all these theoretical analyses considered, the deflections are considered to be of such magnitude that the effect of the stretching of the middle plane of the plate on its curvature can be neglected. When the lateral deflection of the plate is moderately large, that is, in the neighbourhood of one half the plate thickness or more, the linear theory of thin plates is no longer applicable and the effect of the forces acting in the middle surface must be taken into account.

Throughout this theoretical work of linear and nonlinear analyses of skewed plates, the following assumptions are made:

i) points which lie on a normal to the midplane of the undeflected plate lie on a normal to the mid-plane of the deflected plate.

ii) the stresses normal to the mid-plane of the plate, arising from the applied loading, are negligible in comparison with the stresses in the plane of the plate.

iii) the slope of the deflected plate in any direction is small so that its square may be neglected in comparison with unity.

Also, for the linear (small deflection) analysis, the forces in the middle plane of the plate is neglected and this entails one additional assumption, viz.,

iv) the mid-plane of the plate is a neutral plane, i.e., any mid-plane stresses arising from the deflection of the plate into a non-developable surface is ignored.

(b) Formulation of the Governing Partial Differential Equations

The nonlinear large deflection behaviour of thin elastic plates is governed by three coupled nonlinear partial differential equations. When the boundary conditions of the plate are known, it is often convenient to express these equations in terms of the displacement components u , v , and w (parallel to the rectangular co-ordinate axes x , y , and z respectively) of a point in the middle plane of the plate.

i) Equilibrium of the Plate Element in the x and y directions

Consider the equilibrium of a small element cut out from the middle plane of the plate with sides dx and dy as shown in Fig. 1. Let N_x , N_y and N_{xy} be the in-plane forces per unit length of the plate.

Neglecting body forces, the equilibrium of the plate element in the x and y directions yields respectively,

$$N_{x,x} + N_{xy,y} = 0 \dots\dots\dots(3-1)$$

$$N_{xy,x} + N_{y,y} = 0 \dots\dots\dots(3-2)$$

where the comma notation signifies differentiation.

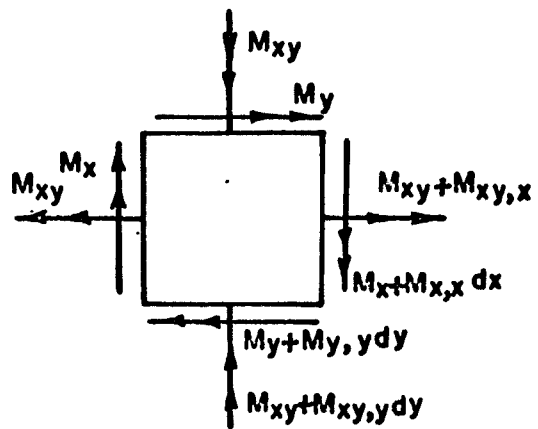
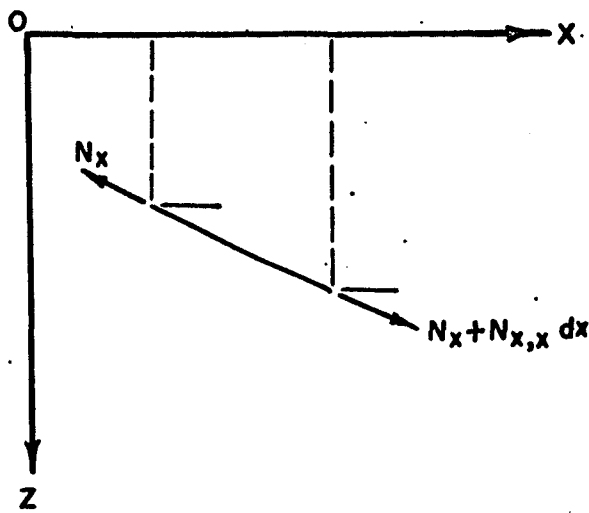
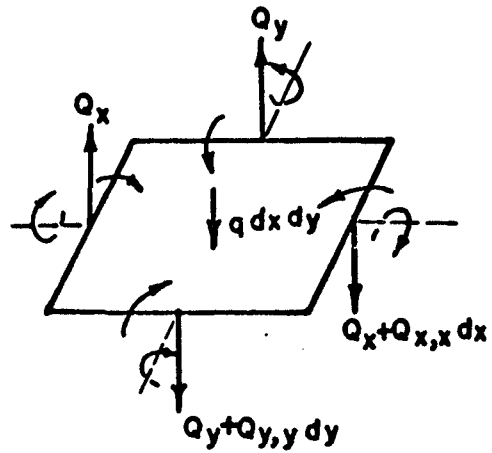
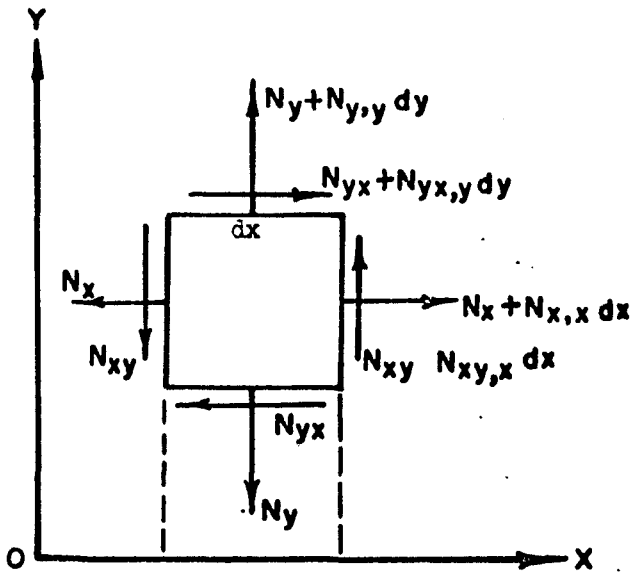


Fig. 1. In-plane Forces on Plate Element

Fig. 2. Moments and Shear Forces on Plate Element

ii) Equilibrium of the plate element in the z direction

Forces in the z direction due to the in-plane forces:

From Figure 1, it is easily seen that the net contribution of the downward force by N_x in the plate element is

$$-N_x w_{,x} dy + (N_x w_{,x} dy)_{,x} dx$$

or $(N_x w_{,xx} + N_{x,x} w_{,x}) dx dy \dots\dots\dots(3-3)$

Similarly, the net downward contribution of N_y on the plate element is

$$(N_y w_{,yy} + N_{y,y} w_{,y}) dx dy \dots\dots\dots(3-4)$$

The net downward contribution of N_{xy} on the plate element is

$$-N_{xy} w_{,y} dy + N_{xy} w_{,y} dy + (N_{xy} w_{,y} dy)_{,x} dx$$

or $(N_{xy} w_{,xy} + N_{xy,x} w_{,y}) dx dy \dots\dots\dots(3-5)$

Similarly, the net downward contribution of N_{yx} is

$$(N_{yx} w_{,xy} + N_{yx,y} w_{,x}) dx dy \dots\dots\dots(3-6)$$

Hence, the net downward contribution of all the in-plane forces can be obtained by adding Eqs. (3-3) through (3-6), viz.,

$$(N_x w_{,xx} + 2 N_{xy} w_{,xy} + N_y w_{,yy}) dx dy \dots\dots(3-7)$$

Forces in the z direction due to lateral loads:

Let Q_x, Q_y be the shear forces per unit length (Fig. 2).

Also shown on the same figure are the direction of the bending and twisting moments acting per unit length.

Equilibrium in the downward direction (along the z axis)

gives:

$$Q_{x,x} + Q_{y,y} + q = 0 \quad \dots\dots\dots(3-8)$$

Also, by taking moments about an axis parallel to the x axis and ignoring terms of lower order of magnitude gives:

$$Q_y dx dy - M_{y,y} dy dx + M_{xy,x} dx dy = 0$$

or $M_{y,y} - M_{xy,x} - Q_y = 0 \quad \dots\dots\dots(3-9)$

Similarly, by taking moments about an axis parallel to the y axis, we have,

$$M_{x,x} - M_{xy,y} - Q_x = 0 \quad \dots\dots\dots(3-10)$$

Putting the well-known expressions for moments and curvature relationships (1), viz.,

$$M_x = -D (w_{,xx} + \nu w_{,yy})$$

$$M_y = -D (w_{,yy} + \nu w_{,xx})$$

$$M_{xy} = D (1-\nu) w_{,xy}$$

into expression (3-9) and (3-10), we get

$$Q_x = -D (w_{,xxx} + w_{,xyy}) \quad \dots\dots\dots(3-11)$$

$$Q_y = -D (w_{,yyy} + w_{,yxx}) \quad \dots\dots\dots(3-12)$$

Substituting Eqs. (3-11) and (3-12) into Eq. (3-8) gives,

$$w_{,xxxx} + 2 w_{,xxyy} + w_{,yyyy} = q/D \quad \dots\dots\dots(3-13)$$

If we now add to this equilibrium equation in the vertical direction due to the lateral loads the effect due to the in-plane forces Eq. (3-7), we finally arrive at the equilibrium equation

in the vertical direction due to the combined action of the lateral and membrane forces,

$$D (w_{,xxxx} + 2 w_{,xxyy} + w_{,yyyy}) = q + N_x w_{,xx} + 2 N_{xy} w_{,xy} + N_y w_{,yy} \dots\dots\dots(3-14)$$

In terms of stresses, Eqs. (3-1), (3-2) and (3-14) can be written as

$$\sigma_{x,x} + \tau_{xy,y} = 0 \dots\dots\dots(3-15)$$

$$\sigma_{y,y} + \tau_{xy,x} = 0 \dots\dots\dots(3-16)$$

and

$$D \nabla^2 \nabla^2 w = q + h (\sigma_x w_{,xx} + \sigma_y w_{,yy} + 2 \tau_{xy} w_{,xy}) \dots\dots(3-17)$$

But, from the elementary theory of elasticity (23), the equations of plane strain are:

$$\begin{aligned} \sigma_x &= E / (1-\nu^2) (\epsilon_x + \nu \epsilon_y) \\ \sigma_y &= E / (1-\nu^2) (\epsilon_y + \nu \epsilon_x) \dots\dots(3-18) \\ \tau_{xy} &= E / 2(1+\nu) \gamma_{xy} \end{aligned}$$

and, the equations of compatibility are:

$$\begin{aligned} \epsilon_x &= u_{,x} + 1/2 (w_{,x})^2 \\ \epsilon_y &= v_{,y} + 1/2 (w_{,y})^2 \dots\dots\dots(3-19) \\ \gamma_{xy} &= u_{,y} + v_{,x} + w_{,x} w_{,y} \end{aligned}$$

Substituting equations (3-18) and (3-19) into Eqs. (3-15), (3-16) and (3-17), the three general differential equations in

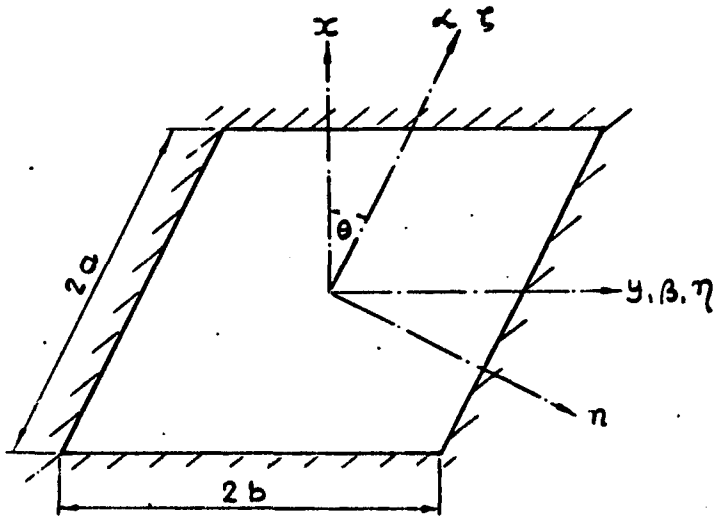


Fig. 3. The Rectangular and Skewed Co-ordinate Systems.

rectangular cartesian co-ordinates governing the large deflection of thin elastic plates are obtained:

$$u_{,xx} + w_{,x} w_{,xx} + \nu(v_{,xy} + w_{,y} w_{,xy}) + \frac{1}{2}(1-\nu)(u_{,yy} + v_{,xy} + w_{,x} w_{,yy} + w_{,y} w_{,xy}) = 0 \quad \dots\dots\dots (3-20)$$

$$v_{,yy} + w_{,y} w_{,yy} + \nu(u_{,xy} + w_{,x} w_{,xy}) + \frac{1}{2}(1-\nu)(v_{,xx} + u_{,xy} + w_{,y} w_{,xx} + w_{,x} w_{,xy}) = 0 \quad \dots\dots\dots (3-21)$$

$$D \nabla^2 \nabla^2 w = q + h \left(\frac{E}{(1-\nu^2)} \left\{ u_{,x} + \frac{1}{2}(w_{,x})^2 + \nu \left[v_{,y} + \frac{1}{2}(w_{,y})^2 \right] \right\} w_{,xx} + \frac{E}{(1-\nu^2)} \left\{ v_{,y} + \frac{1}{2}(w_{,y})^2 + \nu \left[u_{,x} + \frac{1}{2}(w_{,x})^2 \right] \right\} w_{,yy} + \frac{E}{(1+\nu)} \cdot (u_{,y} + v_{,x} + w_{,x} w_{,y}) w_{,xy} \right) \quad \dots\dots\dots (3-22)$$

where ∇ is the Laplacian operator, ν being Poisson's ratio, D , the flexural rigidity, E , the modulus of elasticity of the plate material, q , the intensity of uniformly distributed load, and h is the thickness of the plate. The comma notation signifies differentiation.

(c) The Oblique Co-ordinate System

In investigating the small and large deflection problem of skewed plates, it is often advantageous to adopt a co-ordinate system parallel to the edges of the plate, namely the oblique co-ordinate system α and β as shown in Fig. 3.

By the transformation

$$\left. \begin{aligned} x &= \alpha \cos \theta \\ y &= \beta + \alpha \sin \theta \end{aligned} \right\} \dots\dots\dots(3-23)$$

in which θ is the skew angle, the following relationships between the rectangular and oblique co-ordinate systems hold:

$$u_{,x} = u_{,\alpha} \sec \theta - u_{,\beta} \tan \theta$$

$$u_{,xx} = u_{,\alpha\alpha} \sec^2 \theta - 2 u_{,\alpha\beta} \sec \theta \tan \theta + u_{,\beta\beta} \tan^2 \theta$$

$$u_{,xy} = u_{,\alpha\beta} \sec \theta - u_{,\beta\beta} \tan \theta$$

$$u_{,y} = u_{,\beta}$$

$$u_{,yy} = u_{,\beta\beta}$$

$$v_{,x} = v_{,\alpha} \sec \theta - v_{,\beta} \tan \theta$$

$$v_{,xy} = v_{,\alpha\beta} \sec \theta - v_{,\beta\beta} \tan \theta$$

$$v_{,xx} = v_{,\alpha\alpha} \sec^2 \theta - 2 v_{,\alpha\beta} \sec \theta \tan \theta + v_{,\beta\beta} \tan^2 \theta$$

$$v_{,y} = v_{,\beta}$$

$$v_{,yy} = v_{,\beta\beta}$$

$$w_{,x} = w_{,\alpha} \sec \theta - w_{,\beta} \tan \theta$$

$$w_{,xy} = w_{,\alpha\beta} \sec \theta - w_{,\beta\beta} \tan \theta$$

$$w_{,xx} = w_{,\alpha\alpha} \sec^2 \theta - 2 w_{,\alpha\beta} \sec \theta \tan \theta + w_{,\beta\beta} \tan^2 \theta$$

$$w_{,xxxx} = w_{,\alpha\alpha\alpha\alpha} \sec^4 \theta - 4 w_{,\alpha\alpha\alpha\beta} \sec^3 \theta \tan \theta$$

$$+ 6 w_{,\alpha\alpha\beta\beta} \sec^2 \theta \tan^2 \theta - 4 w_{,\alpha\beta\beta\beta} \sec \theta \tan^3 \theta$$

$$+ w_{,\alpha\beta\beta\beta} \sec \theta \tan^3 \theta + w_{,\beta\beta\beta\beta} \tan^4 \theta$$

$$w_{,xxyy} = w_{,\alpha\alpha\beta\beta} \sec^2 \theta - 2 w_{,\alpha\beta\beta\beta} \sec \theta \tan \theta$$

$$+ w_{,\beta\beta\beta\beta} \tan^2 \theta$$

$$w_{,yyyy} = w_{,\beta\beta\beta\beta}$$

Using these transformation relationships and, by defining further the dimensionless quantities

$$R = \frac{b}{a} ; \quad \zeta = \frac{\alpha}{a} ; \quad \eta = \frac{\beta}{b} ; \quad U = \frac{ua}{h^2} ;$$

$$V = \frac{va}{h^2} ; \quad W = \frac{w}{h} ; \quad Q = \frac{qb^4}{Dh}$$

Eqs. (3-20), (3-21) and (3-22) can be re-written into the oblique dimensionless form as:

$$2R^3 c U_{,\zeta\zeta} - 4R^2 sc U_{,\zeta\eta} + R(2s^2 c + (1-\nu)c^3) U_{,\eta\eta} + R(1+\nu) c (R V_{,\zeta\eta} - s V_{,\eta\eta})$$

$$+ 2R^2 W_{,\zeta\zeta} (R W_{,\zeta} - s W_{,\eta}) + R W_{,\zeta\eta} \{ -4Rs W_{,\zeta} + W_{,\eta} [4s^2 + (1+\nu)c^2] \}$$

$$+ W_{,\eta\eta} [R W_{,\zeta} (1 + s^2 - \nu c^2) - 2s W_{,\eta}] = 0 \dots\dots\dots (3-24)$$

$$R(1 + c^2 - \nu s^2) V_{,\eta\eta} - 2R^2(1-\nu)s V_{,\zeta\eta} + R^3(1-\nu)V_{,\zeta\zeta} + (1+\nu)(R^2 c U_{,\zeta\eta} - Rsc U_{,\eta\eta})$$

$$+ W_{,\eta\eta} [2W_{,\eta} - R(1+\nu)s W_{,\zeta}] + R W_{,\zeta\eta} [(-3+\nu)s W_{,\eta} + R(1+\nu)W_{,\zeta}] + R^2 W_{,\zeta\zeta} [(1-\nu)W_{,\eta}]$$

$$= 0 \dots\dots\dots (3-25)$$

$$R^4 W_{,\zeta\zeta\zeta\zeta} - 4s(R^3 W_{,\zeta\zeta\zeta\eta} + R W_{,\zeta\eta\eta\eta}) + 2R^2(1+2s^2) W_{,\zeta\zeta\eta\eta} + W_{,\eta\eta\eta\eta} =$$

$$Qc^4 + 12\{ (R^2 c U_{,\zeta} - Rsc U_{,\eta}) + \frac{1}{2} (R W_{,\zeta} - s W_{,\eta})^2 + \nu [Rc^2 V_{,\eta} + \frac{1}{2} (c W_{,\eta})^2] \}$$

$$(R^2 W_{,\zeta\zeta} - 2Rs W_{,\zeta\eta} + s^2 W_{,\eta\eta}) + 12c^2 (Rc^2 V_{,\eta} + \frac{1}{2} c^2 (W_{,\eta})^2 + \nu [(R^2 c U_{,\zeta} - Rsc U_{,\eta})$$

$$+ \frac{1}{2} (R W_{,\zeta} - s W_{,\eta})^2]) W_{,\eta\eta} + 12(1-\nu) [(R^2 c V_{,\zeta} - Rsc V_{,\eta}) + (Rc W_{,\zeta} - sc W_{,\eta}) W_{,\eta}$$

$$+ R c^2 U_{,\eta}] (Rc W_{,\zeta\eta} - sc W_{,\eta\eta}) \dots\dots\dots (3-26)$$

where, for brevity, $s = \sin \theta$ and $c = \cos \theta$, θ being the skew angle, $2a$ and $2b$ are the oblique dimensions of the plate.

Hence, the problem of large deflections of skewed plates is reduced to finding a solution to Eqs. (3-24), (3-25) and (3-26).

(d) Method of Solution

The small parameter perturbation method is now used to obtain approximate solutions to Eqs. (3-24), (3-25) and (3-26) for clamped skewed plates subjected to lateral uniform pressure. This method requires the expansion of the displacement components and the dimensionless load quantity in a power series of ascending powers of the dimensionless centre deflection parameter W_0 . Thus we let,

$$Q = \gamma_1 W_0 + \gamma_3 W_0^3 + \gamma_5 W_0^5 + \dots \dots \dots (3-27)$$

$$W = w_1(\zeta, \eta) W_0 + w_3(\zeta, \eta) W_0^3 + w_5(\zeta, \eta) W_0^5 + \dots \dots (3-28)$$

$$U = s_2(\zeta, \eta) W_0^2 + s_4(\zeta, \eta) W_0^4 + \dots \dots \dots (3-29)$$

$$V = t_2(\zeta, \eta) W_0^2 + t_4(\zeta, \eta) W_0^4 + \dots \dots \dots (3-30)$$

where $\gamma_1, \gamma_3, \gamma_5 \dots$ are the undetermined parameters relating the dimensionless centre deflection W_0 to the dimensionless load Q , $s_2, s_4, \dots, t_2, t_4, \dots$, and w_1, w_3, w_5, \dots , are functions of the dimensionless oblique co-ordinates ζ and η , relating the in-plane and lateral displacements to the same perturbation parameter W_0 .

From the series for W , Eq. (3-27), it is evident that, in order that the centre deflection be W_0 as defined, it is necessary to require

$$w_1(0,0) = 1 \quad \text{and} \quad w_3(0,0) = w_5(0,0) = 0 \dots(3-31)$$

The prescribed boundary conditions for the clamped edges are:

$$w_{,n} = v \cos \theta = w = 0 \quad \text{at } \eta = \pm 1$$

and $w_{,x} = u = w = 0 \quad \text{at } \zeta = \pm 1$ (3-32)

Solution to the Linear Small Deflection Problem

(First Order Approximation)

Substituting Eqs. (3-27) and (3-28) into Eq. (3-26) and equating coefficients of the terms containing W_0 , yield the following differential equation governing the linear (small deflection) behaviour of skewed plates:

$$R^4 w_{1,\zeta\zeta\zeta\zeta} - 4R^3 s w_{1,\zeta\zeta\zeta\eta} - 4Rs w_{1,\zeta\eta\eta\eta} + 2R^2(1+2s^2) w_{1,\zeta\zeta\eta\eta} + w_{1,\eta\eta\eta\eta} = \gamma_1 c^4 \dots\dots\dots(3-33)$$

The associated boundary conditions for this first order approximation are:

$$\left. \begin{aligned} w_{1,n} = w_1 = 0 & \quad \text{at } \eta = \pm 1 \\ \text{and} & \\ w_{1,x} = w_1 = 0 & \quad \text{at } \zeta = \pm 1 \end{aligned} \right\} \dots\dots\dots(3-34)$$

It can be readily verified that conditions (3-34) are identically satisfied when

$$w_1 = (1-\eta^2)^2 (1-\zeta^2)^2 (1-\zeta\eta)(1+C_1\eta^2+C_2\zeta^2+C_3\eta^4+C_4\zeta^4+C_5\zeta^2\eta^2) \dots (3-35)$$

where $C_1 \dots C_5$ are undetermined coefficients. It is perhaps worth noting that the deflection function assumed, Eq. (3-35) not only meets the conditions set out in (3-31) but also satisfies the inherent condition of polar symmetry, i.e.,

$$w_1(\zeta, \eta) = w_1(-\zeta, -\eta), \text{ and } w_1(-\zeta, \eta) = w_1(\zeta, -\eta)$$

----- a necessary condition for a uniformly loaded skewed plate.

Substituting expression (3-35) into Eq. (3-33) and equating corresponding powers of η and ζ we obtain six linear algebraic equations for the six undetermined coefficients, C_1, \dots, C_5 . The solution of this matrix equation defines uniquely the value of the small lateral displacement (deflection) of the plate anywhere within the plate boundary.

Solution to the Nonlinear Large Deflection Problem (Higher Order Approximations)

Making use of Eqs. (3-28) through (3-30) in Eqs. (3-24) and (3-25) and collecting coefficients of W_0^2 terms, result in two differential equations governing the in-plane displacement components of the plate:

$$\begin{aligned}
& 2 R^3 c s_{2, \zeta\zeta} - 4 R^2 s c s_{2, \zeta\eta} + R(2s^2 c + (1-\nu)c^3) s_{2, \eta\eta} + (1+\nu) R^2 c^2 t_{2, \zeta\eta} \\
& - R(1+\nu) s c^2 t_{2, \eta\eta} + 2 R^3 w_{1, \zeta\zeta} w_{1, \zeta} - 2 R^2 s w_{1, \zeta\zeta} w_{1, \eta} - 4 R^2 s w_{1, \zeta\eta} w_{1, \zeta} \\
& + R[4s^2 + (1+\nu)c^2] w_{1, \zeta\eta} w_{1, \eta} + R(1+s^2 - \nu c^2) w_{1, \eta\eta} w_{1, \zeta} - 2s w_{1, \eta\eta} w_{1, \eta} = 0 \dots (3-36)
\end{aligned}$$

$$\begin{aligned}
& R(1+c^2 - \nu s^2) t_{2, \eta\eta} - 2R^2(1-\nu)s t_{2, \zeta\eta} + R^3(1-\nu) t_{2, \zeta\zeta} + R(1+\nu) c s_{2, \zeta\eta} \\
& - R(1+\nu) s c s_{2, \eta\eta} + 2 w_{1, \eta\eta} w_{1, \eta} - R(1+\nu) s w_{1, \eta\eta} w_{1, \zeta} + R(\nu-3) s w_{1, \zeta\eta} w_{1, \eta} \\
& + R^2(1+\nu) w_{1, \zeta\eta} w_{1, \zeta} + R^2(1-\nu) w_{1, \zeta\zeta} w_{1, \eta} = 0 \dots (3-37)
\end{aligned}$$

The boundary conditions for the in-plane displacements require

$$\begin{aligned}
& s_2 = t_2 \cos \theta = 0 \\
& \text{at } \eta = 1 \text{ and } \zeta = 1 \dots (3-38)
\end{aligned}$$

which are satisfied if we take,

$$\begin{aligned}
& s_2 = (1 - \zeta^2)(1 - \eta^2)(D_2 \zeta + D_3 \eta + D_4 \zeta^3 + D_5 \eta^3 + D_6 \zeta\eta^2 + D_7 \zeta^2 \eta \\
& + D_8 \zeta^3 \eta^2 + D_9 \zeta^2 \eta^3) \dots (3-39)
\end{aligned}$$

$$\begin{aligned}
& t_2 = (1 - \zeta^2)(1 - \eta^2)(E_2 \eta + E_3 \zeta + E_4 \eta^3 + E_5 \zeta^3 + E_6 \zeta^2 \eta + E_7 \zeta\eta^2 \\
& + E_8 \zeta^2 \eta^3 + E_9 \zeta^3 \eta^2) \dots (3-40)
\end{aligned}$$

Employing expression (3-35), (3-39) and (3-40) as dictated by Eqs. (3-36) and (3-37) and equating powers of x and y, yield sufficient linear equations to determine the twelve undetermined coefficients $D_2, \dots, D_9, E_2, \dots, E_9$, and hence the in-plane displacement components.

Collecting the coefficients of W_0^3 terms in equation (3-26),
the differential equation governing the first nonlinear term of
the lateral displacement expression is obtained, namely,

$$\begin{aligned}
& R^4 w_{3,\zeta\zeta\zeta\zeta} - 4Rs(R^2 w_{3,\zeta\zeta\zeta\eta} + w_{3,\zeta\eta\eta\eta}) + 2R^2(1+2s^2)w_{3,\zeta\zeta\eta\eta} + w_{3,\eta\eta\eta\eta} \\
& = \gamma_3 c^4 + 12 \left\{ [R^4 c s_{2,\zeta} w_{1,\zeta\zeta} - 2R^3 s c s_{2,\zeta} w_{1,\zeta\eta} + R^2 s^2 c s_{2,\zeta} w_{1,\eta\eta} - R^3 s c s_{2,\eta} w_{1,\zeta\zeta} \right. \\
& + 2R^2 s^2 c s_{2,\eta} w_{1,\zeta\eta} - R s^3 c s_{2,\eta} w_{1,\eta\eta}] + \frac{1}{2} [R^4 w_{1,\zeta\zeta} (w_{1,\zeta})^2 \\
& - 2R^3 s w_{1,\zeta\eta} (w_{1,\zeta})^2 + R^2 s^2 w_{1,\eta\eta} (w_{1,\zeta})^2 - 2R^3 s w_{1,\zeta\zeta} w_{1,\zeta} w_{1,\eta} \\
& + 4R^2 s^2 w_{1,\zeta\eta} w_{1,\zeta} w_{1,\eta} - 2R s^3 w_{1,\eta\eta} w_{1,\zeta} w_{1,\eta} + R^2 s^2 w_{1,\zeta\zeta} (w_{1,\eta})^2 \\
& - 2R s^3 w_{1,\zeta\eta} (w_{1,\eta})^2 + s^4 w_{1,\eta\eta} (w_{1,\eta})^2] + \nu [R^3 c^2 w_{1,\zeta\zeta} t_{2,\eta} \\
& - 2R^2 s c^2 w_{1,\zeta\eta} t_{2,\eta} + R s^2 c^2 w_{1,\eta\eta} t_{2,\eta} + \frac{1}{2} R^2 c^2 w_{1,\zeta\zeta} (w_{1,\eta})^2 \\
& - R s c^2 w_{1,\zeta\eta} (w_{1,\eta})^2 + \frac{1}{2} s^2 c^2 w_{1,\eta\eta} (w_{1,\eta})^2] \left. \right\} + 12 \left\{ [R c^4 w_{1,\eta\eta} t_{2,\eta} \right. \\
& + \frac{1}{2} c^4 w_{1,\eta\eta} (w_{1,\eta})^2 + \nu (R^2 c^3 w_{1,\eta\eta} s_{2,\zeta} - R s c^3 w_{1,\eta\eta} s_{2,\eta} \\
& + \frac{1}{2} c^2 [R^2 (w_{1,\zeta})^2 (w_{1,\eta\eta}) - 2Rs w_{1,\eta\eta} w_{1,\zeta} w_{1,\eta} + s^2 w_{1,\eta\eta} (w_{1,\eta})^2]) \\
& + 12(1-\nu) [R^2 c^3 w_{1,\zeta\eta} s_{2,\eta} - R s c^3 w_{1,\eta\eta} s_{2,\eta} + R^3 c^2 w_{1,\zeta\eta} t_{2,\zeta} \\
& - R^2 s c^2 w_{1,\eta\eta} t_{2,\zeta} - R^2 s c^2 w_{1,\zeta\eta} t_{2,\eta} + R s^2 c^2 w_{1,\eta\eta} t_{2,\eta} + R^2 c^2 w_{1,\eta} w_{1,\zeta} w_{1,\zeta\eta} \\
& \left. - R s c^2 w_{1,\eta\eta} w_{1,\eta} w_{1,\zeta} - R s c^2 w_{1,\zeta\eta} (w_{1,\eta})^2 + s^2 c^2 w_{1,\eta\eta} (w_{1,\eta})^2 \right] \quad (3-41)
\end{aligned}$$

The boundary conditions to be met here are:

$$\begin{aligned}
 w_{3,n} = w_3 = 0 & \quad \text{at } \eta = \pm 1 \\
 \text{and } w_{3,x} = w_3 = 0 & \quad \text{at } \xi = \pm 1 \quad \dots\dots\dots(3-42)
 \end{aligned}$$

which are identically satisfied by the following expression:

$$w_3 = (1 - \eta^2)^2 (1 - \xi^2)^2 (1 - \zeta \eta) (F_1 \eta^2 + F_2 \xi^2 + F_3 \eta^4 + F_4 \xi^4 + F_5 \xi^2 \eta^2) \quad (3-43)$$

Substituting Eq. (3-43) into expression (3-41) and again equating powers of η and ξ , the undetermined coefficients $\delta_3, F_1, \dots, F_5$ are evaluated by solving the resulting set of simultaneous equations.

Repeating the same procedure, i.e., now collecting coefficients of W_0^4 , equations governing the next approximation for the in-plane displacements can be written as:

$$\begin{aligned}
 & 2R^3 c s_{4,\xi\xi} - 4R^2 s c s_{4,\xi\eta} + R(2s^2 c + (1-\nu)c^3) s_{4,\eta\eta} \\
 & + (1+\nu) R^2 c^2 t_{4,\xi\eta} - (1+\nu) R c^2 s t_{4,\eta\eta} + 2R^3 (w_{1,\xi} w_{3,\xi\xi} + w_{3,\xi} w_{1,\xi\xi}) \\
 & - 2R^2 s (w_{1,\eta} w_{3,\xi\xi} + w_{3,\eta} w_{1,\xi\xi}) - 4R^2 s (w_{3,\xi} w_{1,\xi\eta} + w_{1,\xi} w_{3,\xi\eta}) \\
 & + R(4s^2 + (1+\nu)c^2) (w_{1,\eta} w_{3,\xi\eta} + w_{3,\eta} w_{1,\xi\eta}) + R(1+s^2-\nu)c^2 \\
 & (w_{1,\xi} w_{3,\eta\eta} + w_{3,\xi} w_{1,\eta\eta}) - 2s (w_{1,\eta} w_{3,\eta\eta} + w_{3,\eta} w_{1,\eta\eta}) = 0 \\
 & \dots\dots\dots(3-44)
 \end{aligned}$$

169928

$$\begin{aligned}
& R(1+c^2 - s^2)t_{4,\eta\eta} - 2(1-\nu)R^2st_{4,\xi\eta} + (1-\nu)R^3t_{4,\xi\xi} + (1+\nu)R^2cs_{4,\xi\eta} \\
& - (1+\nu)Rcs_{4,\eta\eta} + 2(w_1,\eta w_3,\eta\eta + w_3,\eta w_1,\eta\eta) - R(1+\nu)s(w_1,\xi w_3,\eta\eta + w_3,\xi w_1,\eta\eta) \\
& + R(-3+\nu)s(w_1,\eta w_3,\xi\eta + w_3,\eta w_1,\xi\eta) + R^2(1+\nu)(w_3,\xi w_1,\xi\eta + w_1,\xi w_3,\xi\eta) \\
& + R^2(1-\nu)(w_1,\eta w_3,\xi\xi + w_3,\eta w_1,\xi\xi) = 0 \quad \dots\dots\dots (3-45)
\end{aligned}$$

The associated boundary conditions for this approximation are:

$$s_4 = t_4 \cos \theta = 0$$

$$\text{at } \eta = \pm 1 \text{ and } \xi = \pm 1 \quad \dots\dots\dots (3-46)$$

Eq.(3-46) are satisfied by assuming the following forms for the in-plane displacements:

$$s_4 = (1-\xi^2)(1-\eta^2)(1-\xi\eta)(G_2\xi + G_3\eta + G_4\xi^3 + G_5\eta^3 + G_6\xi\eta^2 + G_7\xi^2\eta + G_8\xi^3\eta^2 + G_9\xi^2\eta^3) \dots\dots\dots (3-47)$$

$$t_4 = (1-\xi^2)(1-\eta^2)(1-\xi\eta)(H_2\xi + H_3\eta + H_4\xi^3 + H_5\eta^3 + H_6\xi\eta^2 + H_7\xi^2\eta + H_8\xi^3\eta^2 + H_9\xi^2\eta^3) \dots\dots\dots (3-48)$$

The undetermined coefficients $G_2, \dots, G_6, \dots, H_2, \dots, H_6$ are again evaluated by substituting Eqs (3-47) and (3-48) into Eqs. (3-44) and (3-45).

As a last approximation in this analysis, we put Eqs.(3-27) through (3-30) into Eq. (3-26) and collect coefficients w_0^5 . This yields the differential equation:

$$\begin{aligned}
& R^4w_{5,\xi\xi\xi\xi} - 4Rs(R^2w_{5,\xi\xi\xi\eta} + w_{5,\xi\eta\eta\eta}) + 2R^2(1+2s^2)w_{5,\xi\xi\eta\eta} + w_{5,\eta\eta\eta\eta} = \delta_s^4 + 12 \\
& \{ [R^4c(w_{1,\xi\xi}s_{4,\xi} + w_{3,\xi\xi}s_{2,\xi}) - 2R^3sc(w_{1,\xi\eta}s_{4,\xi} + w_{3,\xi\eta}s_{2,\xi}) + R^2cs^2(w_{1,\eta\eta} \\
& s_{4,\xi} + w_{3,\eta\eta}s_{2,\xi}) - R^3cs(w_{3,\xi\xi}s_{2,\eta} + w_{1,\xi\xi}s_{4,\eta}) + 2R^2cs^2(w_{1,\xi\eta}s_{4,\eta} + w_{3,\xi\eta} \\
& s_{2,\eta}) - Rcs^3(w_{1,\eta\eta}s_{4,\eta} + w_{3,\eta\eta}s_{2,\eta})] + 1/2[R^4(2w_{1,\xi\xi}w_{1,\xi}w_{3,\xi} + w_{3,\xi\xi}
\end{aligned}$$

$$\begin{aligned}
& (w_{1,\xi})^2) - 2R^3 s (2w_{1,\xi\eta} w_{1,\xi} w_{3,\xi} + w_{3,\xi\eta} (w_{1,\xi})^2) + R^2 s^2 (2w_{1,\eta\eta} w_{1,\xi} w_{3,\xi} + w_{3,\eta\eta} \\
& (w_{1,\xi})^2) - 2R^3 s (w_{1,\xi\xi} w_{1,\xi} w_{3,\eta} + w_{1,\xi\xi} w_{3,\xi} w_{1,\eta} + w_{3,\xi\xi} w_{1,\xi} w_{1,\eta}) \\
& + 4R^2 s^2 (w_{1,\xi\eta} w_{1,\xi} w_{3,\eta} + w_{1,\xi\eta} w_{3,\xi} w_{1,\eta} + w_{3,\xi\eta} w_{1,\xi} w_{1,\eta}) - 2R s^3 (w_{1,\eta\eta} \\
& w_{1,\xi} w_{3,\eta} + w_{1,\eta\eta} w_{3,\xi} w_{1,\eta} + w_{3,\eta\eta} w_{1,\xi} w_{1,\eta}) + R^2 s^2 (2w_{1,\xi\xi} w_{1,\eta} w_{3,\eta} \\
& + w_{3,\xi\xi} w_{1,\eta} w_{1,\eta}) - 2R s^3 (2w_{1,\xi\eta} w_{1,\eta} w_{3,\eta} + w_{3,\xi\eta} (w_{1,\eta})^2) + s^4 (2w_{1,\eta\eta} \\
& w_{1,\eta} w_{3,\eta} + w_{3,\eta\eta} (w_{1,\eta})^2) + \nu [R^3 c^2 (w_{1,\xi\xi} t_{4,\eta} + w_{3,\xi\xi} t_{2,\eta}) - 2R^2 s c^2 \\
& (w_{1,\xi\eta} t_{4,\eta} + w_{3,\xi\eta} t_{2,\eta}) + R s^2 c^2 (w_{1,\eta\eta} t_{4,\eta} + w_{3,\eta\eta} t_{2,\eta}) \\
& + 1/2c^2 (R^2 (2w_{1,\xi\xi} w_{1,\eta} w_{3,\eta} + w_{3,\xi\xi} (w_{1,\eta})^2) \\
& - 2R s (2w_{1,\xi\eta} w_{1,\eta} w_{3,\eta} + w_{3,\xi\eta} (w_{1,\eta})^2) + s^2 (2w_{1,\eta\eta} w_{1,\eta} w_{3,\eta} + w_{3,\eta\eta} \\
& (w_{1,\eta})^2))] + 12[Rc^4 (w_{1,\eta\eta} t_{4,\eta} + w_{3,\eta\eta} t_{2,\eta}) + 1/2c^4 (2w_{1,\eta\eta} w_{1,\eta} w_{3,\eta} \\
& + w_{3,\eta\eta} (w_{1,\eta})^2) + \nu [R^2 c^3 (w_{1,\eta\eta} s_{4,\xi} + w_{3,\eta\eta} s_{2,\xi}) - R s c^3 (w_{1,\eta\eta} s_{4,\eta} \\
& + w_{3,\eta\eta} s_{2,\eta}) + 1/2[R^2 c^2 (2w_{1,\eta\eta} w_{1,\xi} w_{3,\xi} + w_{3,\eta\eta} (w_{1,\xi})^2) - 2R s c^2 (w_{1,\eta\eta} \\
& w_{1,\xi} w_{3,\eta} + w_{1,\eta\eta} w_{3,\xi} w_{1,\eta} + w_{3,\eta\eta} w_{1,\xi} w_{1,\eta}) + c^2 s^2 (2w_{1,\eta\eta} w_{1,\eta} w_{3,\eta} \\
& + w_{3,\eta\eta} w_{1,\eta} w_{1,\eta})]] + 12(1-\nu) \{R^2 c^3 (w_{1,\xi\eta} s_{4,\eta} + w_{3,\xi\eta} s_{2,\eta}) - R s c^3 \\
& (w_{1,\eta\eta} s_{4,\eta} + w_{3,\eta\eta} s_{2,\eta}) + R^3 c^2 (w_{1,\xi\eta} t_{4,\xi} + w_{3,\xi\eta} t_{2,\xi}) - R^2 s c^2 (w_{1,\eta\eta} \\
& t_{4,\xi} + w_{3,\eta\eta} t_{2,\xi}) - R^2 s c^2 (w_{1,\xi\eta} t_{4,\eta} + w_{3,\xi\eta} t_{2,\eta}) \\
& + R s^2 c^2 (w_{1,\eta\eta} t_{4,\eta} + w_{3,\eta\eta} t_{2,\eta}) + R^2 c^2 (w_{1,\xi\eta} w_{1,\eta} \\
& w_{3,\xi} + w_{1,\xi\eta} w_{3,\eta} w_{1,\xi} + w_{3,\xi\eta} w_{1,\eta} w_{1,\xi}) - R s c^2 (w_{1,\eta\eta} w_{1,\eta} w_{3,\xi} + w_{1,\eta\eta} \\
& w_{3,\eta} w_{1,\xi} + w_{3,\eta\eta} w_{1,\eta} w_{1,\xi}) - R s c^2 (2w_{1,\xi\eta} w_{3,\eta} w_{1,\eta} + w_{3,\xi\eta} (w_{1,\eta})^2) \\
& + s^2 c^2 (w_{1,\eta\eta} w_{1,\eta} w_{3,\eta} + w_{1,\eta\eta} w_{3,\eta} w_{1,\eta} + w_{3,\eta\eta} (w_{1,\eta})^2) \dots \dots \dots (3-49)
\end{aligned}$$

The boundary conditions for this last approximation are:

$$\begin{aligned}
w_{5,\eta} = w_5 = 0 & \quad \text{at } \eta = \pm 1 \\
& \dots \dots \dots (3-50) \\
\text{and} \\
w_{5,x} = w_5 = 0 & \quad \text{at } \xi = \pm 1
\end{aligned}$$

which are met if we choose:

$$w_5 = (1-\xi^2)^2 \cdot (1-\eta^2)^2 (1-\xi\eta) (T_1\eta^2 + T_2\xi^2 + T_3\eta^4 + T_4\xi^4 + T_5\xi^2\eta^2) \dots\dots\dots(3-51)$$

Using this expression in Eq. (3-49) and equating powers of ξ and η , provide six linear simultaneous equations from which the undetermined coefficients, T_1, \dots, T_5 are found.

The above perturbation procedure has provided a means of determining uniquely the coefficients in all the dimensionless load and displacement functions represented by Eqs. (3-27) through Eq. (3-30). From these displacement functions, the principal bending and membrane stresses at any point within the plate boundary can be obtained.

(e) Displacement and Stress Relationships

It is well known that, in the theory of thin flat plates, the bending and membrane stresses can be expressed in terms of the displacements.¹ In terms of rectangular coordinates x and y , these displacements and stress relationships are given by:

$$\begin{aligned} \sigma_x'' &= \frac{-6D}{h^2} (w_{,xx} + \nu w_{,yy}) \\ \sigma_y'' &= \frac{-6D}{h^2} (w_{,yy} + \nu w_{,xx}) \dots\dots\dots(3-52) \\ \tau_{xy}'' &= \frac{6D}{h^2} (1-\nu) w_{,xy} \end{aligned}$$

$$\sigma_x' = \frac{E}{(1-\nu^2)} \left\{ u_{,x} + \frac{1}{2} (w_{,x})^2 + \nu \left[v_{,y} + \frac{1}{2} (w_{,y})^2 \right] \right\}$$

$$\sigma_y' = \frac{E}{(1-\nu^2)} \left\{ v_{,y} + \frac{1}{2} (w_{,y})^2 + \nu \left[u_{,x} + \frac{1}{2} (w_{,x})^2 \right] \right\} \dots\dots (3-53)$$

$$\tau_{xy}' = G (u_{,y} + v_{,x} + w_{,x} w_{,y})$$

where σ_x'' , σ_y'' and τ_{xy}'' are the extreme-fibre bending and shearing stresses, σ_x' , σ_y' and τ_{xy}' are the membrane stresses in the middle surface of the plate, and G is the shear modulus.

By means of the transformation Eqs. (4) and, by adding further the following dimensionless ratios for stress, viz.,

the nondimensional bending stresses:

$$S_x'' = \frac{\sigma_x'' b^2 (1-\nu^2)}{Eh^2} ; S_y'' = \frac{\sigma_y'' b^2}{Eh^2} (1-\nu^2) ; S_{xy}'' = \frac{\tau_{xy}'' b^2}{Gh^2}$$

and, the nondimensional membrane stresses:

$$S_x' = \frac{\sigma_x' b^2}{Eh^2} (1-\nu^2) ; S_y' = \frac{\sigma_y' b^2}{Eh^2} (1-\nu^2) ; S_{xy}' = \frac{\tau_{xy}' b^2}{Gh^2} \dots (3-54)$$

Eqs. (25) can be readily expressed in terms of

the dimensionless oblique co-ordinates as follows:

$$S_x'' = -\frac{1}{2} [R^2 \sec^2 \theta W_{,\xi\xi} - 2R \sec \theta \tan \theta W_{,\xi\eta} + (\tan^2 \theta + \nu) W_{,\eta\eta}]$$

$$S_y'' = -\frac{1}{2} [(1+\nu \tan^2 \theta) W_{,\eta\eta} + \nu (R^2 \sec^2 \theta W_{,\xi\xi} - 2R \sec \theta \tan \theta W_{,\xi\eta})] \dots\dots (3-55)$$

$$S_{xy}'' = R \sec \theta W_{,\xi\eta} - \tan \theta W_{,\eta\eta}$$

$$\begin{aligned}
S'_x &= R^2 \sec^2 \theta U_{,\zeta} - R \tan \theta U_{,\eta} + \nu R v_{,\eta} + \frac{1}{2} [R^2 \sec^2 \theta (W_{,\zeta})^2 \\
&+ (\nu + \tan^2 \theta) (W_{,\eta})^2 - 2 R \sec \theta \tan \theta W_{,\zeta} W_{,\eta}] \\
S'_y &= R v_{,\eta} + \frac{1}{2} (1 + \nu \tan^2 \theta) (W_{,\eta})^2 + \nu \{ R^2 \sec^2 \theta U_{,\zeta} - R \tan \theta U_{,\eta} \\
&+ \frac{1}{2} [(R W_{,\zeta})^2 \sec^2 \theta - 2 R W_{,\zeta} W_{,\eta} \sec \theta \tan \theta] \} \\
S''_{xy} &= R U_{,\eta} + R^2 \sec \theta v_{,\zeta} - R \tan \theta v_{,\eta} + W_{,\eta} (R \sec \theta W_{,\zeta} - \tan \theta W_{,\eta})
\end{aligned} \tag{3-56}$$

From these dimensionless bending and membrane stresses, the dimensionless principal stresses can be calculated in the usual manner:

$$\begin{aligned}
S''_{\max} &= 1/2 (S''_x + S''_y) + 1/2 \sqrt{(S''_x - S''_y)^2 + 4(S''_{xy})^2} \\
S''_{\min} &= 1/2 (S''_x + S''_y) - 1/2 \sqrt{(S''_x - S''_y)^2 + 4(S''_{xy})^2}
\end{aligned} \tag{3-57}$$

The solution to the problem was programmed in Fortran for an IBM 1620. To guard against round-off errors, all computations were carried to 16 significant figures.

(f) Observation and Discussion of Theoretical Results

Deflections (Lateral Displacements):

Results for the small deflection problem, obtained from the first order approximation, are shown in Table 1 for various skew angles and aspect ratios. It can be observed that the results are in close agreement with those obtained by Morley (4) and Kennedy (5). The results were also compared with experimental values obtained recently by the authors (6); the agreement was found to be good with the theoretical results being on the conservative side.

Results for the large deflection problem are shown graphically in Figures 4, 5, and 6, for aspect ratio $R = 1/2, 2/3,$ and 1 respectively. To exhibit the difference between the linear and non-linear behaviour, results based on the small deflection theory are shown plotted in the above-mentioned figures.

For a given aspect ratio R , each of the Figures 4, 5, or 6 shows that the maximum deflection at the centre of the plate decreases with an increase in the skew angle. A similar observation can be made regarding deflections governed by the small deflection theory. (See also Table 1). This is due mainly to the increased rigidity of the obtuse corners with increase in skew, thus reducing the central deflection.

Furthermore, comparison of results for different aspect ratios R , indicates that the effect of skew on the central deflection decreases with decreasing R ; this is expected since the influence of the plate corners on the central deflection diminish with decreasing R .

TABLE I. COEFFICIENTS w FOR MAXIMUM SMALL DEFLECTION AT CENTER FOR
VARIOUS SKEW ANGLES AND RATIOS OF SIDES

$$R = b/a \quad W_{\max.} = w \frac{b^4 q}{D} (10)^{-2}$$

Skew Angle θ	R = 1		R = 0.8		R = 0.667		R = 0.5	
	Present Method	Reference [5]	Present Method	Reference [5]	Present Method	Reference [5]	Present Method	Reference [5]
15°	1.797	1.793 1.792*	2.583	2.576 2.581*	3.123	3.093 3.098*	3.616	3.536 3.552*
30°	1.219	1.181	1.760	1.699 1.792*	2.096	2.050 2.081*	2.400	2.352 2.320*
45°	0.549	0.508	.791	.735	0.951	0.896 0.997*	1.088	1.056 1.040*
60°	0.128	.120	.186	.175	.230	0.216	.275	.259
75°	.00864	.00826	.0127	.0121	.0160	.0150	.0195	.0182

* Values obtained by Morley (4)

Results from the present method of solution are compared to those obtained by Way (2) for rectangular plates with small and large deflections, Figures 4, 5, and 6. Excellent agreement is shown for the small deflection results for all the aspect ratios considered, and for the large deflection results for aspect ratio $R = 1/2$; whereas for $R = 2/3$ and $R = 1$, the agreement is not as close, the difference not exceeding 5% for $R = 1$ and a dimensionless uniformly distributed load of 200. This discrepancy can be explained by the fact that the expressions assumed here for the displacement components, u , v , and w provide polar symmetry only in contrast to the rectangular plate where quadrant symmetry is required. The effect of this difference in symmetry on the behaviour of the plate under load seems to increase with increase in the aspect ratio R .

Figures 4, 5, and 6 also indicate that results obtained from small deflection and large deflection theories are sensibly the same when the central deflection is small compared to the thickness of the plate. However, the ratio, w_{\max}/h at which the results from the two theories begin to deviate significantly is influenced by the aspect ratio, $R = b/a$. For example, Figure 4 ($R = 1/2$) shows that a distinct deviation between the small and large deflection results occurs when w_{\max}/h exceeds a value of approximately 0.4; whereas Figure 5 ($R = 2/3$) and Figure 6 ($R = 1$) show such deviations occurring at ratios w_{\max}/h approximately equal to 0.35 and 0.22 respectively. Thus we may conclude that the ratio w_{\max}/h , at which

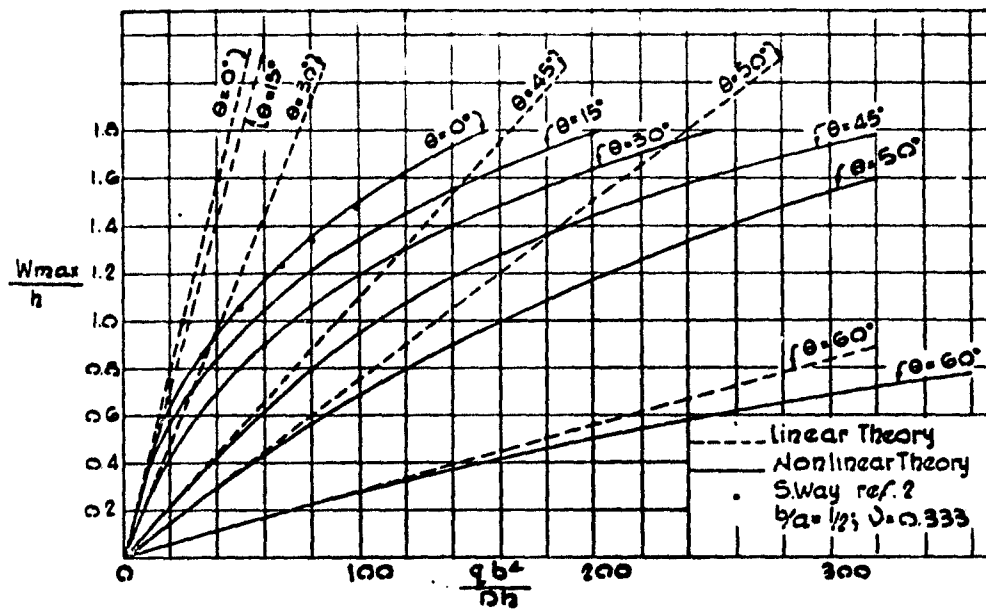


Fig. 4. Variation of Centre Deflections with Skew for Aspect Ratio = 1/2

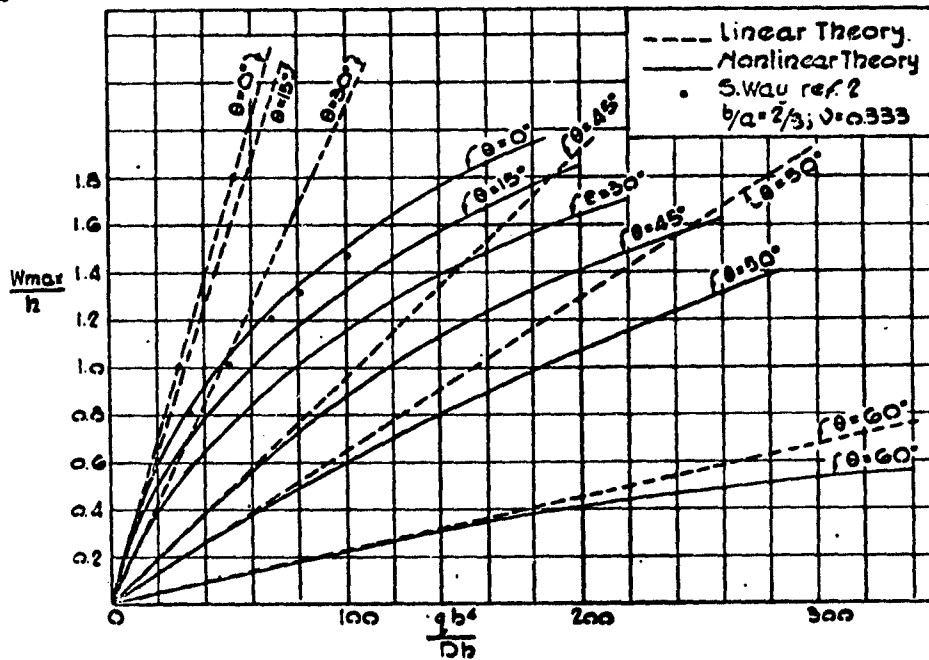


Fig. 5. Variations of Centre Deflections with Skew for Aspect Ratio = 2/3.

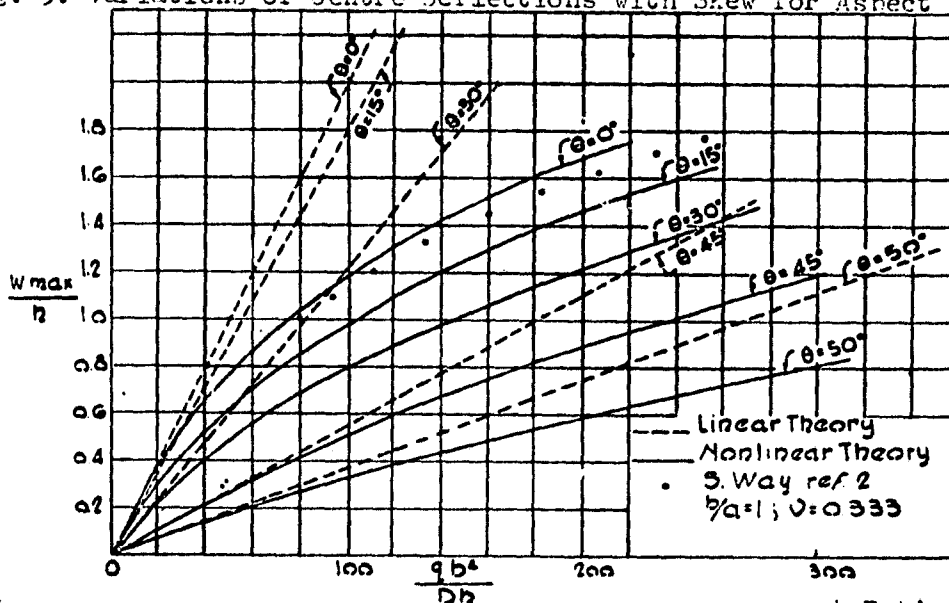


Fig. 6. Variation of Centre Deflection with Skew for Aspect Ratio = 1.

marked deviations of results from the two theories occur, decreases with increasing aspect ratio, R . It may be added also that the above w_{\max}/h ratios do not appear to be sensitive to changes in the skew angle. In general, as the load on the plate is increased, the effect of the membrane forces on the deflection of the plate also increases, thus substantially reducing the lateral deflection as observed from Figures 4, 5, and 6.

The influence of the nonlinear terms on the deflection appears to diminish with increase in skew. Thus, for any given aspect ratio, the large deflection curves tend to become increasingly linear for large angles of skew.

Bending and Membrane Stresses:

Variations of the maximum principal bending and membrane stresses, at the edge and centre of the plate, with maximum centre deflection are shown in Figures 7 through 12 for several aspect ratios and skew angles. For the limiting case of zero skew ($\theta = 0^\circ$) and all the aspect ratios considered, the edge bending stresses are in close agreement with those obtained by Way (2). However, the corresponding membrane edge stresses reported by Way are approximately 30% higher. This discrepancy is probably due partly to the approximations in Way's energy solution, noted also by Timoshenko (1), and partly to the difference in symmetry existing between the skew and rectangular plate problems.

DIMENSIONLESS BENDING AND MEMBRANE EDGE STRESSES

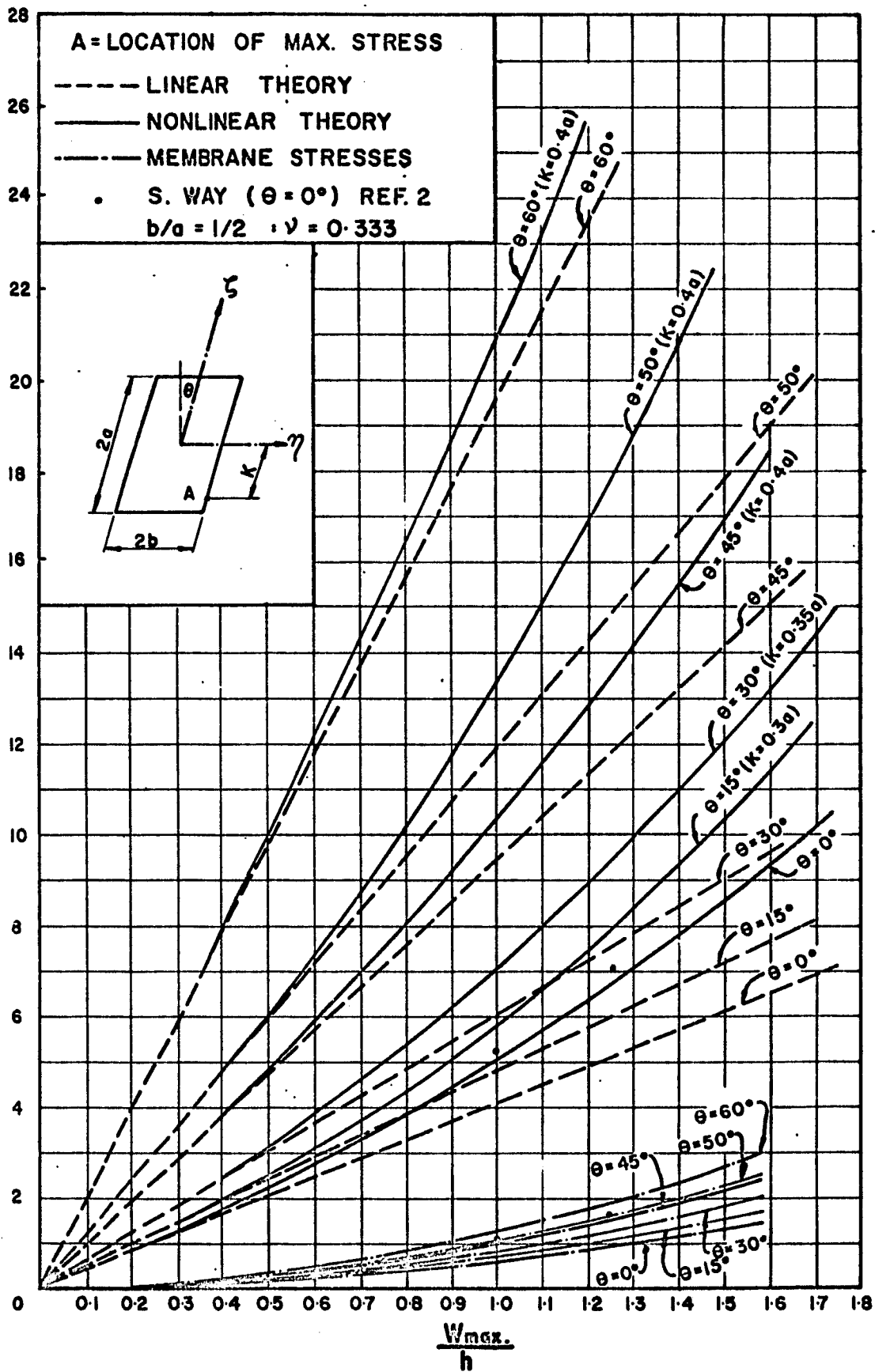


Fig. 7. Variations of Bending and Membrane Edge Stresses with Centre Deflections for Aspect Ratio $b/a = 1/2$

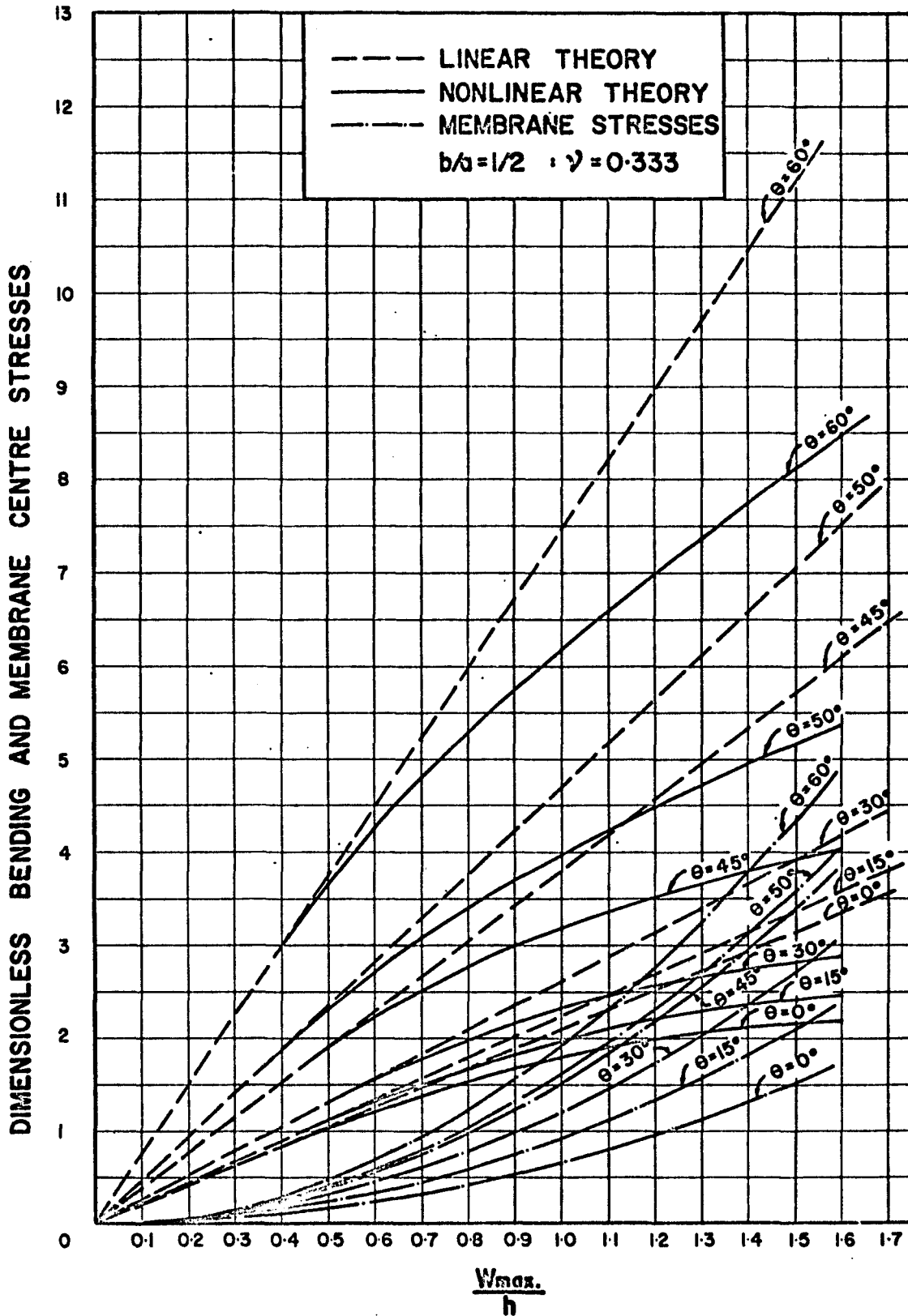


Fig. 8. Variations of Bending and Membrane Stresses at Centre of Plate with Centre Deflections for Aspect Ratio $b/a = 1/2$

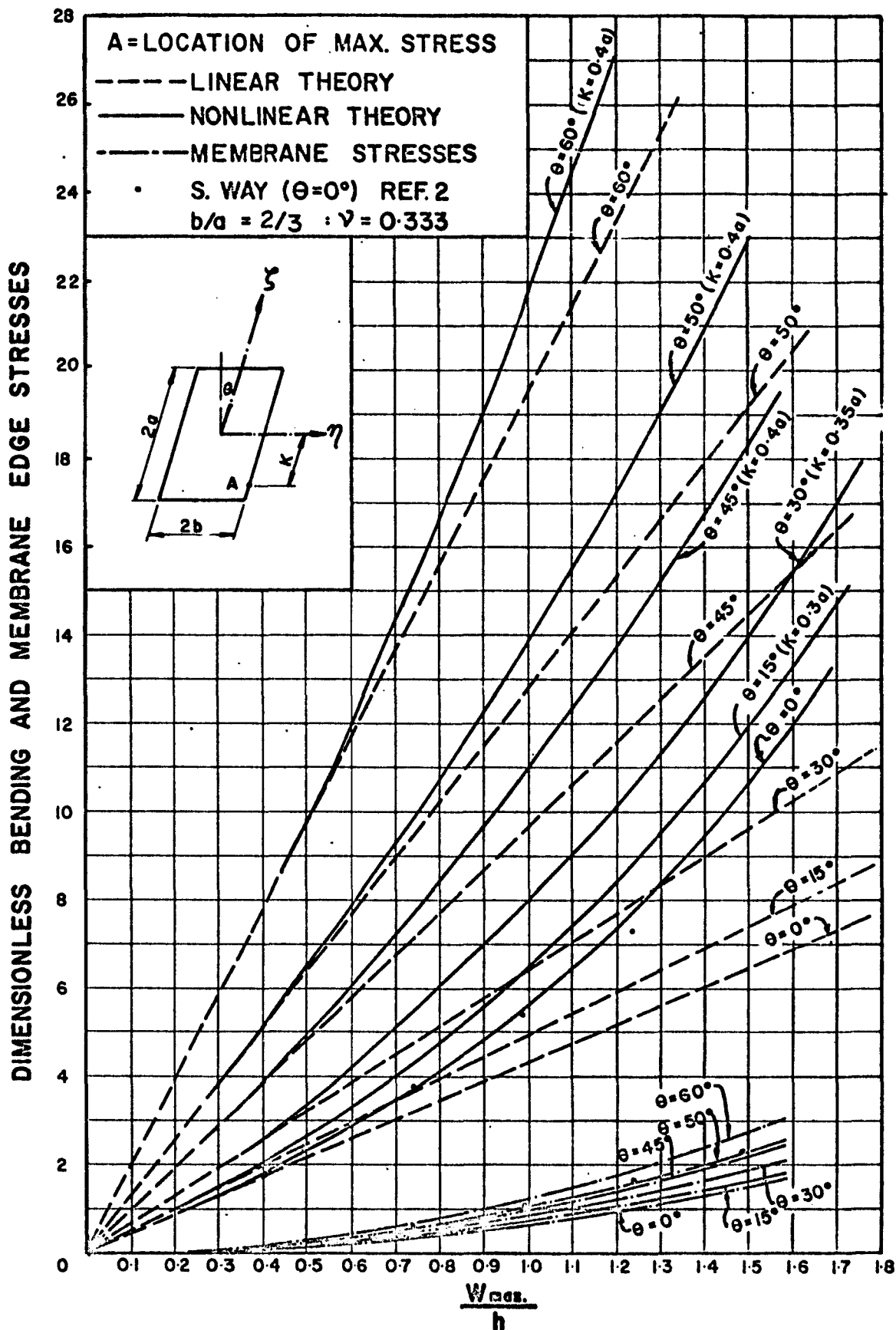


Fig. 9. Variations of Bending and Membrane Edge Stresses with Centre Deflections for Aspect Ratio $b/a = 2/3$

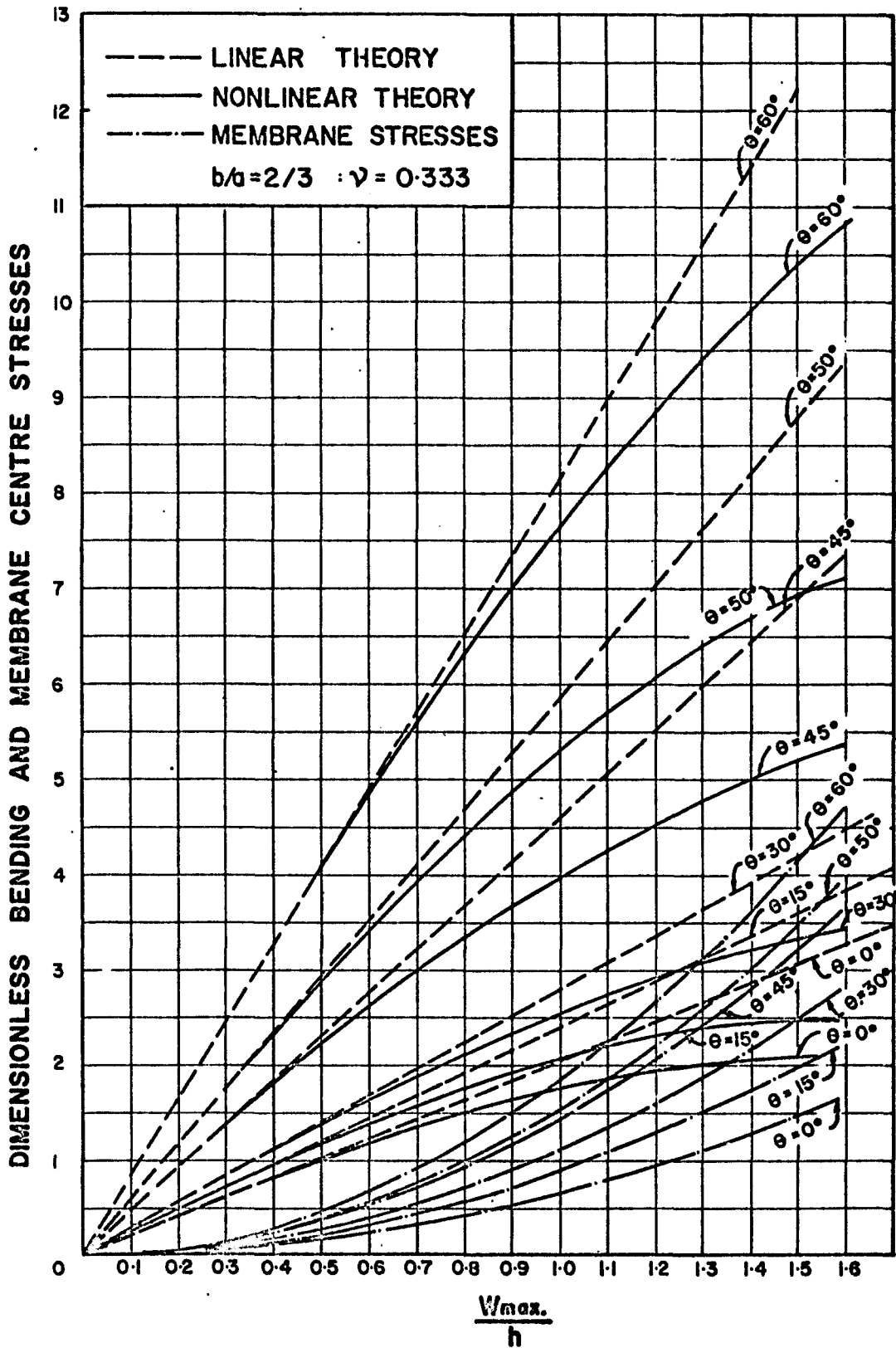


Fig. 10. Variation of Bending and Membrane Stresses at Centre of Plate with Centre Deflections for Aspect Ratio $b/a = 2/3$

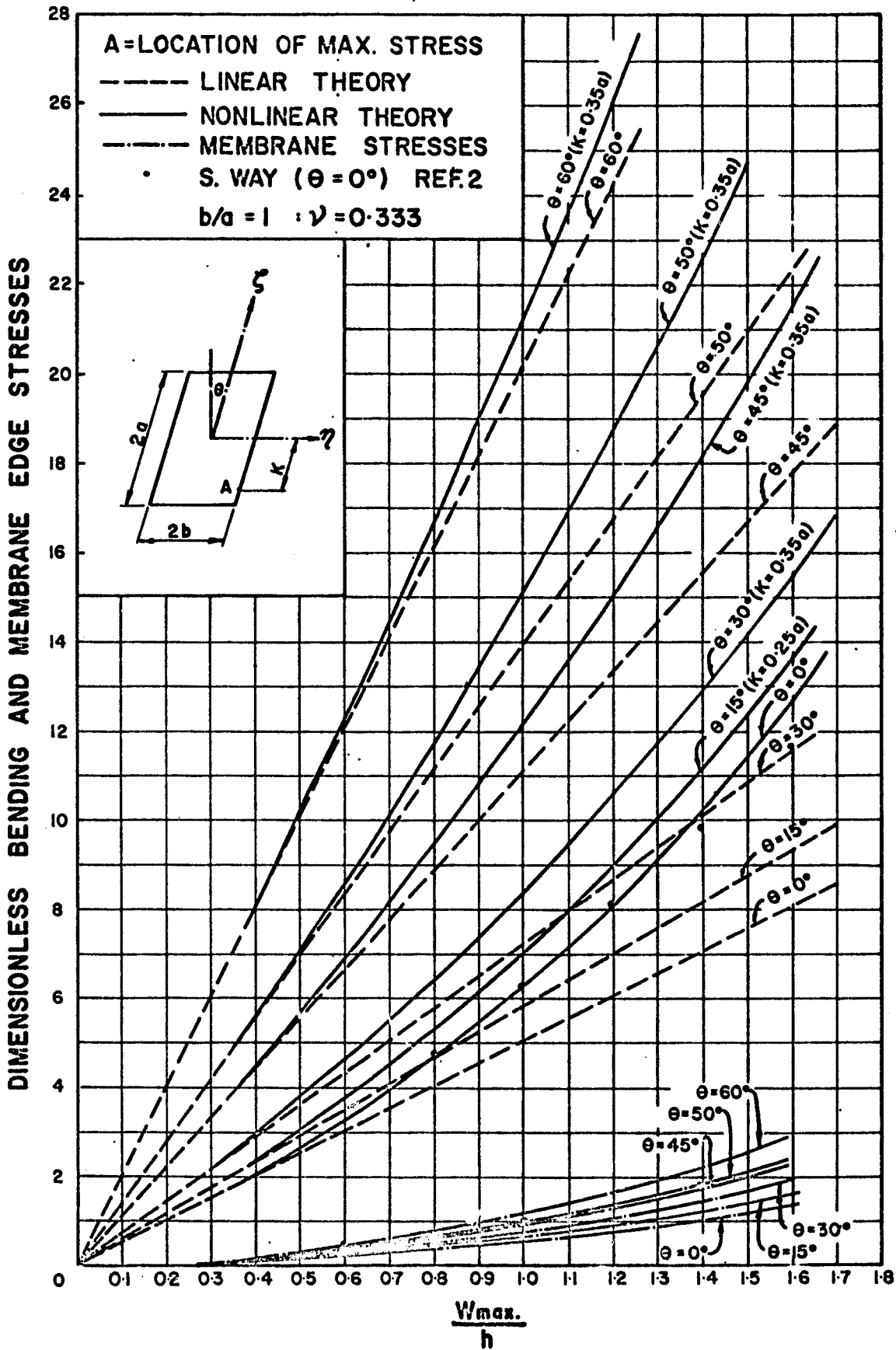


Fig. 11. Variation of Bending and Membrane Edge Stresses with Centre Deflection for Aspect Ratio $b/a = 1$

DIMENSIONLESS BENDING AND MEMBRANE CENTRE STRESSES

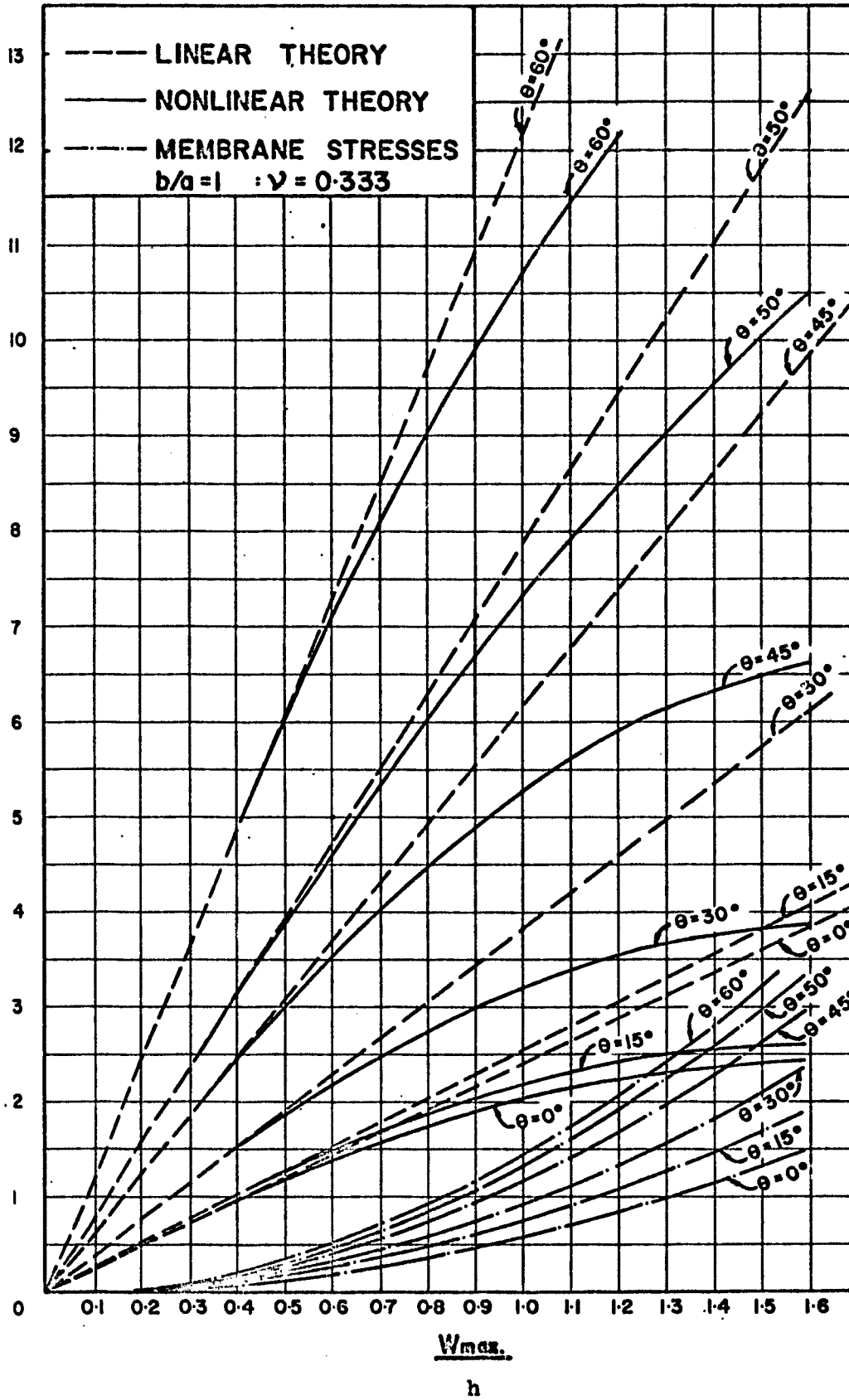


Fig. 12. Variation of Bending and Membrane Stresses at Centre of Plate with Centre Deflection for Aspect Ratio $b/a = 1$

Inspection of Figures 7 through 12 indicates that the maximum resultant or total stress occurs along the longer edge of the plate. The location of this resultant stress is invariably displaced towards the obtuse corners, and increasingly so with higher skew. It can also be observed from the above figures that, for a particular lateral displacement at centre, both the maximum edge and centre stresses increase with increasing skew; this is to be expected since more load is required to produce the same lateral centre displacement in a plate with a large skew than one with a small skew.

For different values of skew and aspect ratio considered, the curves representing the bending and membrane stresses are sensibly linear up to a point where the ratio w_{\max} / h is between 0.35 and 0.40. This observation confirms the generally accepted criterion as to the limit of applicability of the small deflection theory.

Although the maximum membrane stresses along the edge and at the centre do increase with skew, they are relatively insensitive to changes in the aspect ratio, R . For any particular plate geometry the membrane stresses at the centre are invariably larger than those along the edge. However, for the entire combinations of independent variables considered, the magnitude of the membrane stresses is quite small when compared with the maximum resultant stresses along the longer edge of the plate.

(g) Convergence of the Results:

Although the convergence of the perturbation method has not been fully and rigorously clarified (25) (26), the method has been used successfully in solving many practical problems. Invariably, when the method was employed in solving plate problems, approximations beyond the third were not considered, mainly because of the formidable computational labour entailed. However, due to the restrictive symmetry of the problem treated herein, approximations up to and including the 5th were considered to obtain the results reported. It should be mentioned that in some cases with skew angles as high as 60° , the 5th order approximations were discarded, since with their inclusion the results began to diverge. The convergence and divergence of series solutions used in perturbation methods are fully discussed by Van Dyke (26). To illustrate the convergence, typical values for γ , in Equation (3-27), are given below:

For

$$R = 1/2, \theta = 15^\circ : \gamma_1 = 27.654, \gamma_3 = 25.274, \gamma_5 = 0.792$$

$$R = 1, \theta = 45^\circ : \gamma_1 = 181.149, \gamma_3 = 38.745, \gamma_5 = 15.253$$

(h) Plastic Analysis

As a result of foregoing theoretical analysis, it has been found that the maximum principal stress of a clamped skewed plate occurs along the longer edge of the plate and is displaced towards the obtuse corners (Figures 7, 9, and 11.) This maximum principal stress acts perpendicular to the edge of the plate and increases with increasing lateral centre deflection. When the yielding stress of the plate material is reached, the bending strength at the edge would break gradually.

The condition of yielding along the edge can be computed most simply by following the assumptions of the von-mises-Hencky theory of plastic failure. If σ_1 , σ_2 , and σ_3 are the principal stresses in the three perpendicular directions, the yielding condition is (23):

$$(\sigma_1 - \sigma_2)^2 + (\sigma_2 - \sigma_3)^2 + (\sigma_3 - \sigma_1)^2 = \dots\dots\dots(3-58)$$

Where E_0 is the yielding stress in simple tension.

At the edge of the plate, we may identify σ_1 , the maximum principal stress perpendicular to the edge of the plate as σ_x , and

σ_2 , the principal stress parallel to the edge of the plate as σ_y ; and, due to the assumption of plane stress (assumption 2), σ_3 in the von Mises equation is neglected and Equation (3-58) is

reduced to :

$$\sigma_x^2 - \sigma_x \sigma_y + \sigma_y^2 = E_o^2 \dots\dots\dots(3-59)$$

Using equations (3-18) and (3-19) and recalling that the boundary conditions at the longer edge of the plate are:

$$w_{,x} = w_{,n} = w_{,y} = v_{,y} = 0 \text{ at } y = \pm 1 \dots\dots(3-60)$$

we have,

$$\sigma_x = \frac{E}{(1 - \nu^2)} u_{,x}$$

$$\sigma_y = \frac{E}{(1 - \nu^2)} \nu u_{,x}$$

or $\sigma_y = \nu \sigma_x \dots\dots\dots(3-61)$

Putting Equation (3-61) into Equation (3-59) and, after simplification, the yield condition at the edge of the plate on the convex side is obtained:

$$\frac{E_o b^2 (1 - \nu^2)}{E h^2} = \sqrt{(1 - \nu + \nu^2)} (S''_{max} + S'_{max}) \dots\dots(3-62)$$

This equation for the yield condition is plotted for aspect ratios $R = 1/2$, $R = 2/3$, and $R = 1$ respectively for various skew angles in Figures 13, 14, and 15.

$$\frac{E_0 h^2 (1-\nu^2)}{E h^2}$$

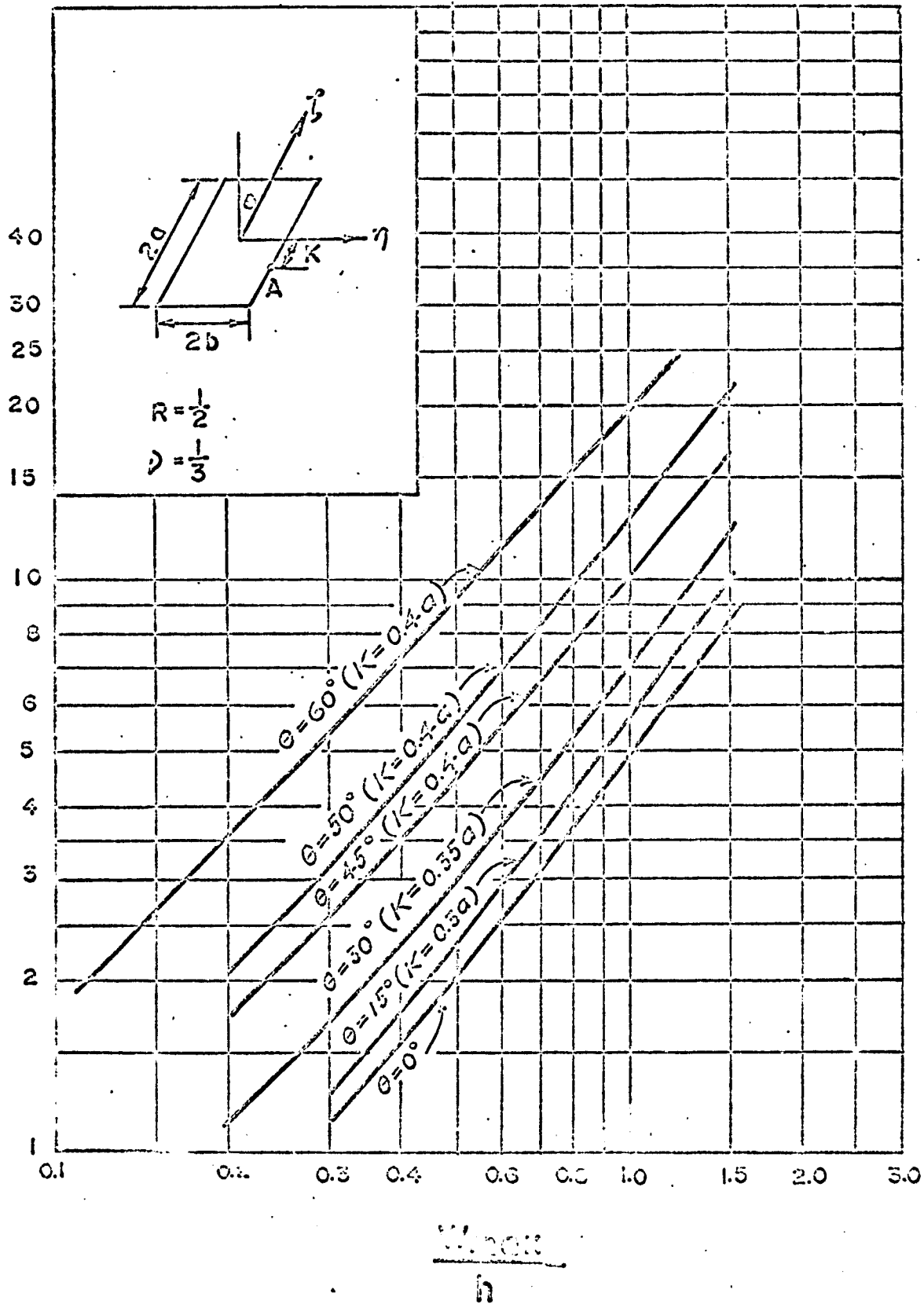


Fig. 13. Initiation of Yield at A for Various Skew Angles for Aspect Ratio $b/a = 1/2$

$\frac{F_0 b^2 (1-\nu^2)}{E h^2}$

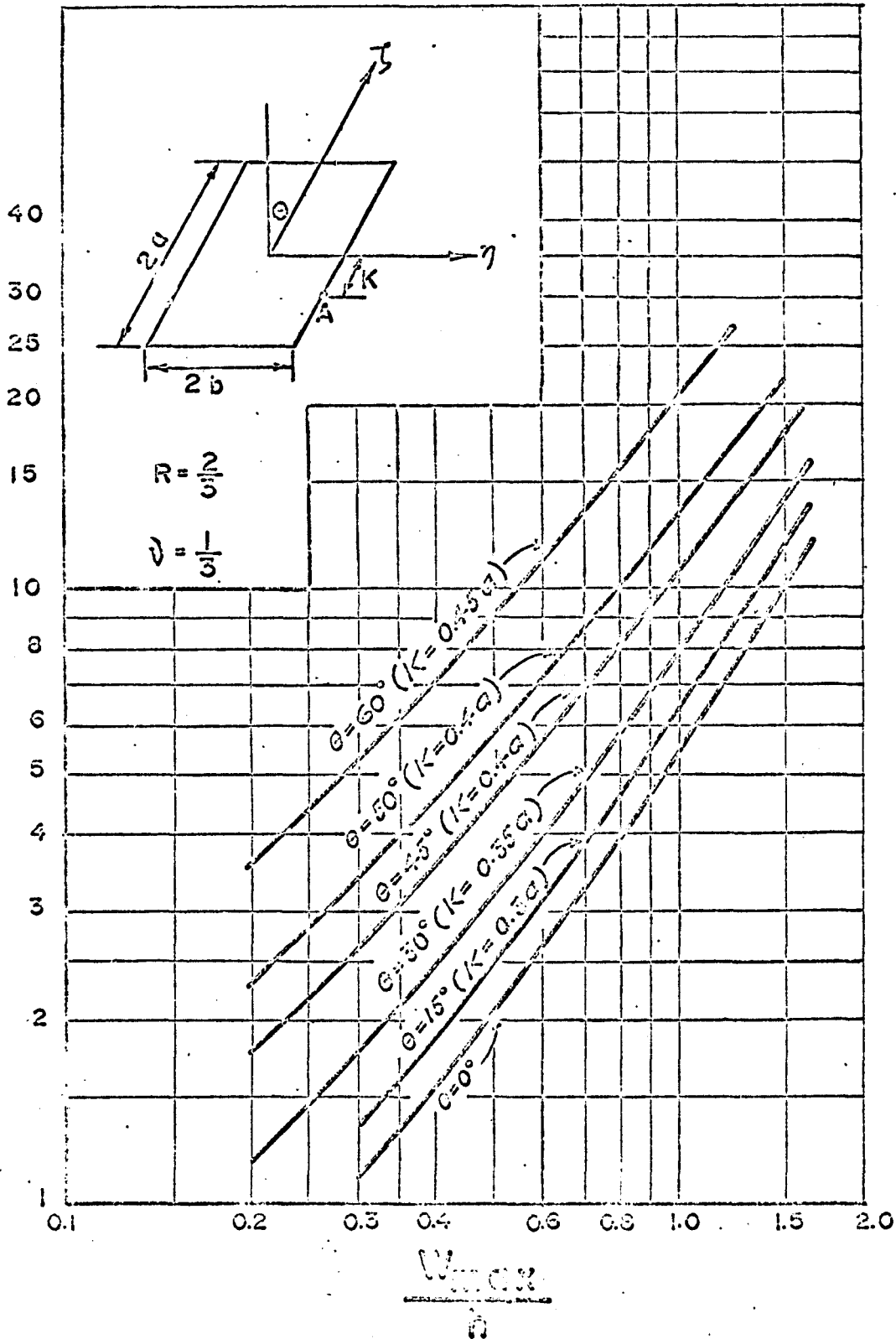


Fig. 14. Initiation of Yield at A for Various Skew Angles for Aspect Ratio $b/a = 2/3$

$$\frac{E_0 b^2 (1-\nu^2)}{E h^2}$$

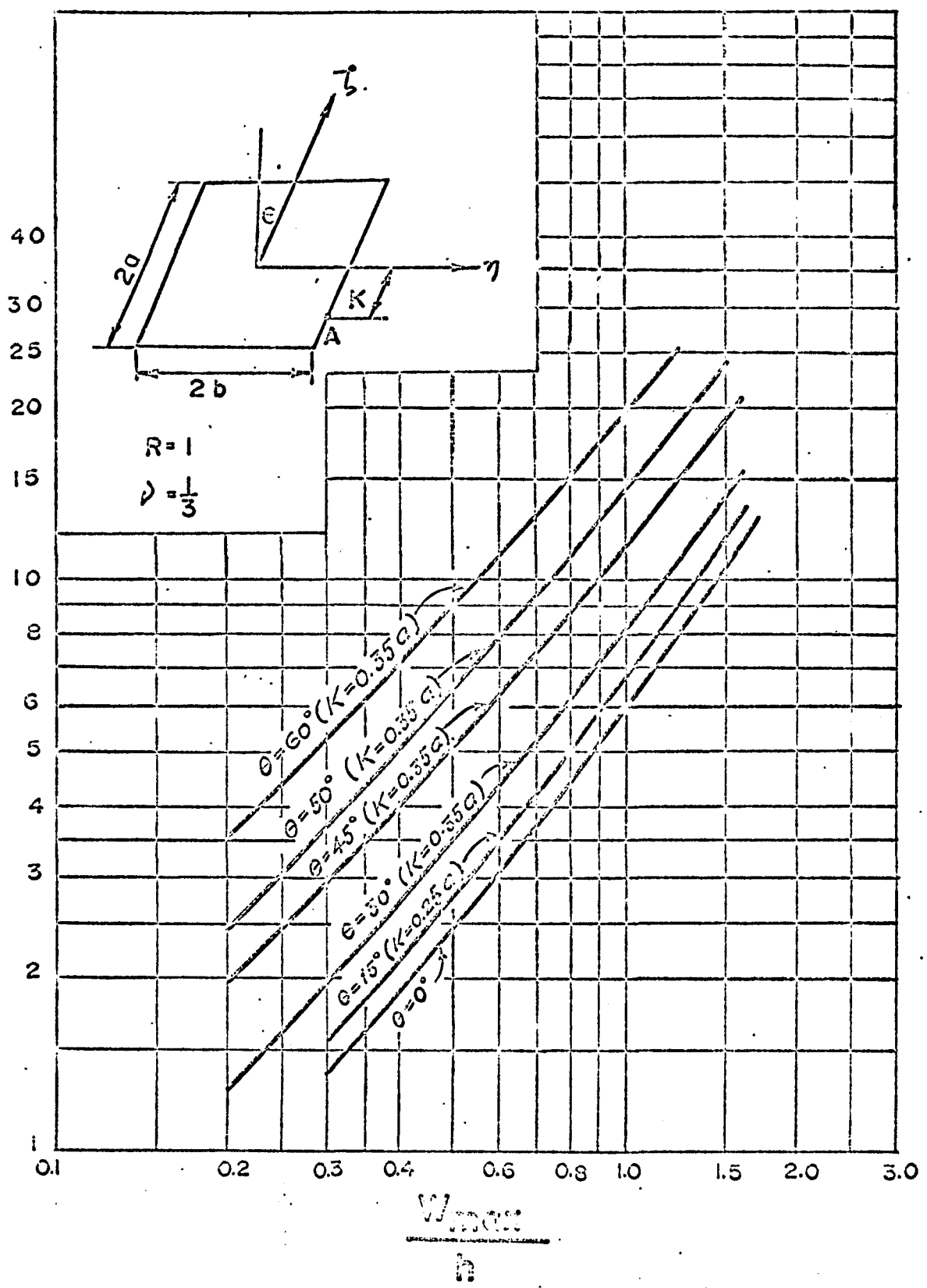


Fig. 15. Initiation of Yield at A for Various Skew Angles for Aspect Ratio $b/a = 1$

From these figures, it can be seen that, apart from the elastic and plastic properties of the plate material, the initiation of the yield condition in a clamped skewed plate depends largely on the angle of skew and is rather insensitive to changes in the aspect ratio R of the plate. For skewed plates with a given plate material, aspect ratio and oblique dimensions, the yielding occurs at a much lower dimensionless centre deflection ratio w_{\max} / h for large skew angles than it is with small skews. This is to be expected since, for a given aspect ratio R , the maximum stress of the plate increases with the angle of skew for a particular dimensionless centre deflection w/h (Figures 7, 9, and 11). Due to the assumptions on which the large deflection equations (3-20), (3-21), (3-22) are based, the results from this analysis are applicable only to those skewed panels where the plate material has a very low yield strength so that yielding occurs in a region where the von Karman equations are still valid ($w_{\max} / h \leq 2$).

CHAPTER IV
EXPERIMENTAL ANALYSIS

(a) Materials and Apparatus

Four aluminum alloy (24) 6061-T6 skewed panels were tested. The aspect ratio, skew angle, thickness and dimensions of these test panels are given in Table 2. A total of 18 metal-foil strain rosette gauges were installed on each panel, equally divided between the top and bottom surfaces of each test plate. All these rosette gauges are of the 3-gauge 45° rectangular type, having a gauge factor of 2.05 and a resistance of 120 ohms. Since the stress gradient near the edges of the plate is expected to be high, all the rosette gauges installed near the edge of the plate have a gauge length of 1/16 in. For gauges installed near the centre portion of the plate, gauges of gauge length 1/8 in were used. Terminal strips (type T-50) were used to connect the lead wires to the gauge tabs. All the lead wires are sixteen feet long, made of No. 26 stranded copper wire and with vinyl insulation. To provide mechanical protection and waterproofing, all gauges after installation were covered with gauge coat No. 1 (synthetic resin compound), gauge coat No. 2 (nitrite rubber) and gauge coat No. 5 (a two-component rubber epoxy resin)

A skewed frame left over from a previous experiment (7) on skewed plates was re-used as the supporting structure. The

Table 2. Geometries of test plates

	Panel 1	Panel 2	Panel 3	Panel 4
2b, in.	26	26	20	20
2a, in.	52	52	30	30
θ , degree	50	50	30	30
h, in.	0.125	0.0625	0.0625	0.125

Table 3. Location of rosette gauges in inches

Point	Panels 1 and 2		Panels 3 and 4	
	α	β	α	β
A	-11.0	12.6	-5.25	9.6
B	0.0	12.6	0.0	9.6
C	0.0	0.0	0.0	0.0
D	-25.0	12.6	-14.0	9.6
E	-13.0	0.0	-7.5	0.0
F	-25.0	11.5	-14.0	8.5
G	-25.0	-12.6	-14.0	-9.6
H	-24.0	12.6	-13.0	9.6
I	11.0	-12.6	5.25	-9.6

frame was made from four standard steel channels twelve inches deep and weighing 20.7 pounds per foot. To increase the rigidity of the skew frame, 1/4 in. thick vertical stiffeners were welded to the channels and were spaced approximately six inches apart. The plate and channel assembly was then seated on steel angles which were in turn bolted to heavy structural posts.

To assimilate the built-in condition, the aluminum test plate was sandwiched between the flange of the channels and a 1 in. thick cold-rolled steel cover plate, 3 inches wide. The test panels were all cut in such a way so as to provide a clamping edge of three inches while the flange width of the channel was also three inches. Heavy structural erection clamps were used to clamp down the edges of the plate. These clamps are spaced approximately three inches apart centre to centre.

For tests within the elastic limit, the 1/16 in. thick plate models 2 and 3 required relatively low pressures and hence, for these two models, the uniformly distributed load was provided hydrostatically. In this connection, for each plate model, a one-foot tall wooden tank having the same dimensions and skew as the plate model was made and a waterproof sheet of polyethylene material lined the inside of the wooden tank and test plate.

Plate models 1 and 4 are relatively thick and hence to exhibit large deflection behaviour, a high intensity of lateral uniform pressure was required. For each of these plate models,

a 1/4 in. thick plate was used together with leather gaskets to form an airtight connection. Air presser was used to provide the uniformly distributed load, this presser being regulated and recorded by means of two pressure gauges, one placed at the entrance to the test plate, the other in the vicinity of the centre of the plate. Similar experimental set-ups using air as a loading medium were also used for yield tests on plate models 3 and 4.

During the test , the strains were measured by means of three switch and balancing units(model C-10T and C-10 LTC, Budd Instrument Division), a digital strain indicator and an automatic print out unit (photograph A) which can print out strains in micro-inches per inch at all gauge locations for the different intensities of loadings. Dial indicators which permitted the measurement of lateral deflections in one-thousandth of an inch were installed at the bottom of the plate to measure the deflection of the centre and quarter points of each test plate. To clarify the description of the aforementioned apparatus and the general set-up of the experiments, photographs were taken and are included on pages 57 and 59 .

(b) Procedures and Results

For each of the four plate models, the plate was first cut to the required dimensions and skew, leaving three inches all around for clamping purposes. The plate was then cleaned with acetone and the locations for both the top and bottom surface gauges laid with reference to the oblique co-ordinates α and β (Fig. 3). In order to ascertain the magnitude of the membrane stresses, care was taken to ensure that all the top gauges are in proper alignment with the corresponding gauges at the bottom of the test plate. The co-ordinates of the gauge locations are given in Table 3. The installation of these rosette gauges followed a set procedure. The spot where the rosette was to be placed was first wiped clean with acetone and then sanded with a metal conditioner using silicon carbide paper. The exact location of the gauge was then marked and then cleaned in turn first with a metal conditioner and then with a neutralizer. With the rosette and the terminal strip properly lined Eastman 910 cement was applied to cement the assembly onto the plate. The gauge and terminal were then left to dry for approximately one minute during which time pressure was applied to the gauge by means of the thumb. The installation of both ends of the lead wires was next stripped and the bare copper strands twisted. Each lead wire consisted of three copper strands, one strand was soldered to one tab of the terminal strip while the other two strands were twisted together and soldered to the other tab of the terminal. The tabs of the terminal strip

were then connected in turn with the tabs of the gauges by means of thin copper jumper wires. After the lead wires were soldered into position, the gauge is then covered with gauge coats for waterproof and mechanical protection. Photographs B and D show a clear picture of some of the gauges completely installed on the plate models.

The skewed supporting structure was next prepared by first cutting the standard steel channels to the required dimensions and skew as the test plate and then welded and seated onto four heavy structural posts (photograph C). Each test plate with all the rosette gauges installed on both the top and bottom surfaces was then placed on top of the skewed supporting frame with the edges of the plate sandwiched between the flanges of the steel channels and a one inch thick cold rolled steel cover plate. A 1/4 in. thick plate cut into the same skew and dimensions as the plate model was in turn laid on top of the cold-rolled steel cover plate and the entire edge assembly was then clamped by closely spaced special structural clamps; allowance was made here to have clamps placed closer together near the corners of the plate. All four edges of the plate model were made airtight by inserting thin leather gaskets both immediately above and below the edges of the test plate. Compressed air, regulated and measured by means of two Bourdon type gauges was used to provide the uniform lateral pressure (photograph C). For plate models 1 and 4 with plate thickness equal to 1/16 in., a relatively low pressure was required to produce the desired centre deflection and hence for these two

models, hydrostatic pressure was used to provide the uniformly distributed load

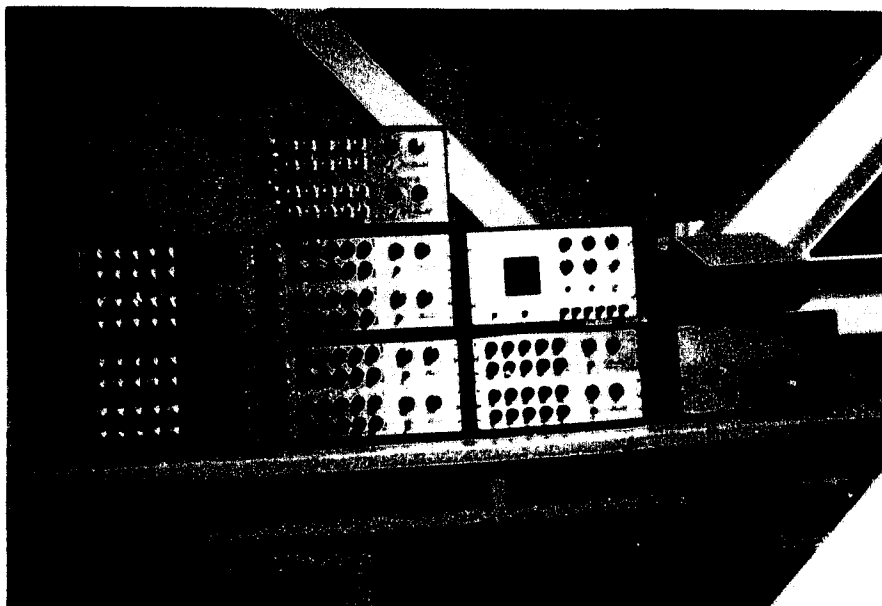
Next, gauge lead wires from the rosette gauges were soldered to ten 5-channel receptacles especially provided for the three switch and balance units. Unit strains for different intensities of loadings were automatically recorded by a precise digital strain indicator and printer.

To allow a direct measurement of the lateral deflections, four dial indicators graduated in one thousandth of an inch were installed for each plate model in locations previously marked on the bottom of the plate. The locations of these dial indicators in terms of the oblique co-ordinate axes α and β are tabulated in Table 4.

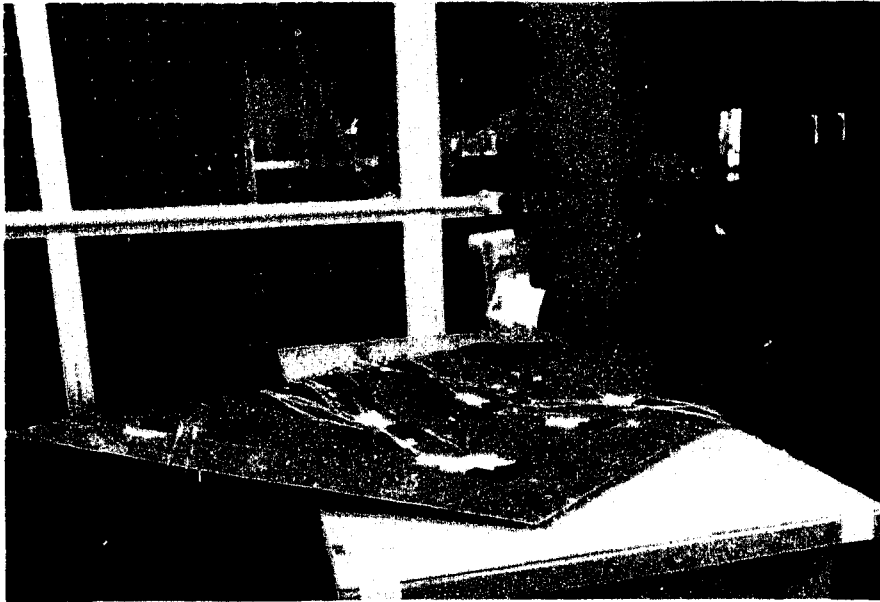
Three independent tests were performed on each of the four plate models loaded within the elastic limit with test data obtained for both loading and unloading. All experimental results for deflection and principal stresses reported herein represent an average value of these tests. To avoid the tedious task of copying the experimental results, strain readings from the digital indicators were photographically reduced and are included in Appendix B. Test data for experimental lateral deflections of each plate model recorded by means of the dial indicators are also reported in the same Appendix.

Table 4. Location of Dial Indicators (in.)

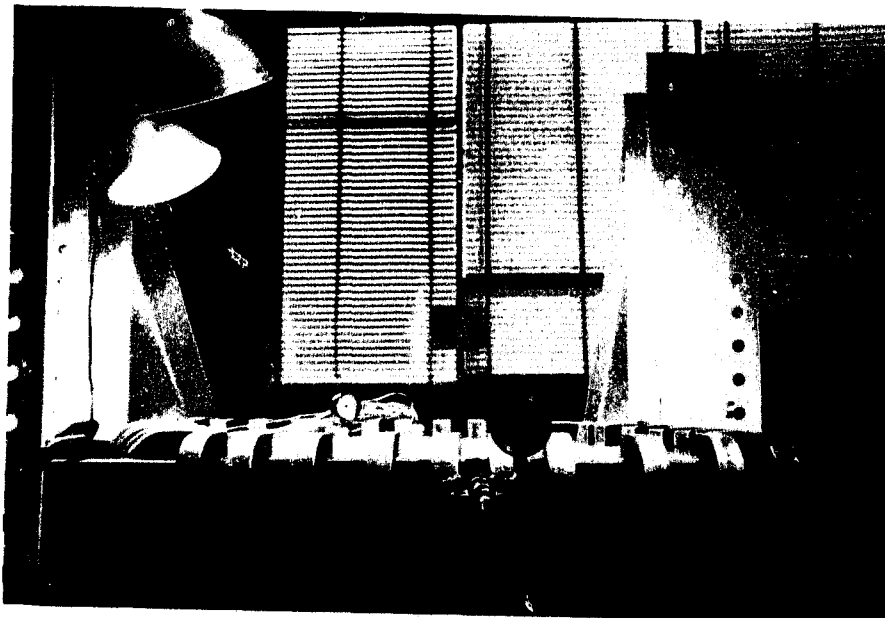
Dial Gauge	Panels 1 and 2		Panels 3 and 4	
	α	β	α	β
1	0.0	0.0	0.0	0.0
2	13.0	-6.5	5.0	-7.5
3	-13.0	6.5	-5.0	7.5
4	13.0	6.5	5.0	7.5



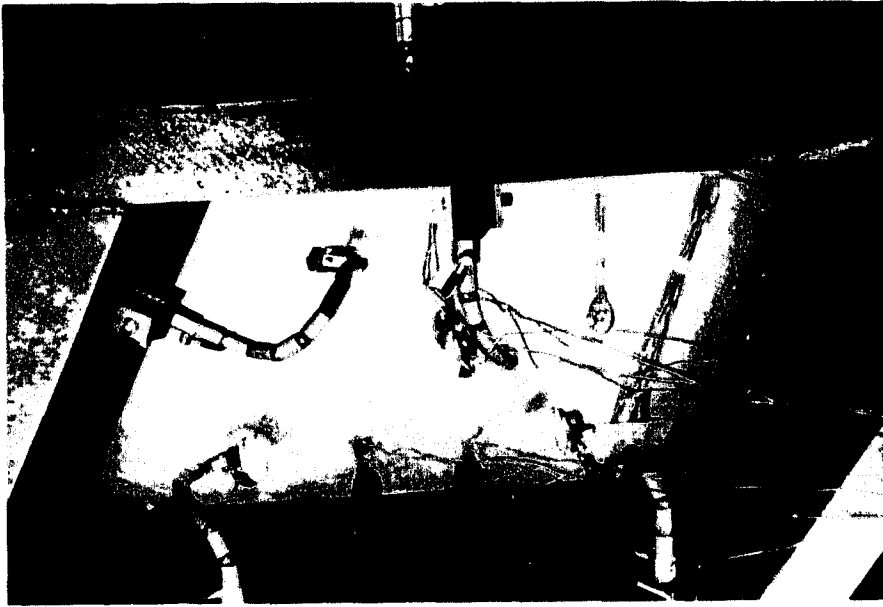
Photograph A. Digital Strain Indicator and Automatic Print-out Device



Photograph B. Test Plate Permanently Deformed after Yield Test.



Photograph C. Photograph showing air-tight Chamber and Supporting Structure.



Photograph D. Bottom View of Test Plate showing Dial Indicators in position

From the values of unit strains e_a , e_b , and e_c obtained from each rosette gauge, the principal stresses can be obtained in the usual manner:

$$\sigma_{\max} = \frac{E}{2} \left(\frac{e_a + e_c}{(1-\nu)} + \frac{1}{1+\nu} \sqrt{2(e_a - e_b)^2 + 2(e_b - e_c)^2} \right) \dots\dots (4-1)$$

$$\sigma_{\min} = \frac{E}{2} \left(\frac{e_a + e_c}{(1-\nu)} - \frac{1}{1+\nu} \sqrt{2(e_a - e_b)^2 + 2(e_b - e_c)^2} \right) \dots\dots (4-2)$$

To facilitate the computation of principal stresses from the unit strains, a small programme in Fortran was written and is included in Appendix A.

(c) Comparison and Discussion of Experimental and Theoretical

Results

Deflections (Lateral displacements)

Experimental and theoretical results for the centre deflections of the four test panels are plotted in Figure 16. From this figure, it is noted that, for low intensities of the uniformly distributed lateral pressure, the agreement between the theoretical and experimental values is excellent. However, as the lateral pressure increases and the centre deflection exceeds the thickness of the test plate, the measured experimental centre deflection starts to deviate from the theoretical values. This deviation may be due to a slight slippage of the test plate taking place at the edges of the test model, with the result that the experimental deflections range from 4-8 % higher than those predicted analytically. Since the ideal theoretical clamping conditions assumed in the analytical solution can never be realized in practice, this discrepancy between the experimental and theoretical values in the lateral displacement of clamped plates will always exist and must be taken into account in the design of such plates.

The variation of the plate thickness does not seem to affect appreciably the deflection pattern of the plate models as deflection measurements from test plates 1 and 2 (or test plates 3 and 4) do not differ significantly.

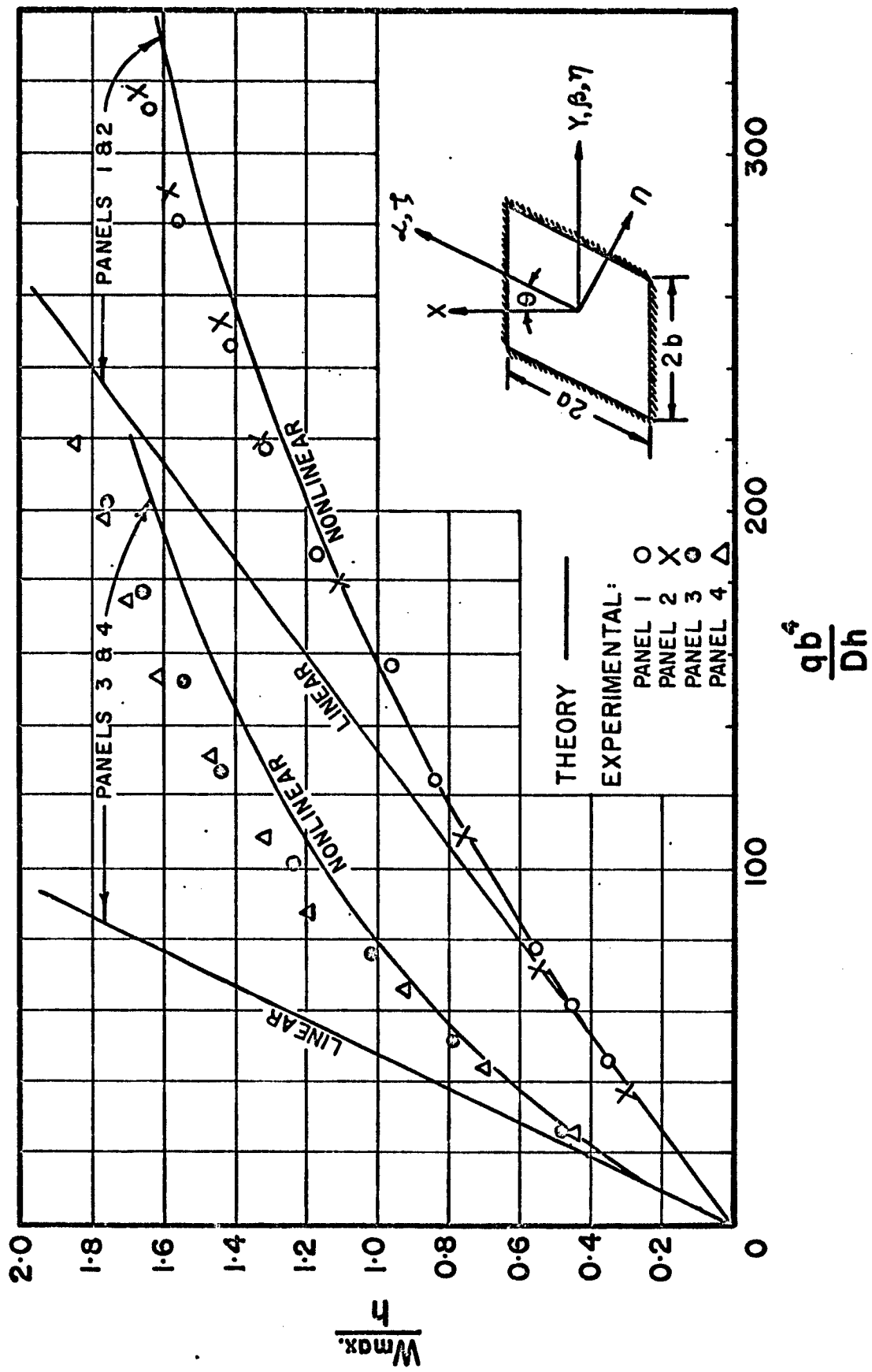


Fig. 16. Comparison of Experimental Centre Deflections with Theory.

Total Principal Stresses

Figures 17 and 18 show comparisons between the theoretical and experimental maximum total principal edge and centre stresses for panels 1 and 2 and 3 and 4, respectively. The agreement is quite good, with the theoretical predictions invariably on the conservative side. Here the degree of skew does affect the closeness of the results since with a high skew of 50° (Figure 17) the results from the 1/16 inch plate is shown to be closer to theory than those from a panel with the same thickness but with a moderate skew of 30° (Figure 18). Analytical results based on the linear theory are shown for comparison.

Typical experimental and the corresponding theoretical variations of the bending and membrane edge and centre stresses with the centre deflection are given in Figure 19. It can be observed that the results compare quite well generally, with the exception of the theoretical and experimental membrane stresses for test plate 3. This discrepancy may be due to a slight relaxation of the test panel along the clamped edges, resulting in an appreciable relief in the membrane stresses. Such discrepancies are of no great significance since, within the range of the centre deflections considered in the analytical solution ($w/h \leq 2$), the membrane stress accounted for a relatively small percentage of the total stress; hence, despite the apparent discrepancy between the theoretical and experimental membrane stresses, the agreement between the total stresses remains close (Figures 17 and 18).

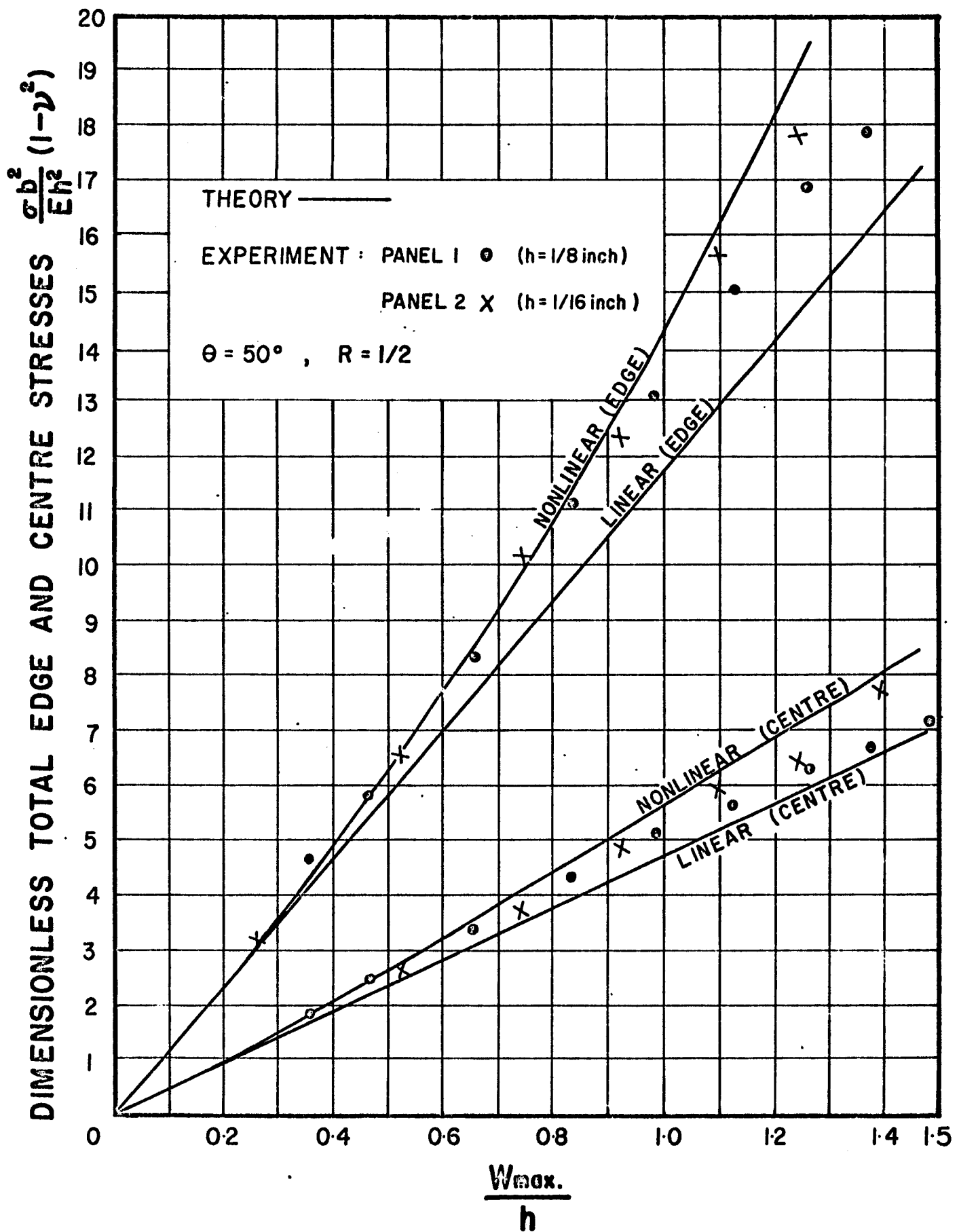


Fig. 17. Comparison of Experimental Edge and Centre Stresses with Theory for Test Plates 1 and 2

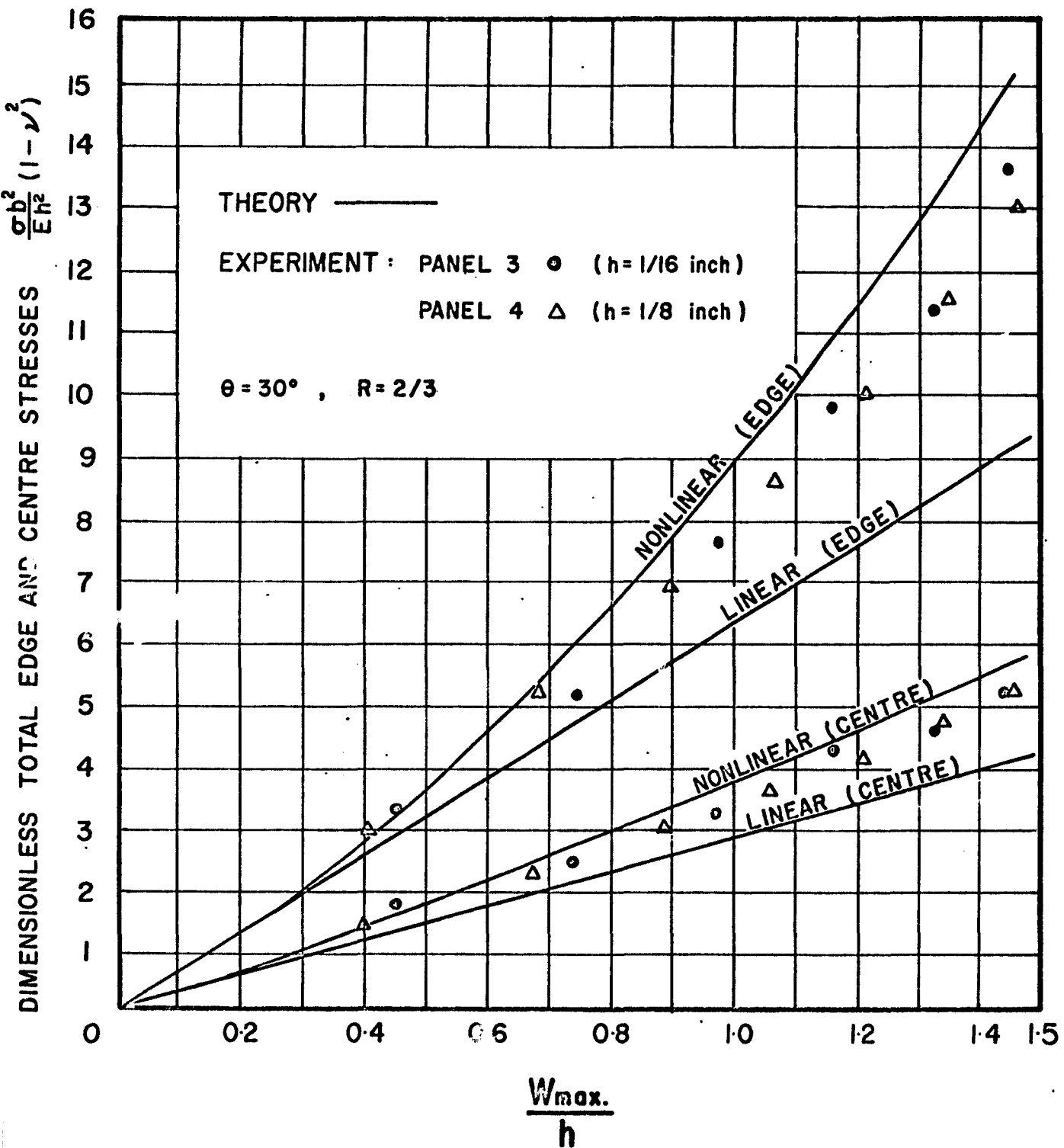


Fig. 18. Comparison of Experimental Edge and Centre Stresses with Theory for Test Plates 3 and 4.

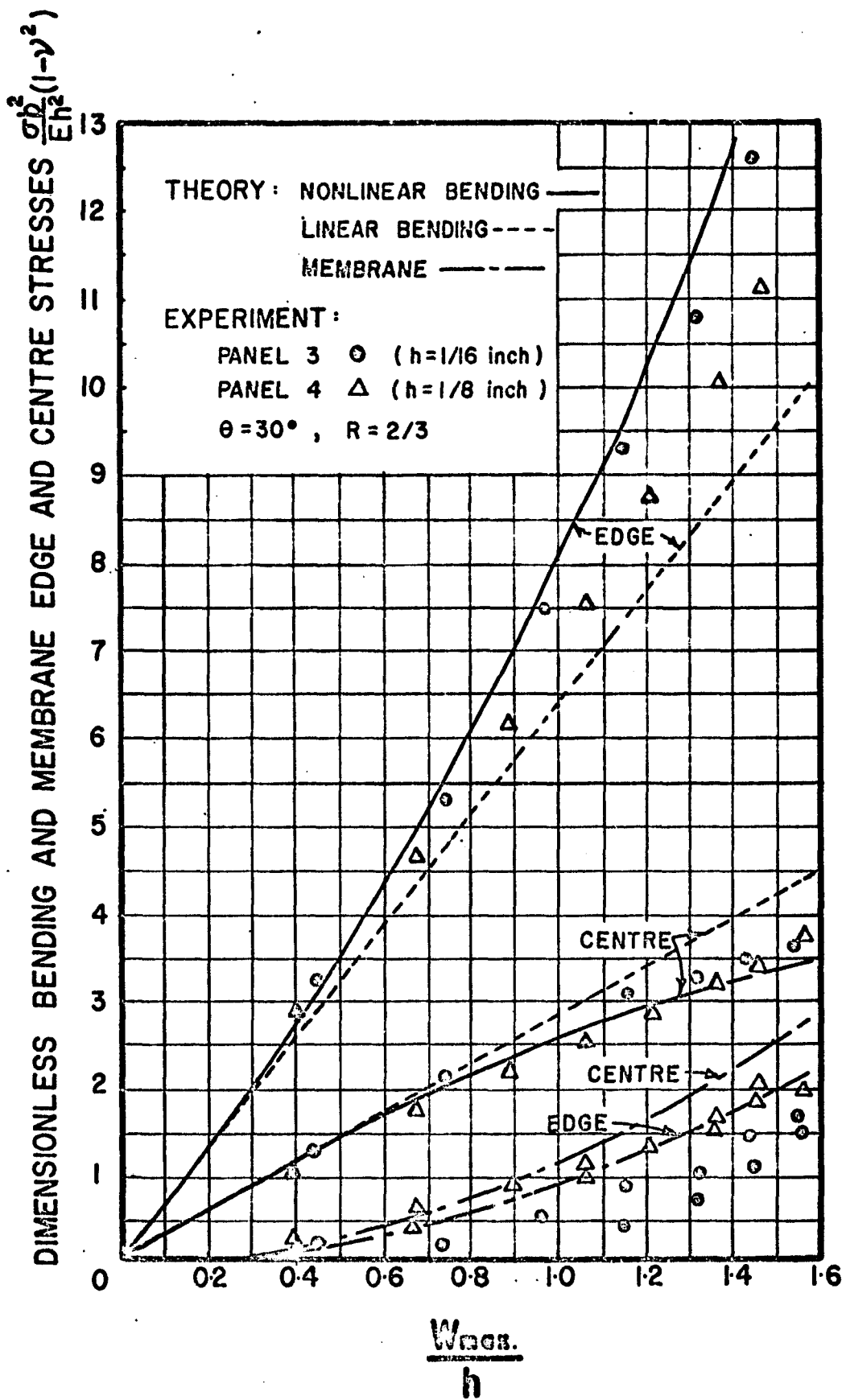


Fig. 19. Experimental and Theoretical Results for Bending and Membrane Stresses.

To exhibit the relative magnitude of the maximum total principal stresses at critical locations on the test panels, such stresses are shown plotted versus the applied pressure in Figures 20-23. Examination of these figures shows that for low intensities of pressure, the principal stress increases linearly with the applied pressure, producing a centre deflection not exceeding half the plate thickness and with insignificant membrane forces. However, with higher intensities of load (producing large deflections), the membrane forces become more pronounced, effecting a decrease in the slope of the stress-pressure curves shown. The total principal stresses at different locations will now be discussed:

As predicted by the analytical solution the experimental maximum total stress occurs along the longer edge of the plate and is displaced towards the obtuse corners, point A. [Compare with theoretical investigations of clamped rectangular plates (2) (3) where such stress occurs at the middle of the longer edge]. The total stress at the middle of the longer edge, point B, is about 85% of that at point A for test panels 1 and 2 with a skew of 50° . This percentage increases to approximately 90% for test panels 3 and 4 where the skew is 30° . Variations in the thickness of the plates do not seem to affect this percentage.

The variations of the experimental total stress at the panel centre (point C) with load are shown in Figures 20-23. It can be observed that for the entire range of loading considered, the total stresses at the centre of the test panels are approximately 35 to

45% of the corresponding maximum total edge stresses. This observation seems to indicate that the ratio of total stress at centre to maximum total edge stress is sensibly unaffected by changes in skew, aspect ratio, or plate thickness.

Results from the experimental study have revealed, as expected, severe concentration of stress in the vicinity of the obtuse corners. [Theoretically, stresses at the corners are zero, due to the nature of the mathematical model of the problem.] Figures 20-23 show that for low intensities of loading the total stress at the obtuse corners is of the same order of magnitude as the stress at centre of panel. With increased loading, the magnitude of the total stress at the obtuse corners can exceed that at the centre by approximately 10% for plates 1 and 4 (with 1/8 inch thickness) and by as much as 20% for plates 2 and 3 (with 1/16 inch thickness). Therefore, it may be surmised that the stress concentration at the obtuse corners, relative to the stress at the centre of the plate, is more affected by the plate thickness than by changes in skew or aspect ratio.

In contrast to the high level of stress in the vicinity of the obtuse corners, only nominal stresses were recorded in the vicinity of the acute corners. The experimental results obtained indicate that the total stress at such corners remains insignificant until parts of the edges yield due to excessive lateral loading. This will be expounded on in the next section.

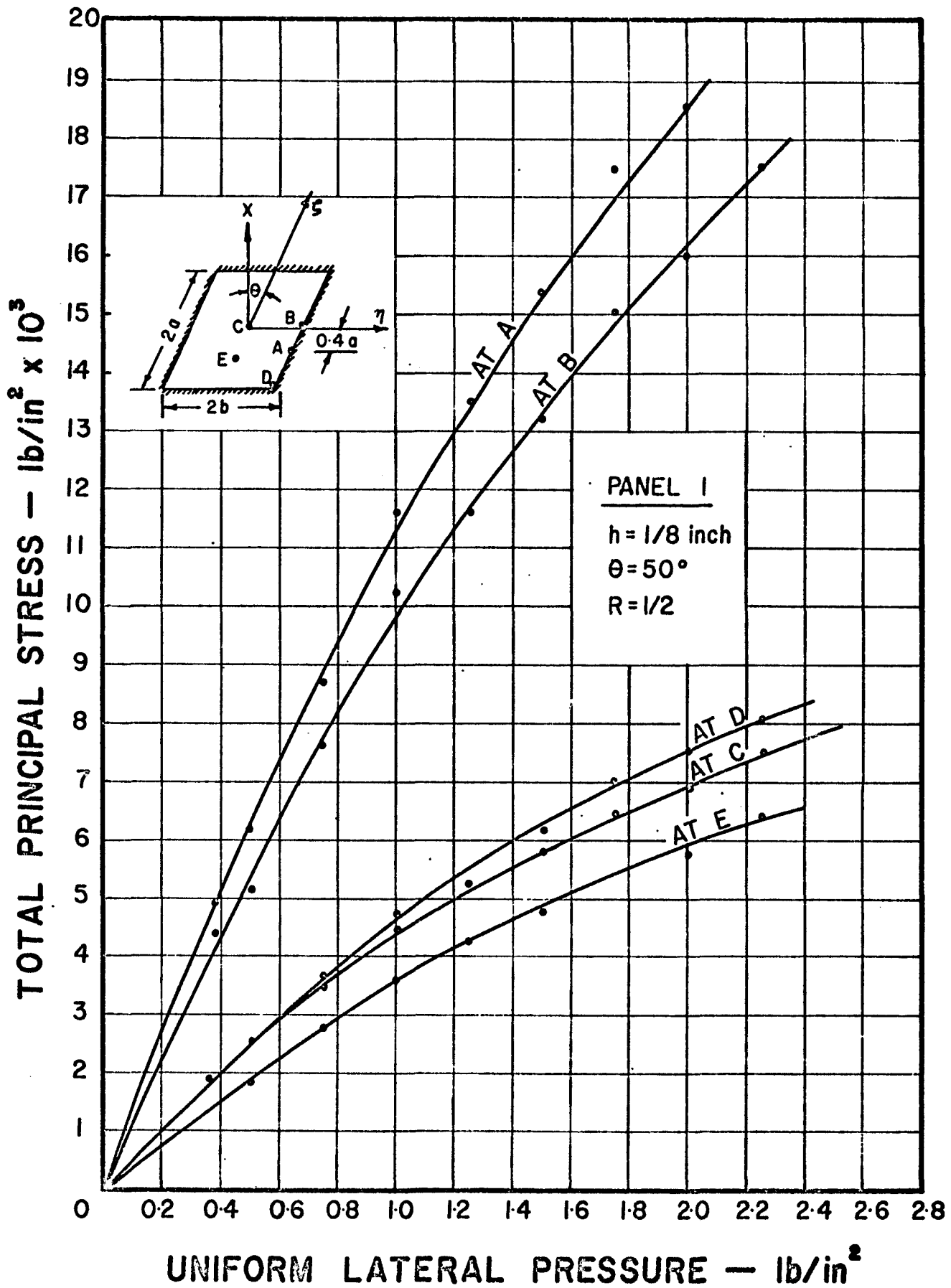


Fig. 20. Experimental Stresses at various Locations on Test Plate 1

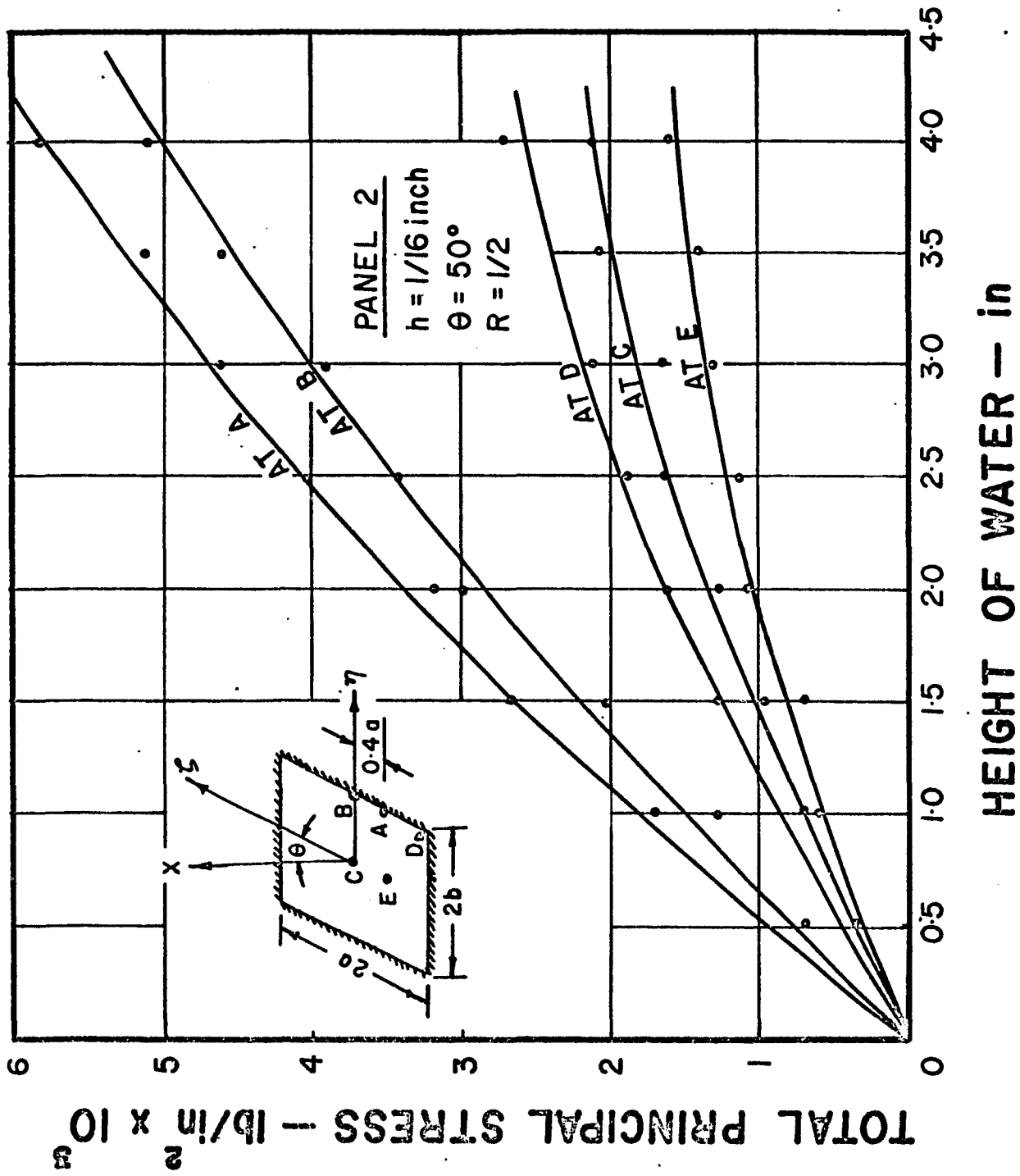


Fig. 21. Experimental Stresses at Various Locations on Test Plate 2

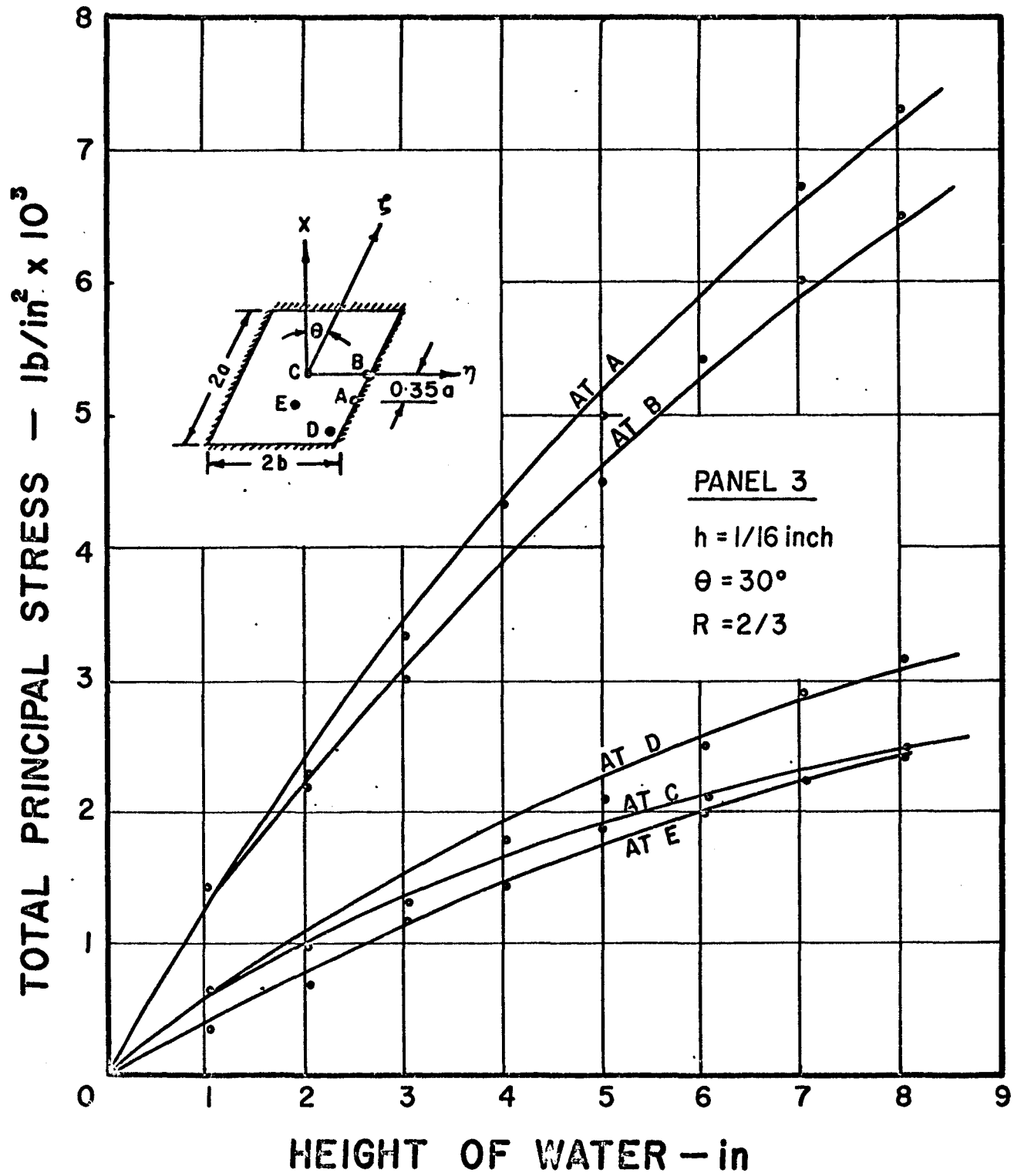


Fig. 22. Experimental Stresses at Various Locations on Test Plate 3.

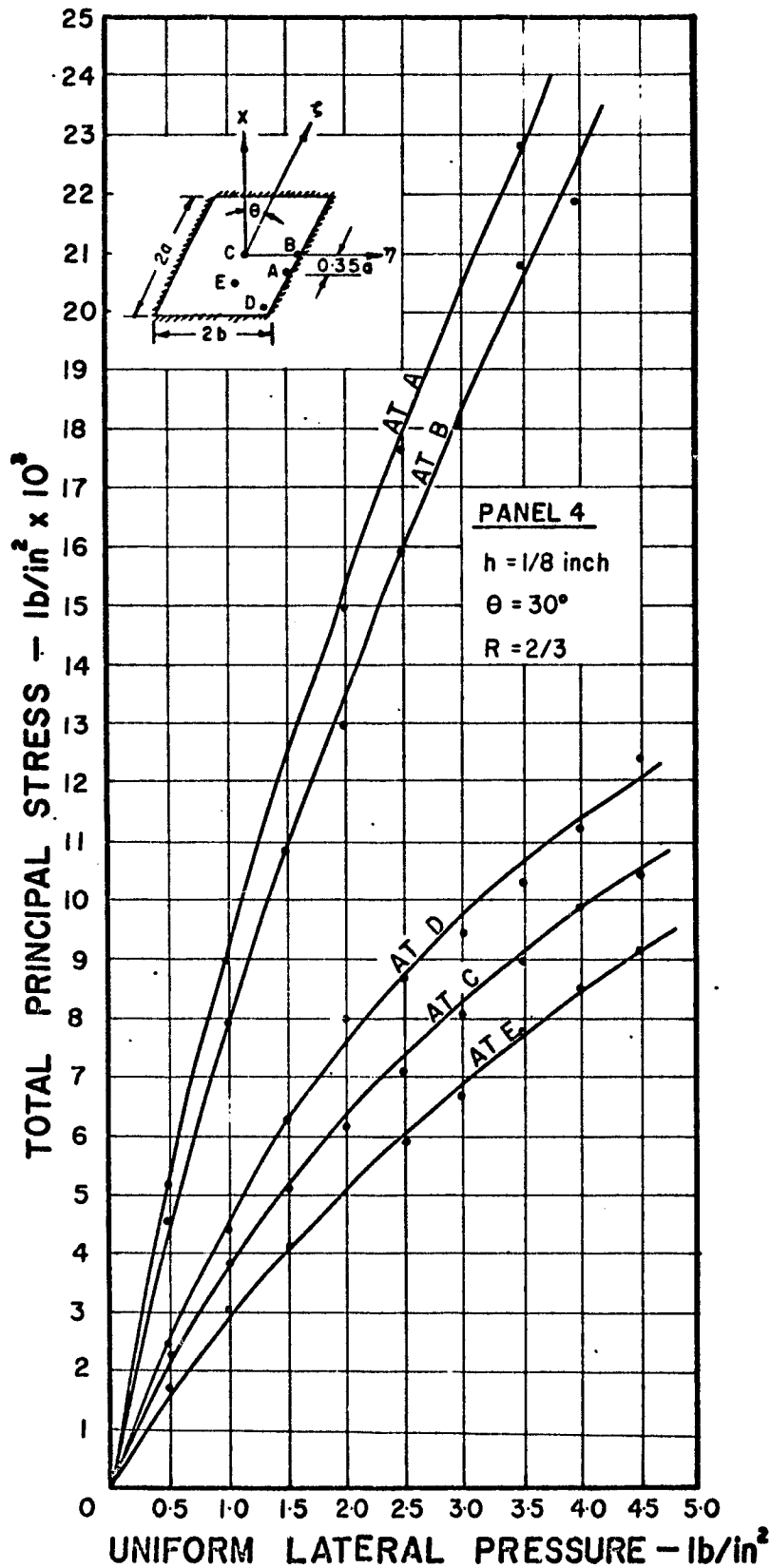


Fig. 23. Experimental Stresses at Various Locations on Test Plate 4.

Yield Tests:

In order to study the behaviour of clamped skewed plates beyond the validity of the Von Karman equations (9), where the centre deflection should not exceed 2 to 2.5 times the panel thickness, plates 3 and 4 were loaded until plastic regions were formed. The results of such tests are shown in Figures 24-26.

The variation of the total principal strain at the plate centre with applied pressure is shown in Figure 24. It is interesting to observe that when these plates were loaded excessively the strain in the middle plan of the plate increased to such a level that it nullified the compressive strain at the top of the panel at centre. This is not surprising since it was shown in Figure 15 that the magnitude of the membrane stress at centre increases rapidly with increase in centre deflection.

Figure 25 exhibits the behaviour and the distribution of principal strain in the vicinity of the obtuse corner when the panels are loaded beyond the elastic region. A sudden reversal in strain at these corners is noted when a certain critical load on the plate is reached. Such instability is preceded by progressive yielding of the panel edges towards the obtuse corners. (The variation of the maximum principal strain along the longer edge with lateral load is given in Figure 26) Ideally, one would have expected the curves from the top and bottom gauges to cross the horizontal axis at the same load. However, this was not the case and the discrepancy seems to be more pronounced for

plate 4 (1/8 inch thick) than plate 3 (1/16 inch thick). This can be attributed mainly to experimental errors such as those incurred in gauge alignment, support conditions, etc. It may be mentioned that results from a bottom gauge located less than 1 inch away, at point F, do indicate the expected reversal in strain.

Variation of the total principal strain at the maximum point along the longer edges of plates 3 and 4 with load are shown in Figure 12. It can be observed that after the yield stress of the material is reached the total strain decreases with further increase in strain in the vicinity of the acute corners after the edges have yeilded; reversal of strain is also possible at such corners as evidenced from the results obtained, although the observed instability here is not as pronounced as was found for the obtuse corners.

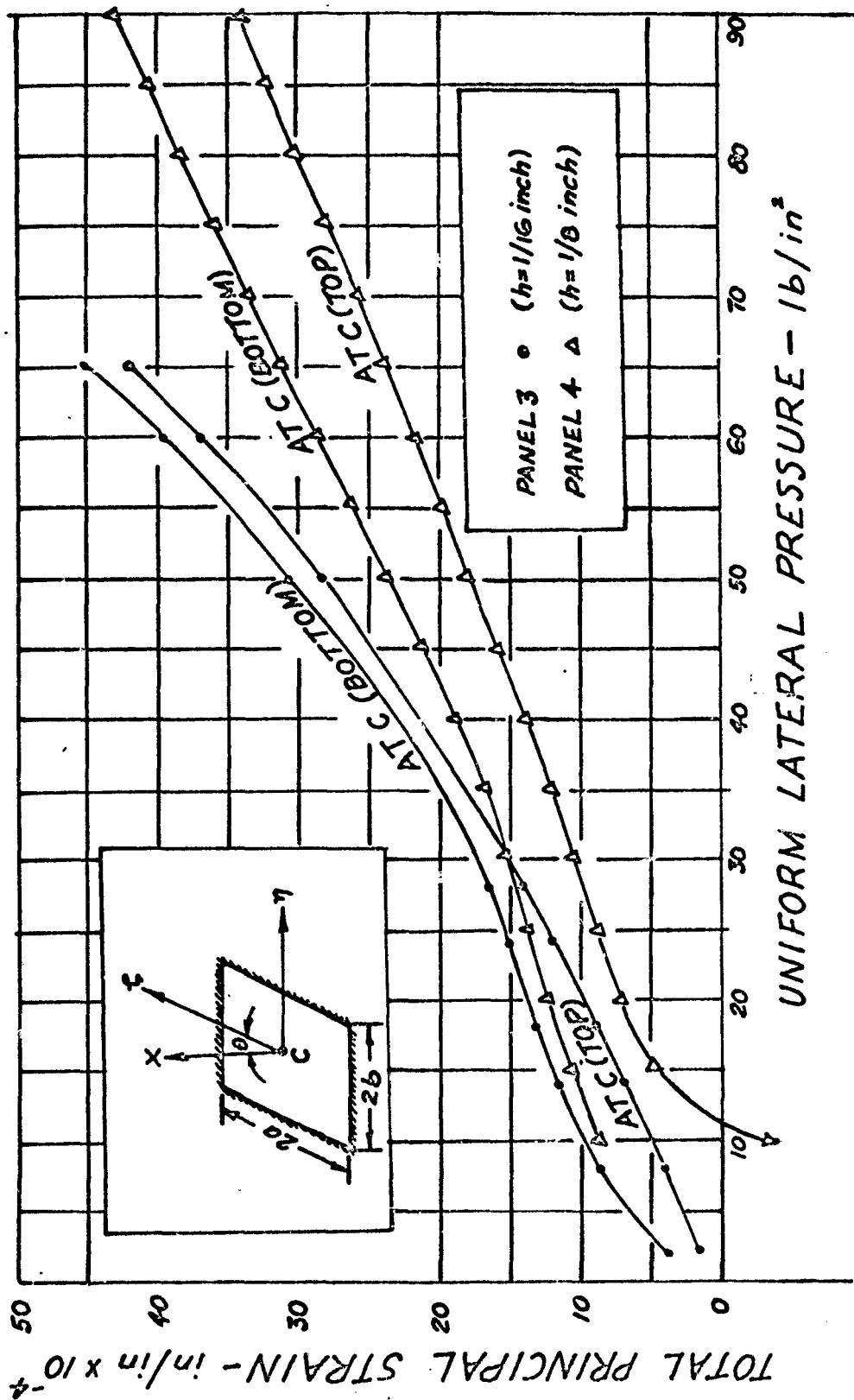


Fig. 24. Centre Stresses at Large Lateral Pressures

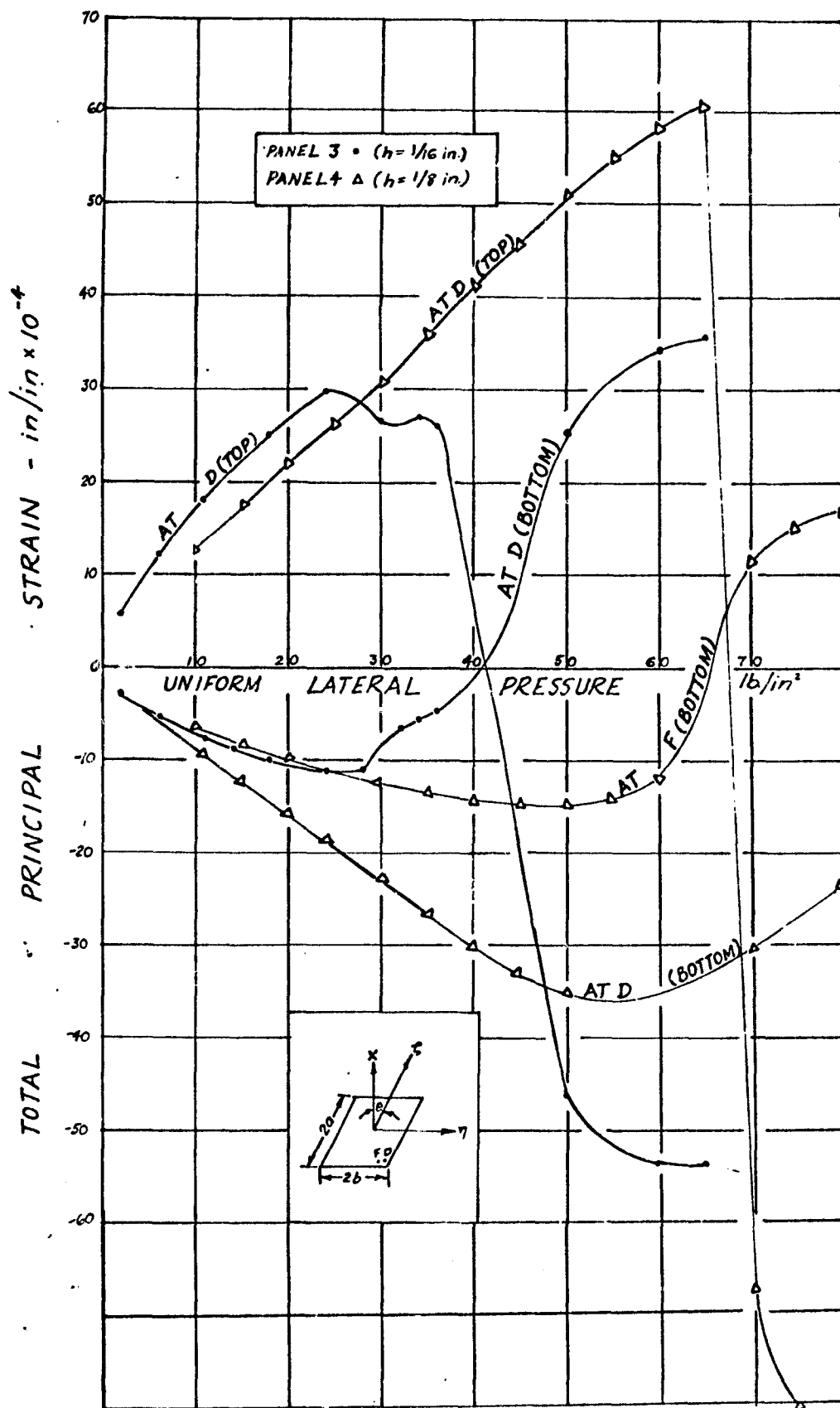


Fig. 25. Obtuse Corner Stresses at Large Lateral Pressures

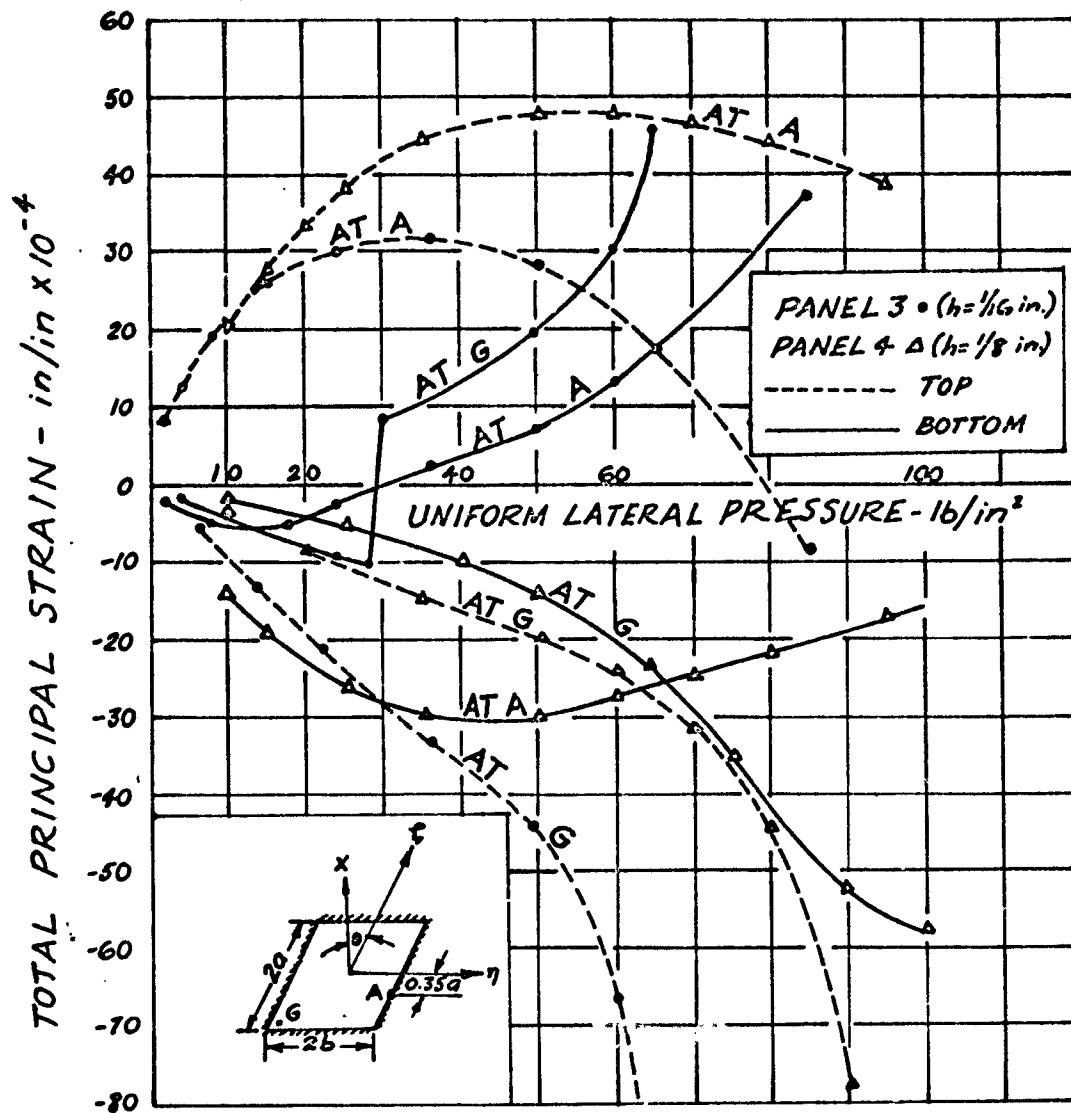


Fig. 26. Acute Corner and Maximum Edge Stresses at Large Lateral Pressures

CHAPTER V

CONCLUSIONS

As a result of this theoretical and experimental investigation on the small and large deflection behaviour of clamped skewed plates, the following conclusions may be drawn:

1. For the limiting case where the skew angle is reduced to zero, the perturbation method yields results which are in good agreement with those obtained for rectangular plates, analysed by more laborious methods.
2. The small deflection results for clamped skewed plates are in close agreement with those obtained by experiments and by other analytical methods.
3. For a given aspect ratio and a given uniformly distributed load, the maximum deflection at the centre of skewed plates decreases with increase in skew.
4. The effect of skew on the centre deflection decreases with decreasing aspect ratio R , where $R < 1$.
5. The ratios w_{max}/h , at which results from the linear and nonlinear theories begin to deviate significantly from each other are influenced by the aspect ratio, R ; the ratio w_{max}/h decreasing with increasing R . Thus the deflection value, at which the influence of the in-plane forces begins to be effective, can be assessed.

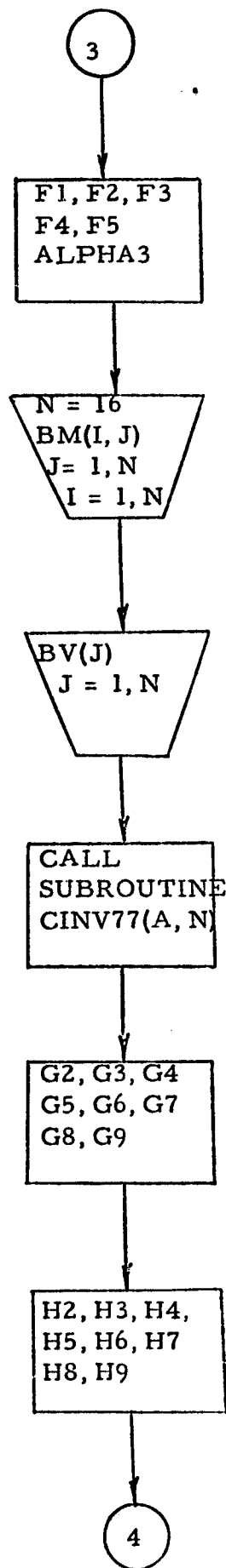
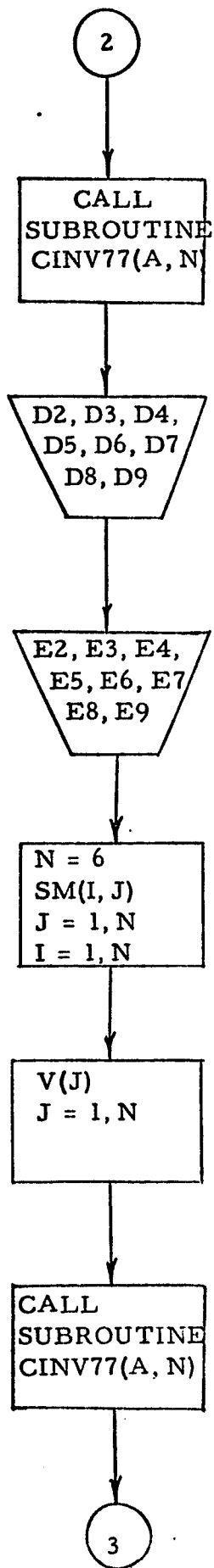
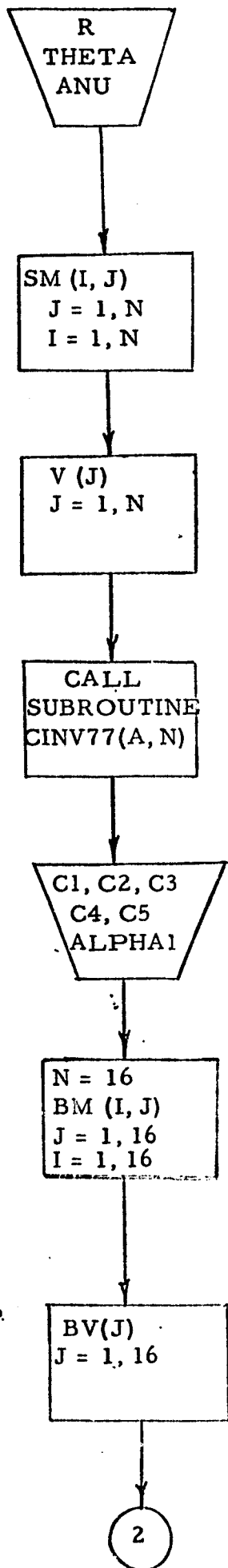
6. Analytical nonlinear (large deflection) results have been substantiated by model tests. Notwithstanding the experimental errors inherent in such tests, the agreement between theory and experiment is found to be quite close.
7. Nonlinear deflection of clamped skewed plates tend to become increasingly linear with increase in skew.
8. The maximum resultant stress occurs along the longer edge of the plate and is displaced towards the obtuse corners. Such stress increases with skew for any specified aspect ratio and centre deflection.
9. Invariably membrane stresses are relatively insignificant in magnitude when compared to the maximum resultant edge stresses.
10. Experimental results obtained for very large loads, producing plastic regions, and outside the range of applicability of the analytical solution of the Von Karman equations have indicated that:

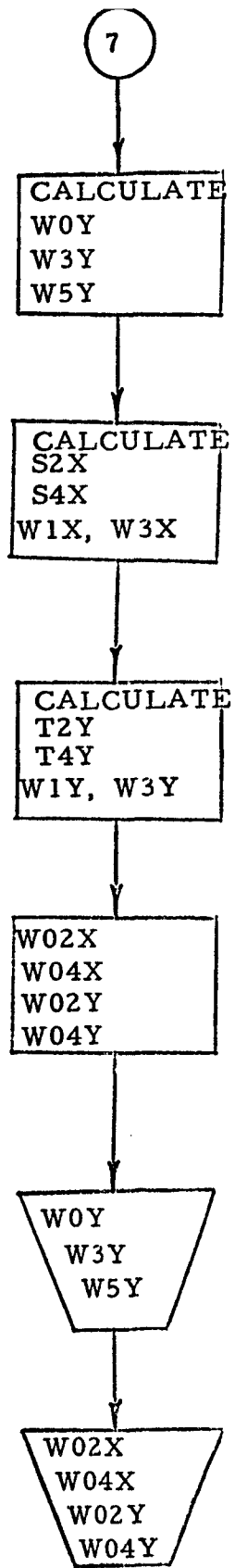
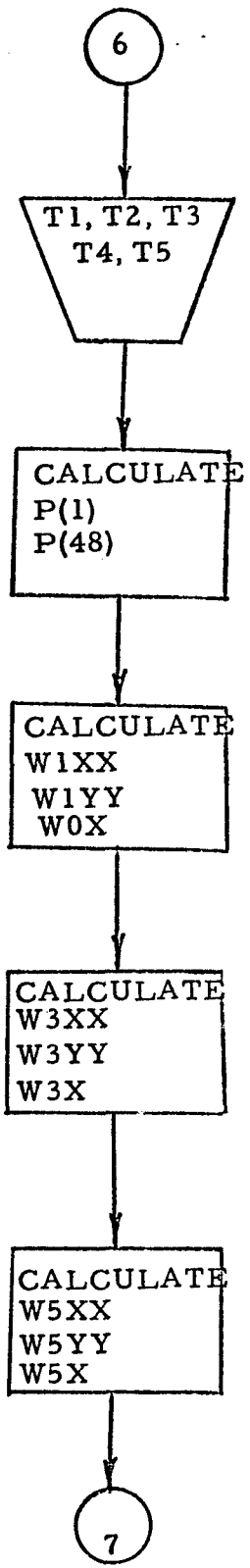
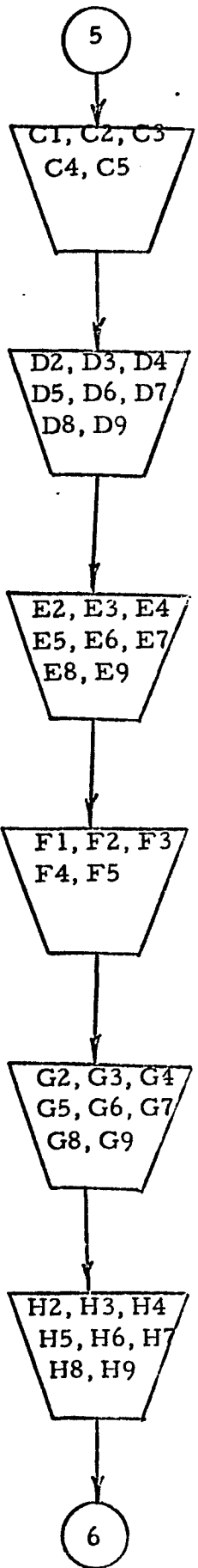
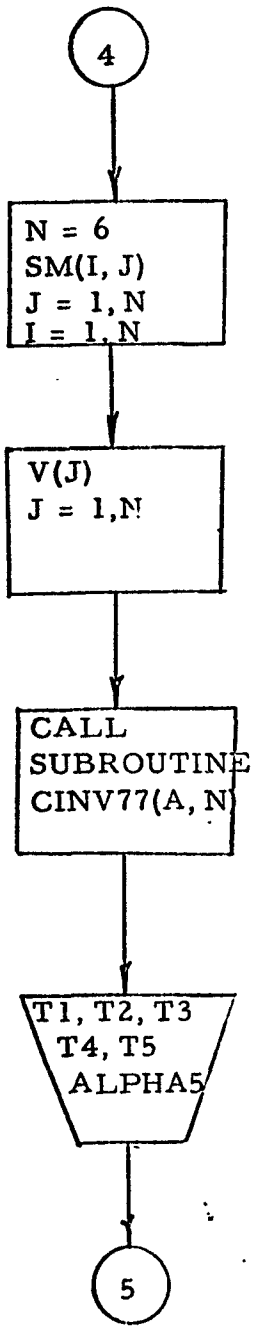
(a) The obtuse corners of clamped skewed plates are not only regions of severe stress concentrations, but also of instability, giving rise to sudden reversal of stresses.

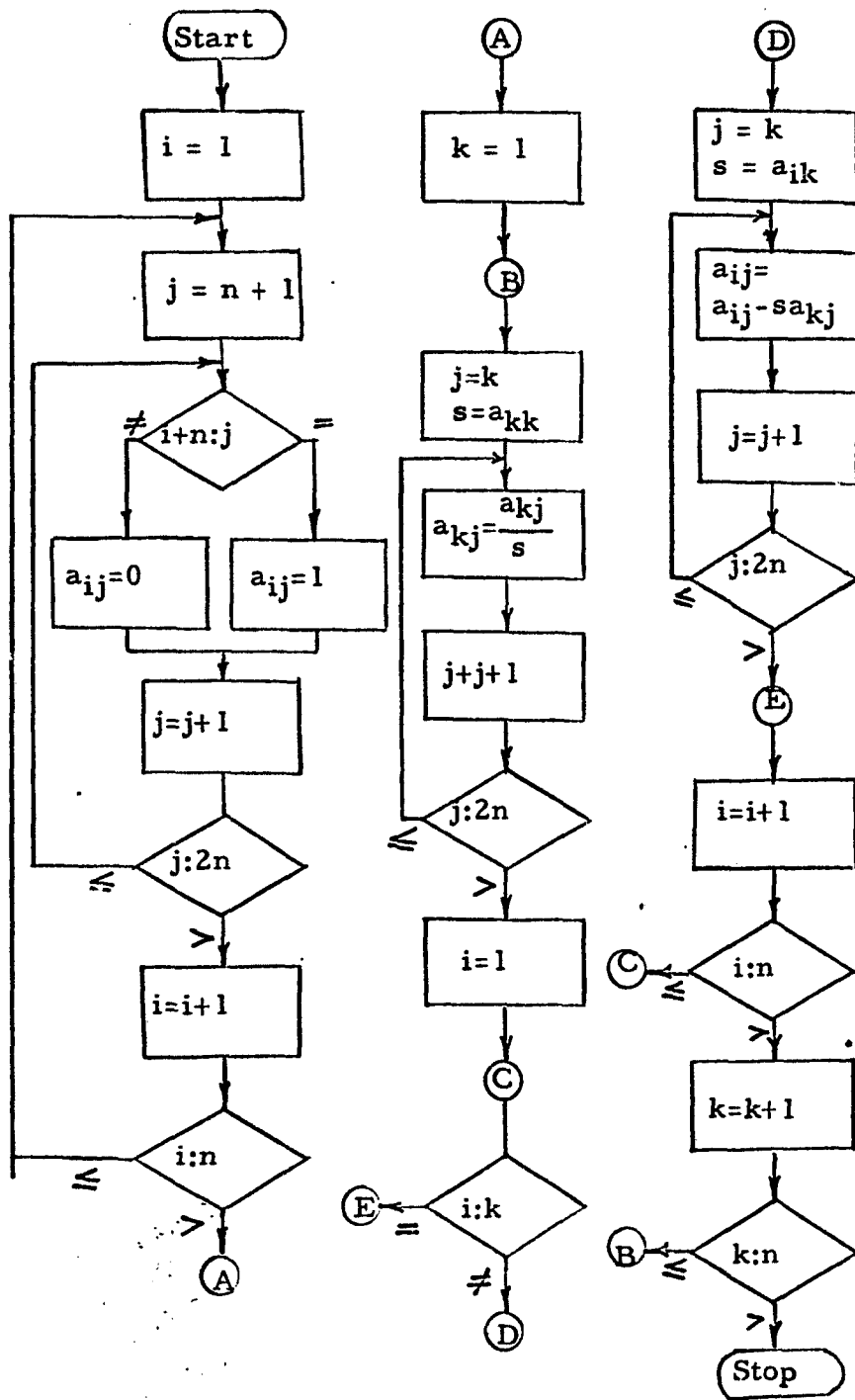
(b) The stress in the vicinity of the acute corners are relatively insignificant; however, when the edges have yielded, the stresses in such corners increase sharply with possible stress reversal at very large loads.

APPENDIX A

FORTRAN PROGRAMS FOR THEORETICAL AND EXPERIMENTAL
ANALYSIS







CALL LINK(RC,SUR2)
E

0.0000 00. 0.

LPISRRCSA

```

1=10
D. 01 1=1,10
D. 01 1=1,10
D1 01(1,3)=-.
D. 01(1,1)=-1.*R2*R*C-2.*A44
D. 01(1,2)=1.*R
D. 01(1,3)=12.*R2*R*C
D. 01(1,4)=1.*A44
D. 01(1,5)=-2.*R
D. 01(1,6)=1.*A11
D. 01(1,10)=-2.*R10
D. 01(1,13)=-2.*A11
D. 01(1,14)=2.*A10
D. 01(2,1)=1.*R1
D. 01(2,2)=-4.*R2*R*C-6.*A44
D. 01(2,4)=1.*A44
D. 01(2,5)=-2.*R
D. 01(2,6)=4.*R2*R*C
D. 01(2,8)=-2.*A10
D. 01(2,10)=6.*A11
D. 01(2,12)=-4.*A11
D. 01(2,13)=2.*A10
D. 01(3,1)=1.*A44
D. 01(3,5)=-40.*R2*R*C-2.*A44
D. 01(3,6)=-2.*A44
D. 01(3,8)=4.*R
D. 01(3,10)=2.*A44
D. 01(3,11)=-2.*A11
D. 01(3,12)=1.*A11
D. 01(3,13)=2.*A11
D. 01(3,14)=-4.*A10
D. 01(3,15)=-2.*A11
D. 01(4,1)=6.*R2*R*C
D. 01(4,5)=-4.*R2*R*C-20.*A44
D. 01(4,6)=6.*R
D. 01(4,8)=-4.*R2*R*C
D. 01(4,10)=6.*R2*R*C
D. 01(4,11)=2.*A11
D. 01(4,12)=-4.*A10
D. 01(4,13)=12.*R2*R*C
D. 01(4,14)=-1.*A10
D. 01(4,15)=-12.*R2*R*C
D. 01(4,16)=1.*R
D. 01(4,17)=-12.*R2*R*C-12.*A44
D. 01(4,18)=6.*R
D. 01(4,19)=12.*R2*R*C
D. 01(4,20)=-5.*A10
D. 01(5,1)=6.*A10

```


END

LDISKKUSAN

N=15

```

D1(10,12)=8.*A14
D1(10,13)=-4.*A7*R2*S
D1(10,14)=1.*A7*R2*R
D1(11,1)=-1.*A6*R*C*S
D1(11,2)=2.*A6*R*C*S
D1(11,3)=2.*A6*R2*C
D1(11,4)=-4.*A6*R2*C
D1(11,7)=-2.*A6*R*C*S
D1(11,8)=2.*A14
D1(11,11)=-2.*A14-20.*A7*R2*R
D1(11,13)=-2.*A14
D1(11,14)=1.*A7*R2*S
D1(11,15)=2.*A14
D1(12,4)=20.*A6*R*C*S
D1(12,5)=-4.*A6*R2*C
D1(12,11)=1.*A7*R2*R
D1(12,12)=-2.*A7*R2*R-20.*A14
D1(12,13)=-1.*A7*R2*S
D1(12,14)=-2.*A7*R2*R
D1(12,15)=2.*A7*R2*R
D1(13,11)=6.*A6*R2*C
D1(13,12)=-1.*A6*R2*C
D1(13,13)=-12.*A6*R*C*S
D1(13,14)=-1.*A6*R2*C
D1(13,15)=1.*A6*R2*C
D1(13,17)=0.*A7*R2*R
D1(13,18)=-12.*A7*R2*S
D1(13,19)=-0.*A7*R2*R
D1(13,20)=12.*A7*R2*S
D1(13,21)=-0.*A7*R2*R-12.*A14
D1(13,22)=12.*A7*R2*S
D1(13,23)=1.*A7*R2*R
D1(13,24)=-12.*A7*R2*S
D1(13,25)=1.*A6*R2*C
D1(13,26)=-6.*A6*R*C*S
D1(13,27)=-6.*A6*R2*C
D1(13,28)=6.*A6*R*C*S
D1(13,29)=6.*A6*R2*C
D1(13,30)=-0.*A6*R2*C
D1(13,31)=-0.*A6*R*C*S
D1(13,32)=-12.*A7*R2*S
D1(13,33)=1.*A14
D1(13,34)=12.*A7*R2*S
D1(13,35)=-1.*A14
D1(13,36)=1.*A7*R2*S
D1(13,37)=-1.*A14-12.*A7*R2*R
D1(13,38)=-1.*A7*R2*S
D1(13,39)=1.*A14
D1(13,40)=-12.*A6*R*C*S

```

```

A(11,1)=1.0*#A7*#R2*#S
A(12,1)=1.0*#A7*#R2*#S
A(13,1)=-1.0*#A7*#R2*#S
A(14,1)=1.0*#A7*#R2*#S
A(15,1)=1.0*#A7*#R2*#S
A(16,1)=1.0*#A7*#R2*#S
A(17,1)=1.0*#A7*#R2*#S
A(18,1)=1.0*#A7*#R2*#S
A(19,1)=1.0*#A7*#R2*#S
A(20,1)=1.0*#A7*#R2*#S
A(21,1)=1.0*#A7*#R2*#S
A(22,1)=1.0*#A7*#R2*#S
A(23,1)=1.0*#A7*#R2*#S
A(24,1)=1.0*#A7*#R2*#S
A(25,1)=1.0*#A7*#R2*#S
A(26,1)=1.0*#A7*#R2*#S
A(27,1)=1.0*#A7*#R2*#S
A(28,1)=1.0*#A7*#R2*#S
A(29,1)=1.0*#A7*#R2*#S
A(30,1)=1.0*#A7*#R2*#S
A(31,1)=1.0*#A7*#R2*#S
A(32,1)=1.0*#A7*#R2*#S
A(33,1)=1.0*#A7*#R2*#S
A(34,1)=1.0*#A7*#R2*#S
A(35,1)=1.0*#A7*#R2*#S
A(36,1)=1.0*#A7*#R2*#S
A(37,1)=1.0*#A7*#R2*#S
A(38,1)=1.0*#A7*#R2*#S
A(39,1)=1.0*#A7*#R2*#S
A(40,1)=1.0*#A7*#R2*#S
CALL L11A(K0SA34)
END

```

LISTING

```

A(1)=-1.0*#A2*#A16*#A16+2.0*#R2*#S*#A16+4.0*#A2*#S*#A16+A12+A13+A14+A15
+2.0*#A17)
A(2)=-1.0*#A2*#R*(-A16)-2.0*#R2*#S*(A16*A17)-4.0*#A2*#S+A12*(-A17)+A13
+1*(-A17)-0.0*#S*(A17*A17))
A(3)=-1.0*#A2*#R*(A16*A24+A16*A25)-2.0*#R2*#S*(A16*A25-A25)-4.0*#A2*#S*
+1(A16*A26-A24)+A12*(-A25-A26)+A13*(A16*A17+A17*(A24)-2.0*#S*(-A16+A27
+2*A25))
A(4)=-1.0*#A2*#R*(A16*A26-A16)-2.0*#R2*#S*(A16*A31+A17*A16)-4.0*#A2*#S*
+1(-A26-A27)+A12*(-A31+A17*A30)+A13*(-A21+A17*A25)-2.0*#S*(A21+A17
+2*A17*A31))
A(5)=-1.0*#A2*#R*(A16*A18-A19+A16*A18)-2.0*#R2*#S*(A16*A20+A17*A18-
+1.16)-4.0*#A2*#S*(A16*A30-A33-A18)+A12*(-A20+A17*A23-A30)+A13*(A16*
+2*A21-A32+A17*A13)-2.0*#S*(-A21+A17*A22+A17*A20))
CALL L11A(K0SA3A)

```

LISTING

```

A(6)=-1.0*#A2*#R*(A16*A26-A25+A19*A16)-2.0*#R2*#S*(A16*A16+A17*A17-+19
+2)-4.0*#A2*#S*(A16*A33-A26-A26)+A12*(-A16+A17*A17-A33)+A13*(A16*(A22-
+2.16+A17*A17)-2.0*#S*(-A22+A17*A16+A17*A16))
A(7)=-1.0*#A2*#R*(2.0*A16*A39+A23*A16+A19*(A26-+40+A24*A17+A16*A39+A13
+1)-0.0*#S*(A16*A16+A23*A26+A16*(A19+A17*(A16+A18*A16)-0.0*#S*(A16
+2.0*#A17*(A16+A24*A26-4.0*#A39*(A17*(A26+A26*A16)-2.0*#A17*(A16
+2*(-0.0*#A17*(A16+A24*A26)+A33*A16)+4.0*#A39*(A17*(A26-+1.16*A29)+A17
+4.0*#A17*(A16+A24*A26)+A33*A16)+A16*(A26*(A22+A17*(A16)+2.0*#A39*(A17))
A(8)=-1.0*#A2*#R*(-0.0*#S*(-0.0*#A27+A25*A21-2.0*A16*A17*A16+A22+A20-+1
+2.0*#A17*(A17))
A(9)=-1.0*#A2*#R*(0.0*#A27*(A16+A17*(A26+A19*(A16+A16*(A27)+A16*(A16-+1
+1.16)-2.0*#A27*(2.0*A16*A27+A16*(A16+A19*(A20-A27*(A16+A17*(A16+A17
+2.0*#A17*(A16+A24*A26)+4.0*#A17*(A27+A16*(A16+A24*A26)-0.0*#A17*(
+2.0*#A17*(A16+A24*A26)+A33*A16)+A25*(A20-4.0*#A27*(A26+A31+1.0*#A29*(A17))
+4.0*#A17*(A16+A24*A26)+A33*A16)+A16*(A27*(A16)+0.0*#A29*(A17))
A(10)=-1.0*#A2*#R*(-2.0*#S*(6.0*#A27*(A17+A31*A16)-4.0*#A32+A20*A22+A16

```



```

      *S*(1-1.)*4)-1.)*C**S**S*(D2*A1+A17*(-3.*D2+B.*D4))-2.*D2*(A17+
      2*(A17*A16*(-D3+D7))+2.*R2*C**S**S*(D2*A26+A3-B7)-1.)*C**S**S*(D2*A17+
      2*(A17*(-D3+D7)))
      U(1)=C(1)+.5*(R2*R2*(A16*A16+A16)-2.*R2**S**S*(-A17+A17)+2.*R2**S**
      S*(A17*A16*A16)-1.*R2**S**S*(-A16*A16)+4.*R2**S**S*(A16)-2.*R2**S**S*(
      2*(-A17*A16)+R2**S**S*(A16)-2.*R2**S**S*(-1.))+S**4*(A17))
      U(2)=U(1)+7.5*(R2*C**C*(B3*A27+A16*(-D3+D7))-2.*R2**S**S*(A16*(A17+
      1+D2-A7)+R2*C**S**S*(D2*A16+A17*(-D3+D7))+0.5*C**C*(A16)-1.)*C**C*(
      2*(-1.))+R2**S**S**S*(A17))
      U(3)=U(1)+S**C**C*(B3*A16+A17*(-D3+D7))+0.5*C**C*(A17)+A16*(D2+D3+
      2*(D2*A1+A17*(-3.*D2+B.*D4))-R2**C**C*(B3*A17+A17*(-D3+D7))-1.)*
      2*C**C*(D2*(A17*A16*A16)-2.*R2**C*(A17*A16)+S**S*(A17))
      U(4)=U(3)+(.5-R2)*C*(R2*C**S*(D2*A26+A3-B7)-R2**S**S*(D2*A16+A17+
      1(-D3+D7))+R2**C**C*(D2*A26+B.*D2-B.*D4)-2*S**C**C*(D2*A16+
      2*A17*(-D3+D7)+.54))-R2*S**C**C*(B3*A26+B3-B7)+S**S**C**C*(D2*A16+
      2*A17*(-D3+D7))+R2*C**C*(A16)-R2*S**C**C*(-A17*A16)-R2*S**C**C*(-1.)
      4+S**S**C**C*(A17))
      U(5)=C(2)*12.
      CALL LINE(RJSA16)

```

*LDIRSKR3A16

```

      U(6)=(.5-R2)*C*(D2*A16+A16*(-D2+D6))-2.*R2**S**C**C*(D2*A16*(D2+D3+
      1+D2+C**S**S*(D2*A21+A17*(-D2+D6))-R2**C**C*(D2*A16+A16*(-3.*D2+B.*D4)-
      2))+2.*R2**C**S**S*(D3*A30+B.*D3-B.*D5)-R2**S**S*(D3*A21+A17*(-3.*D2+
      B.*D4)))
      U(7)=U(6)+0.5*(R2**R2*(A16)-2.*R2**S**S*(-1.))+R2**S**S*(A17)-2.*R2**S**S*(
      1(-A16*A17)+.5.*R2**S**S*(A17)-2.*R2**S**S*(-A17*A17)+R2**S**S*(A16+A17-
      2*A17)-2.*R2**S**S*(A17*A17)+S**4*(A17*A17*A17))
      U(8)=U(6)+A16*(R2**R2*(B3*A16+A16*(-3.*D2+B.*D4))-2.*R2**C**C*(D2+
      1(D3*A30+B.*D3-B.*D5)+R2**C**C**S**S*(D3*A21+A17*(-3.*D2+B.*D4))+.5*C
      2*C**A16*(D2*(A17*A17)-R2**C**C*(-A17*A17)+0.5*C**C**S**S*(A17*A17*A17))
      U(9)=U(8)+R2**C**4*(B3*A21+A17*(-3.*D2+B.*D4))+0.5*C**4*(A17+A17+A17-
      1)+R2**C*(R2**R2*(D2*A21+A17*(-D2+D6))-R2**C**2*(D3*A21+A17*(-3.*D2+
      2+C.*D4))+R2**C**C*(R2*(A17)-2.*R2**S**S*(-A17*A17)+S**S*(A17*A17*A17)))
      U(10)=U(9)+(.5-R2)*C*(R2*C**S*(D3*A30+B.*D3-B.*D5)-R2**C**C*(D3*A1
      1+A17*(-3.*D2+B.*D4))+R2**R2**C**C*(D2*A30+B2-E6)-R2**S**C**C*(A21*A16+A17-
      2*(-D2+D4)-R2**S**C**C*(B3*A30+B.*D3-B.*D5)+R2**S**C**C*(B3*A21+A17*(-
      3-1.)*D2+B.*D4))+R2**C**C*(A17)-R2**C**C*(-A17*A17)-R2**C**C*(-A17*A17)
      4+S**S**C**C*(A17*A17*A17))
      U(11)=U(10)*12.
      CALL LINE(RJSA15)

```

*LDIRSKR3A15

```

      U(12)=(.5-R2)*C*(D2*A35+A16*(-D.*D4)+A23*(-3.*D2+B.*D4))-2.*R2**R2**S**C
      1*(D2*(D2+D3+B.*D4+A26*(-3.*D2+B.*D4))+R2**C**S**S*(D2*A35-B.*D4*A17+D2-
      2(-3.*D2+B.*D4))-R2**R2**C**S*(D3*A35-D7*A16+A23*(-D3+D7))+2.*R2**C**S**S*
      S*(D3*A35+A17(-D3+D7))-R2**C**S**S*(D3*A35-D7*A17+A16*(-D3+D7)))
      U(13)=U(12)+.5*(R2**R2*(A16*2.*A16*A24+A23*A16*A16)-2.*R2**R2**S*(-1.*
      1+D2+D3+D4+D5+D6*A16)+R2**S**S*(2.*A16*A24*A17+A16*A16*A16)-2.*R2**S**S
      2*(A16*(D2*(D2+D3+B.*D4)+A16*A23)+4.*R2**S**S*(A24-A25*A16-A16*A16))-2.*R
      2**S**S*(A17*(D2*(D2+B.*D4)+A16*A16))+R2**S**S*(-2.*A25*A16+A23)-2.*R2**
      4+S**4*(A16+A16+A23)+S**4*(-2.*A25*A17+A16))
      U(14)=U(13)+.5*(R2**R2**C**C*(-E7*A16+B3*A25+A23*(-E3+E7))-2.*R2**C**S**S*
      S*(E3+A16*(A17+D2)*(-E3+E7))+R2**C**S**S*(-E7*A17+B3*A25+A16*(-E3+D7))
      2+0.5*C**C*(R2*(D2*(D2+B.*D4)+A16*A23)-R2**C**C*(2.*A25+A26)+0.5*C**C**S**S*
      S*(-2.*R2*(A17*A16)))

```



```

S(1,1)=350.*K4+A1+192.*K2+24.
S(1,2)=A2.*K2+96.
S(1,3)=-710.*K4-96.*K2
S(1,4)=-A1.
S(1,5)=-96.*K2-48.
S(1,6)=0.
S(2,1)=96.*K4+A1.*K2
S(2,2)=24.*K4+192.*K2+360.*A1
S(2,3)=-48.*K4
S(2,4)=-96.*K2-720.
S(2,5)=-96.*K2-48.*K4
S(2,6)=0.
S(3,1)=-240.*K2-48.*K4-2.*AK
S(3,2)=-A1.
S(3,3)=1680.*K4+24.*K2+410.*K2+AK
S(3,4)=24.
S(3,5)=120.*K2+96.
S(3,6)=0.
S(4,1)=-96.*K4
S(4,2)=-48.*K4-240.*K2-2.*AK
S(4,3)=96.*K4
S(4,4)=24.*K4+480.*K2+1680.*AK
S(4,5)=120.*K2+96.*K4
S(4,6)=0.
S(5,1)=-720.*K4-576.*K2-2.*AK
S(5,2)=-576.*K2-720.*K4-2.*AK
S(5,3)=1440.*K4+240.*K2
S(5,4)=768.*K2+1440.
S(5,5)=360.*K4+1152.*K2+360.*AK
S(5,6)=0.
V(1)=- (24.*K4+32.*K2+24.*AK)
V(2)=2.*AK- (-96.*K2-48.)
V(3)=2.*AK- (-48.*K4-96.*K2)
V(4)=-AK-24.
V(5)=-AK-24.*K4
V(6)=-240.*K2-4.*AK
DO I=1,6
DO J=1,6
15 S(I,J)=S(I,N)
I=6
DO I=1,6
DO J=1,6
25 WRITE(6,1) (S(I,J),J=1,6),I=1,6)
35 FORMAT(/(5X,2E16.5))
CALL AINV77(A,I)
DO I=1,6
ANS(I)=.
DO J=1,6
15 ANS(I)=ANS(I)+A(I,J)*V(J)
35 FORMAT(/(5X,4E16.5))
C1=ANS(1)
C2=ANS(2)
C3=ANS(3)
C4=ANS(4)

```

```

DO 10 I=1,6
  ALPHAI=ALPHAS(I)
  X(1,1)=57,01,02,03,04,05,ALPHAI
  X(1,7)=1,0
  Y(1)=0.
  DO 10 J=1,6
10  Y(1)=Y(1)+X(1,J)*ALPHAS(J)
  READ(1,10) (C1=516.,40 C2=516.,40 C3=516.,/40 C4=516.,,
100 C5=516.,,70 C6=516.,)
  CALL LYSK(X(1,1:6))
  END

```

0.0000 0.10 0.

#L1SARKJ1K2

```

N=12
DO 21 I=1,12
  DO 21 J=1,12
21  S(I,J)=0.
  S(I,1)=-12.*X20*-2.***(1.-ALU)
  S(I,2)=12.*X20
  S(I,3)=2.***(1.-ALU)
  S(I,7)=-7.*(1.-ALU)*X2
  S(I,8)=2.*(1.+ALU)*X2
  S(I,9)=1.*X2*(1.-ALU)
  S(I,10)=-7.*(1.-ALU)-40.**X2**
  S(I,11)=-7.*X2*(1.-ALU)
  S(I,12)=0.**X2**
  S(I,13)=-.5.*X2*(1.-ALU)
  S(I,14)=-.5.*(1.+ALU)*X2
  S(I,15)=7.*X2*(1.+ALU)*X2
  S(I,16)=12.*X2
  S(I,17)=-12.*X2**
  S(I,18)=-12.**X2**X2-12.***(1.-ALU)
  S(I,19)=12.***(1.-ALU)
  S(I,20)=12.**X2**
  S(I,21)=.5*(1.+ALU)*X2
  S(I,22)=-.5*(1.+ALU)*X2
  S(I,23)=-7.*(1.+ALU)*X2
  S(I,24)=6.*(1.+ALU)*X2
  S(I,25)=2.*X2*(1.-ALU)
  S(I,26)=-4.**X2**X2-2.***(1.-ALU)
  S(I,27)=-4.*X2*(1.-ALU)
  S(I,28,11)=-.5*(1.+ALU)*X2
  S(I,29)=12.**X2**
  S(I,30)=-12.**X2**X2-30.***(1.-ALU)
  S(I,31)=-12.**X2**
  S(I,32)=.5*(1.+ALU)*X2
  S(I,33,11)=-.5*(1.+ALU)
  S(I,34,12)=-12.***(1.+ALU)*X2
  S(I,35,11)=6.**X2**
  S(I,36,11)=12.***(1.-ALU)
  S(I,37,11)=-40.**X2**

```



```

BV(7)=-((2.*(2.*F2*(2.*C2-4.)+2.*F2*(2.*C2-4.))+R2*(1.-ANU))
1*(2.*F1*(2.*C2-4.)+(2.*C1-4.)*2.*F2))

```

```

BV(8)=-((2.*(2.*C2-4.)*(-24.*F2+12.*F4)+(-8.*C2+4.*C4+4.)*2.*F2
1+2.*F2*(-24.*C2+12.*C4+12.))+(-8.*F2+4.*F4)*(2.*C2-4.))*R2*(1.
2-ANU)*((2.*C2-4.)*(-4.*F1-4.*F2+2.*F5)+2.*F1*(-8.*C2+4.*C4+4.))
3+(2.*C1-4.)*(-8.*F2+4.*F4)+(-4.*C1-4.*C2+2.*C5+8.)*2.*F2))

```

```

BV(9)=-((2.*(2.*C2-4.)*(-4.*F1-4.*F2+2.*F5)+(-4.*C1-4.*C2+2.*C5
1+8.)*2.*F2+2.*F2*(-4.*C1-4.*C2+2.*C5+8.))+(-4.*F1-4.*F2+2.*F5)
2*(2.*C2-4.))+R2*(1.+ANU)*((-8.*C1-8.*C2+4.*C5+16.)*2.*F1+(2.*C1
3-4.)*(-8.*F1-8.*F2+4.*F5))+R2*(1.-ANU)*((2.*C2-4.)*(-24.*F1
4+12.*F5)+(-4.*C1-4.*C2+2.*C5+8.)*2.*F1))

```

```

BV(9)=BV(9)-(+R2*(1.-ANU))*(+2.*F2*(-24.*C1+12.*C3+12.))+(-4.*F1
1-4.*F2+2.*F5)*(2.*C1-4.))

```

```

CALL LINK(KJEAR7)

```

```

*LDISKKJEAR7

```

```

BV(10)=-((2.*(2.*C2-4.)*(30.*F2-60.*F4)+(-8.*C2+4.*C4+4.)*(-24.
1*F2+12.*F4)+(6.*C2-12.*C4)*2.*F2+2.*F2*(30.*C2-60.*C4)+(-8.*F2
2+4.*F4)*(-24.*C2+12.*C4+12.))+6.*F2-12.*F4)*(2.*C2-4.))+R2*(1.
3-ANU)*((2.*C2-4.)*(2.*F1+8.*F2-4.*F4-4.*F5)+(-8.*C2+4.*C4+4.))
4*(-4.*F1-4.*F2+2.*F5)+(6.*C2-12.*C4)*2.*F1))

```

```

BV(10)=BV(10)-(+R2*(1.-ANU))*(+2.*F2*(2.*C1+8.*C2-4.*C4-4.*C5
1-4.))+(-8.*F2+4.*F4)*(-4.*C1-4.*C2+2.*C5+8.))+6.*F2-12.*F4)
2*(2.*C1-4.))

```

```

BV(11)=-((2.*(2.*C2-4.)*(8.*F1+2.*F2-4.*F3-4.*F5)+(-4.*C1-4.*C2
1+2.*C5+8.))*(-4.*F1-4.*F2+2.*F5)+(8.*C1+2.*C2-4.*C3-4.*C5-4.))
2*2.*F2+2.*F2*(8.*C1+2.*C2-4.*C3-4.*C5-4.))+(-4.*F1-4.*F2+2.*F5)*
3(-4.*C1-4.*C2+2.*C5+8.))+8.*F1+2.*F2-4.*F3-4.*F5)*(2.*C2-4.))
4+R2*(1.+ANU)*((32.*C1+8.*C2-16.*C3-16.*C5-16.)*2.*F1))

```

```

BV(11)=BV(11)-(+R2*(1.+ANU))*((-8.*F1+4.*F3)*(-8.*C1-8.*C2+4.*C5
1+16.))+2.*C1-4.)*(32.*F1+8.*F2-16.*F3-16.*F5)+(-8.*C1+4.*C3+4.))
2*(-8.*F1-8.*F2+4.*F5))+R2*(1.-ANU)*((2.*C2-4.)*(30.*F1-60.*F3)+
3(-4.*C1-4.*C2+2.*C5+8.))*(-24.*F1+12.*F3)+2.*F1*(8.*C1+2.*C2-4.*C3
4-4.*C5-4.))+2.*F2*(30.*C1-60.*C3))

```

```

BV(11)=BV(11)-(+R2*(1.-ANU))*((-4.*F1-4.*F2+2.*F5)*(-24.*C1
1+12.*C3+12.))+8.*F1+2.*F2-4.*F3-4.*F5)*(2.*C1-4.))

```

```

BV(12)=-((2.*(2.*C2-4.)*(12.*F1+48.*F2-24.*F4-24.*F5)+(-8.*C2+
14.*C4+4.))*(-4.*F1-4.*F2+2.*F5)+(-4.*C1-4.*C2+2.*C5+8.))*(-24.*F2
2+12.*F4)+(4.*C1+16.*C2-8.*C4-8.*C5-8.))*2.*F2+2.*F2*(12.*C1+4.*C2
3-24.*C4-24.*C5-24.))+(-8.*F2+4.*F4)*(-4.*C1-4.*C2+2.*C5+8.))+(-4.*
4F1-4.*F2+2.*F5)*(-24.*C2+12.*C4+12.))

```

```

BV(12)=BV(12)-((2.*((4.*F1+16.*F2-8.*F4-8.*F5)*(2.*C2-4.))+R2*
1(1.+ANU))*2.*F1*(8.*C1+32.*C2-16.*C4-16.*C5-16.))+(-4.*F1-4.*F2
2+2.*F5)*(-8.*C1-8.*C2+4.*C5+16.))+2.*C1-4.)*(8.*F1+32.*F2-16.*F4
3-16.*F5)+(-4.*C1-4.*C2+2.*C5+8.))*(-8.*F1-8.*F2+4.*F5))+R2*(1.-
4ANU)*((2.*C2-4.)*(48.*F1+12.*F2-24.*F3-24.*F5))

```

```

BV(12)=BV(12)-(+R2*(1.-ANU))*((-8.*C2+4.*C4+4.))*(-24.*F1+12.*F3)
1+(-4.*C1-4.*C2+2.*C5+8.))*(-4.*F1-4.*F2+2.*F5)+(4.*C1+16.*C2-8.*C4
2-8.*C5-8.))*2.*F1+2.*F2*(48.*C1+12.*C2-24.*C3-24.*C5-24.))+(-8.*F2
3+4.*F4)*(-24.*C1+12.*C3+12.))+(-4.*F1-4.*F2+2.*F5)*(-4.*C1-4.*C2
4+2.*C5+8.))+4.*F1+16.*F2-8.*F4-8.*F5)*(2.*C1-4.))

```

```

DO 15 N=1,12

```

```

DO 15 N=1,12

```

```

15 SM(N,N)=BM(N,N)

```

```

EQUIVALENCE(SM,A)

```

```

N=12
PUNCH 36,((A(I,J),J=1,N),I=1,N)
PUNCH 36,(BV(J),J=1,N)
36 FORMAT(/(6X,4E16.8))
CALL AINV77(A,N)
DO 12 I=1,N
  ANS(I)=0.
DO 13 J=1,N
13 ANS(I)=ANS(I)+A(I,J)*BV(J)
  G1=ANS(1)
  G2=ANS(2)
  G3=ANS(3)
  G4=ANS(4)
  G5=ANS(5)
  G6=ANS(6)
  H1=ANS(7)
  H2=ANS(8)
  H3=ANS(9)
  H4=ANS(10)
  H5=ANS(11)
  H6=ANS(12)
PUNCH 36,G1,G2,G3,G4,G5,G6,H1,H2,H3,H4,H5,H6
DO 14 I=1,12
  BV(I)=0.
DO 14 J=1,12
14 BV(I)=BV(I)+BM(I,J)*ANS(J)
  PUNCH 36,(BV(I),I=1,12)
38 FORMAT(4H G1=E16.8,4H G2=E16.8,4H G3=E16.8/4H G4=E16.8,4H G5=E16.8
1,4H G6=E16.8/4H H1=E16.8,4H H2=E16.8,4H H3=E16.8/4H H4=E16.8,
24H H5=E16.8,4H H6=E16.8)
  CALL LINK(KJEAR8)
  END

```

```

**FOR 5

```

```

*LDISKKJEAR8

```

```

  U(1)=R2*R2*((2.*C1-4.)*G1+2.*F1*D1)+ANU*(R2*R*((2.*C1-4.)*H1
1+2.*F1*E1))+R*(H1*(2.*C2-4.)+2.*F2*E1)+ANU*(R2*(G1*(2.*C2-4.)
2+2.*F2*D1))

```

```

  U(1)=U(1)*12.

```

```

  U(2)=R2*R2*((2.*C1-4.)*(-3.*G1+3.*G2)+(-24.*C1+12.*C3+12.)*G1
1+2.*F1*(-3.*D1+3.*D2)+D1*(-24.*F1+12.*F3))+0.5*(R2*R2*(2.*(2.*C1
2-4.)*2.*F1*(2.*C1-4.)+2.*F1*(2.*C1-4.)*(2.*C1-4.)))+ANU*(R2*R*((
32.*C1-4.)*(-H1+H3)+H1*(-24.*C1+12.*C3+12.))+2.*F1*(-E1+E3)+E1*
4*(-24.*F1+12.*F3)))

```

```

  U(2)=U(2)+R*((2.*C2-4.)*(-H1+H3)+(-4.*C1-4.*C2+2.*C5+8.)*H1
1+2.*F2*(-E1+E3)+(-4.*F1-4.*F2+2.*F5)*E1)+ANU*(R2*(G1*(-4.*C1
2-4.*C2+2.*C5+8.)+(2.*C2-4.)*(-3.*G1+3.*G2)+2.*F2*(-3.*D1+3.*D2)
3+(-4.*F1-4.*F2+2.*F5)*D1)+0.5*(R2*(2.*(2.*C2-4.)*2.*F1*(2.*C1
4-4.))+2.*F2*(2.*C1-4.)*(2.*C1-4.)))

```

```

  U(2)=U(2)*12.

```

```

  U(3)=R2*R2*((2.*C1-4.)*(-G1+G3)+(-4.*C1-4.*C2+2.*C5+8.)*G1
1+2.*F1*(-D1+D3)+D1*(-4.*F1-4.*F2+2.*F5))+ANU*(R2*R*((2.*C1-4.)
2*(-3.*H1+3.*H2)+(-4.*C1-4.*C2+2.*C5+8.)*H1+2.*F1*(-3.*E1+3.*E2)
3+(-4.*F1-4.*F2+2.*F5)*E1)+0.5*(R2*(2.*(2.*C1-4.)*(2.*C2-4.)*2.*F2
4+2.*F1*(2.*C2-4.)*(2.*C2-4.)))

```

U(3)=U(3)+R*((2.*C2-4.)*(-3.*H1+3.*H2)+(-24.*C2+12.*C4+12.)*(-1+2.*F2*(-3.*F1+3.*E2)+(-24.*F2+12.*F4)*F1)+0.5*(2.*(2.*C2-4.)*2.2*F2*(2.*C2-4.))+2.*F2*(2.*C2-4.)*(2.*C2-4.))+ANU*(R2*((2.*C2-4.)*3*(-G1+G3)+(-24.*C2+12.*C4+12.)*G1+2.*F2*(-D1+D3)+(-24.*F2+12.*F4)*4*D1))

U(3)=U(3)*12.

U(4)=R2*R2*((2.*C1-4.)*(-5.*G2+5.*G4)+(-24.*C1+12.*C3+12.)*(-5.1*G1+5.*G2)+(30.*C1-60.*C3)*G1+2.*F1*(-5.*D2+5.*D4)+(-24.*F1+2+12.*F3)*(-3.*D1+3.*D2)+(30.*F1-60.*F3)*D1)+0.5*(R2*R2*(2.*(2.*3C1-4.)*((2.*C1-4.)*(-8.*F1+4.*F3)+(-8.*C1+4.*C3+4.)*2.*F1)+(4-24.*C1+12.*C3+12.)*(2.*C1-4.)*2.*F1))

U(4)=U(4)+0.5*(R2*R2*(+2.*F1*2.*(2.*C1-4.)*(-8.*C1+4.*C3+4.))1+(-24.*F1+12.*F3)*(2.*C1-4.)*(2.*C1-4.))+ANU*(R2*((2.*C1-4.)*2*(-H3+H5)+(-24.*C1+12.*C3+12.)*(-H1+H3)+(30.*C1-60.*C3)*H13+2.*F1*(-E3+E5)+(-24.*F1+12.*F3)*(-E1+E3)+(30.*F1-60.*F3)*E1))

U(4)=U(4)+R*((2.*C2-4.)*(-H3+H5)+(-4.*G1-4.*C2+2.*C5+8.)*(-H1+H3))1+(8.*C1+2.*C2-4.*C3-4.*C5-4.)*H1+2.*F2*(-E3+E5)+(-4.*F1-4.*F22+2.*F5)*(-E1+E3)+(8.*F1+2.*F2-4.*F3-4.*F5)*E1)+ANU*(R2*((2.*C2-4.)*3*(-5.*G2+5.*G4)+(-4.*C1-4.*C2+2.*C5+8.)*(-3.*G1+3.*G2)+(8.*C14+2.*C2-4.*C3-4.*C5-4.)*G1+2.*F2*(-5.*D2+5.*D4)))

U(4)=U(4)+ANU*(R2*((-4.*F1-4.*F2+2.*F5)*(-3.*D1+3.*D2)+(8.*F11+2.*F2-4.*F3-4.*F5)*D1)+0.5*(R2*(2.*(2.*C2-4.)*((2.*C1-4.)*(-8.*2F1+4.*F3)+(-8.*C1+4.*C3+4.)*2.*F1)+(-4.*C1-4.*C2+2.*C5+8.)*3*2.*F1*(2.*C1-4.))+2.*F2*2.*(2.*C1-4.)*(-8.*C1+4.*C3+4.))+(-4.*F14-4.*F2+2.*F5)*(2.*C1-4.)*(2.*C1-4.)))

U(4)=U(4)*12.

U(5)=R2*R2*((2.*C1-4.)*(-G3+G5)+(-4.*C1-4.*C2+2.*C5+8.)*(-G11+G3)+(2.*C1+8.*C2-4.*C4-4.*C5-4.)*G1+2.*F1*(-D3+D5)+(-4.*F1-4.*F22+2.*F5)*(-D1+D3)+(2.*F1+8.*F2-4.*F4-4.*F5)*D1)+ANU*(R2*((2.*C13-4.)*(-5.*H2+5.*H4)+(-4.*C1-4.*C2+2.*C5+8.)*(-3.*H1+3.*H2)+(2.*C14+8.*C2-4.*C4-4.*C5-4.)*H1+2.*F1*(-5.*E2+5.*E4)))

U(5)=U(5)+ANU*(R2*((-4.*F1-4.*F2+2.*F5)*(-3.*E1+3.*E2)+(2.*F11+8.*F2-4.*F4-4.*F5)*E1)+0.5*(R2*(2.*(2.*C1-4.)*((2.*F2*(-8.*C22+4.*C4+4.))+2.*C2-4.)*(-8.*F2+4.*F4))+(-4.*C1-4.*C2+2.*C5+8.)*3*2.*F2*(2.*C2-4.))+2.*F1*2.*(2.*C2-4.)*(-8.*C2+4.*C4+4.))+(-4.*F14-4.*F2+2.*F5)*(2.*C2-4.)*(2.*C2-4.)))

CALL LINK(KJEAR9)

END

*LDISKKJEAR9

U(5)=U(5)+R*((2.*C2-4.)*(-5.*H2+5.*H4)+(-24.*C2+12.*C4+12.)*(-1-3.*H1+3.*H2)+(30.*C2-60.*C4)*H1+2.*F2*(-5.*E2+5.*E4)+(-24.*F22+12.*F4)*(-3.*E1+3.*E2)+(30.*F2-60.*F4)*E1)+0.5*(2.*(2.*C2-4.)*3(2.*F2*(-8.*C2+4.*C4+4.))+2.*C2-4.)*(-8.*F2+4.*F4))+(-24.*C24+12.*C4+12.)*(2.*C2-4.)*2.*F2)

U(5)=U(5)+0.5*(+2.*F2*(2.*C2-4.)*(-8.*C2+4.*C4+4.)*2.+(-24.*F21+12.*F4)*(2.*C2-4.)*(2.*C2-4.))+ANU*(R2*((2.*C2-4.)*(-G3+G5))2+(-24.*C2+12.*C4+12.)*(-G1+G3)+(30.*C2-60.*C4)*G1+2.*F2*(-D33+D5)+(-24.*F2+12.*F4)*(-D1+D3)+(30.*F2-60.*F4)*D1))

U(5)=U(5)*12.

U(5)=R2*R2*((2.*C1-4.)*(3.*G1-3.*G2-3.*G3+3.*G6)+(-24.*C1+12.*C31+12.)*(-G1+G3)+(-4.*C1-4.*C2+2.*C5+8.)*(-3.*G1+3.*G2)+(48.*C12+12.*C2-24.*C3-24.*C5-24.)*G1+2.*F1*(3.*D1-3.*D2-3.*D3+3.*D6))+3(-24.*F1+12.*F3)*(-D1+D3)+(-4.*F1-4.*F2+2.*F5)*(-3.*D1-3.*D2)+

```

4(4*. *F1+12.*F2-24.*F3-24.*F5)*D1)
  U(6)=U(6)+0.5*(R2*R2*(2.*(2.*C1-4.)*(2.*C1-4.)*(-4.*F1-4.*F2
1+2.*F5)+2.*F1*(-4.*C1-4.*C2+2.*C5+8.))*(-4.*C1-4.*C2+2.*C5+8.))
2*(2.*C1-4.)*2.*F1+2.*F1*2.*(2.*C1-4.)*(-4.*C1-4.*C2+2.*C5+8.))
3(-4.*F1-4.*F2+2.*F5)*(2.*C1-4.)*(2.*C1-4.))*ANU*(12.*F1+48.*F2-24.*F4
4*(3.*G1-3.*G2-3.*G3+3.*G6)+(-24.*C1+12.*C3+12.)*(-3.*G1+3.*G2)))
  U(6)=U(6)+ANU*(R2*R2*(+(-4.*C1-4.*C2+2.*C5+8.))*(-H1+H3)+(12.*C1+48.*
112.*C2-24.*C3-24.*C5-24.)*H1+2.*F1*(3.*F1-3.*F2-3.*F3+3.*F6)+
2(-24.*F1+12.*F3)*(-3.*E1+3.*E2)+(-4.*F1-4.*F2+2.*F5)*(-E1+E3)+
3(4*. *F1+12.*F2-24.*F3-24.*F5)*F1)+0.5*(R2*(2.*(2.*C1-4.)*(2.*F2*
4(-4.*C1-4.*C2+2.*C5+8.))+(2.*C2-4.))*(-4.*F1-4.*F2+2.*F5))))
  U(6)=U(6)+ANU*(+0.5*(R2*(+(-24.*C1+12.*C3+12.))*2.*F2*(2.*C2-4.))
1+2.*F1*2.*(2.*C2-4.))*(-4.*C1-4.*C2+2.*C5+8.))+(-24.*F1+12.*F3)*
2(2.*C2-4.)*(2.*C2-4.)))+R*(2.*C2-4.)*(3.*H1-3.*H2-3.*H3+3.*H6)
3+(-4.*C1-4.*C2+2.*C5+8.))*(-3.*H1+3.*H2)+(-24.*C2+12.*C4+12.))*
4(-H1+H3)+(12.*C1+48.*C2-24.*C4-24.*C5-24.)*H1)
  U(6)=U(6)+R*(+2.*F2*(3.*E1-3.*E2-3.*E3+3.*E6)+(-4.*F1-4.*F2+2.*F5)
1*(-3.*E1+3.*E2)+(-24.*F2+12.*F4)*(-E1+E3)+(12.*F1+48.*F2-24.*F4
2-24.*F5)*E1)+0.5*(2.*(2.*C2-4.)*(2.*F2*(-4.*C1-4.*C2+2.*C5+8.))
3+(2.*C2-4.))*(-4.*F1-4.*F2+2.*F5))+(-4.*C1-4.*C2+2.*C5+8.))*2.*F2*
4(2.*C2-4.))+2.*F2*2.*(2.*C2-4.))*(-4.*C1-4.*C2+2.*C5+8.))
  U(6)=U(6)+0.5*(+(-4.*F1-4.*F2+2.*F5)*(2.*C2-4.))*(2.*C2-4.))
1+ANU*(R2*(2.*C2-4.)*(3.*G1-3.*G2-3.*G3+3.*G6)+(-4.*C1-4.*C2+2.*
2C5+8.))*(-G1+G3)+(-24.*C2+12.*C4+12.))*(-3.*G1+3.*G2)+(12.*C1+48.*
3C2-24.*C4-24.*C5-24.)*G1+2.*F2*(3.*D1-3.*D2-3.*D3+3.*D6)+(-4.*F1
4-4.*F2+2.*F5)*(-D1+D3)+(-24.*F2+12.*F4))*(-3.*D1+3.*D2)))
9 U(6)=U(6)+ANU*(R2*(12.*F1+48.*F2-24.*F4-24.*F5)*D1)
1+0.5*(R2*(2.*(2.*C2-4.))*((2.*C1-4.))*(-4.*F1-4.*F2+2.*F5)+2.*F1*(
2-4.*C1-4.*C2+2.*C5+8.))+(-24.*C2+12.*C4+12.))*2.*F1*(2.*C1-4.))
3+2.*F2*2.*(2.*C1-4.))*(-4.*C1-4.*C2+2.*C5+8.))+(-24.*F2+12.*F4)
4*(2.*C1-4.))*(2.*C1-4.)))
  U(6)=U(6)+(1.-ANU)*(R2*((-8.*C1-8.*C2+4.*C5+16.))*(-2.*G1+2.*G3)
1+(-8.*F1-8.*F2+4.*F5)*(-2.*D1+2.*D3))+R2*R*((-8.*C1-8.*C2+4.*C5+
216.))*(-2.*H1+2.*H3)+(-8.*F1-8.*F2+4.*F5)*(-2.*E1+2.*E3))*R2*((-8.*
3*C1-8.*C2+4.*C5+16.))*(2.*F1)*(2.*C2-4.))+(-8.*C1-8.*C2+4.*C5+16.))
4*(2.*C1-4.))*(2.*F2)+(-8.*F1-8.*F2+4.*F5)*(2.*C1-4.))*(2.*C2-4.)))
  U(6)=U(6)*12.
DO 15 N=1,6
DO 15 N=1,6
15 SM(N,A)=DM(N,N)
EQUIVALENCE(SM,A)
N=6
PUNCH B6,((A(I,J),J=1,N),I=1,N)
PUNCH B6,(U(J),J=1,N)
36 FORMAT(/(3X,4E16.8))
CALL AIRV77(A,N)
DO 15 I=1,N
ANS(I)=0.
DO 15 J=1,N
13 ANS(I)=ANS(I)+A(I,J)*U(J)
Y1=ANS(1)
Y2=ANS(2)
Y3=ANS(3)
Y4=ANS(4)

```



```

Y5=ANS(5)
ALPH5=ANS(6)
PUNCH 444,Y1,Y2,Y3,Y4,Y5,ALPH5
DO 14 I=1,6
  U(I)=0.
  DO 14 J=1,6
    14 U(I)=U(I)+DM(I,J)*ANS(J)
  PUNCH 36,(U(I),I=1,6)
444 FORMAT(4H Y1=E16.8,4H Y2=E16.8,4H Y3=E16.8/4H Y4=E16.0,
14H Y5=E16.8,7H ALPH5=E16.8)
CALL LINK(KJEA10)
340003200701360003200702490240251196361130010200
**JOB 5
**PCK 5
**FANCK1510
*LDISKKJEA10
  DIMENSION P(50)
  COMMON R,AK,R2,R4,C1,C2,C3,C4,C5,D1,D2,D3,D4,D5,D6,E1,E2,E3,E4,E5,
1E6,F1,F2,F3,F4,F5,G1,G2,G3,G4,G5,G6,H1,H2,H3,H4,H5,H6,Y1,Y2,Y3,
2Y4,Y5,AMU,P
  AXI=0.
  ETA=1.
77 P(1)=(2.*AXI-8.*(AXI**3)-4.*AXI*(ETA**2)+16.*(AXI**3)*(ETA**2)
1-12.*(AXI**5)*(ETA**2)+2.*AXI*(ETA**4)-8.*(AXI**3)*(ETA**4)
2+6.*(AXI**5)*(ETA**4)+6.*(AXI**5))
  P(2)=(-4.*AXI*(ETA**2)+4.*(AXI**3)*(ETA**2)+8.*AXI*(ETA**4)
1-8.*(AXI**3)*(ETA**4)-4.*AXI*(ETA**6)+4.*(AXI**3)*(ETA**6))
  P(3)=(4.*(AXI**3)-12.*(AXI**5)+8.*(AXI**7)-8.*(AXI**3)*(ETA**2)
1+24.*(AXI**5)*(ETA**2)-16.*(AXI**7)*(ETA**2)+4.*(AXI**5)*(ETA
2**4)-12.*(AXI**5)*(ETA**4)+8.*(AXI**7)*(ETA**4))
  P(4)=(-4.*AXI*(ETA**4)+4.*(AXI**3)*(ETA**4)+8.*AXI*(ETA**6)
1-8.*(AXI**3)*(ETA**6)-4.*AXI*(ETA**8)+4.*(AXI**3)*(ETA**8))
  P(5)=(1.*AXI*(ETA**2)-6.*(AXI**3)*(ETA**2)+6.*(AXI**5)*(ETA**2)
1-4.*AXI*(ETA**4)+16.*(AXI**3)*(ETA**4)-12.*(AXI**5)*(ETA**4)
2+2.*AXI*(ETA**6)-8.*(AXI**3)*(ETA**6)+6.*(AXI**5)*(ETA**6))
  P(6)=(-4.*AXI+4.*(AXI**3)+8.*AXI*(ETA**2)-8.*(AXI**3)*(ETA**2)-4.
1*AXI*(ETA**4)+4.*(AXI**3)*(ETA**4))
  P(7)=(2.-24.*(AXI**2)+30.*(AXI**4)-4.*(ETA**2)+48.*(AXI**2)
1*(ETA**2)-60.*(AXI**4)*(ETA**2)+2.*(ETA**4)-24.*(AXI**2)*(ETA**4)
2+30.*(AXI**4)*(ETA**4))
  P(8)=(-4.*(ETA**2)+12.*(AXI**2)*(ETA**2)+8.*(ETA**4)-24.*(AXI**2)
1*(ETA**4)-4.*(ETA**6)+12.*(AXI**2)*(ETA**6))
  P(9)=(12.*(AXI**2)-60.*(AXI**4)+56.*(AXI**6)-24.*(AXI**2)*(ETA**2)
1+120.*(AXI**4)*(ETA**2)-112.*(AXI**6)*(ETA**2)+12.*(AXI**2)
2*(ETA**4)-60.*(AXI**4)*(ETA**4)+56.*(AXI**6)*(ETA**4))
  P(10)=(-4.*(ETA**4)+12.*(AXI**2)*(ETA**4)+8.*(ETA**6)-24.*(
1AXI**2)*(ETA**6)-4.*(ETA**8)+12.*(AXI**2)*(ETA**8))
  P(11)=(2.*(ETA**2)-24.*(AXI**2)*(ETA**2)+30.*(AXI**4)*(ETA**2)
1-4.*(ETA**4)+48.*(AXI**2)*(ETA**4)-60.*(AXI**4)*(ETA**4)+2.*(ETA
2**6)-24.*(AXI**2)*(ETA**6)+30.*(AXI**4)*(ETA**6))
  P(12)=(-4.+12.*(AXI**2)+8.*(ETA**2)-24.*(AXI**2)*(ETA**2)-4.*
1(ETA**4)+12.*(AXI**2)*(ETA**4))
  P(13)=(-4.*(AXI**2)*ETA+8.*(AXI**4)*ETA-4.*(AXI**6)*ETA+4.
1*(AXI**2)*(ETA**3)-8.*(AXI**4)*(ETA**3)+4.*(AXI**6)*(ETA**3))

```

$P(14) = (2.*ETA-4.*(AXI**2)*ETA+2.*(AXI**4)*ETA-8.*(ETA**3)+16.*$
 $1*(AXI**2)*(ETA**3)-8.*(AXI**4)*(ETA**3)+6.*(ETA**5)-12.*(AXI**2)$
 $2*(ETA**5)+6.*(AXI**4)*(ETA**5))$
 $P(15) = (-4.*(AXI**4)*ETA+7.*(AXI**6)*ETA-4.*(AXI**8)*ETA+4.*$
 $1*(AXI**4)*(ETA**3)-8.*(AXI**6)*(ETA**3)+4.*(AXI**8)*(ETA**3))$
 $P(16) = (4.*(ETA**5)-8.*(AXI**2)*(ETA**3)+4.*(AXI**4)*(ETA**3)$
 $1-12.*(ETA**5)+24.*(AXI**2)*(ETA**5)-12.*(AXI**4)*(ETA**5)+4.*$
 $2*(ETA**7)-16.*(AXI**2)*(ETA**7)+8.*(AXI**4)*(ETA**7))$
 $P(17) = (2.*(AXI**2)*ETA-4.*(AXI**4)*ETA+2.*(AXI**6)*ETA-8.*$
 $1*(AXI**2)*(ETA**3)+16.*(AXI**4)*(ETA**3)-8.*(AXI**6)*(ETA**3)$
 $2+6.*(AXI**2)*(ETA**5)-12.*(AXI**4)*(ETA**5)+6.*(AXI**6)*(ETA**5))$
 $P(18) = (-4.*ETA+8.*(AXI**2)*ETA-4.*(AXI**4)*ETA+4.*(ETA**3)-4.*$
 $1*(AXI**2)*(ETA**3)+4.*(AXI**4)*(ETA**3))$
 $P(19) = (-4.*(AXI**2)+8.*(AXI**4)-4.*(AXI**6)+12.*(AXI**2)*(ETA**2)$
 $1-24.*(AXI**4)*(ETA**2)+12.*(AXI**6)*(ETA**2))$
 $P(20) = (2.-4.*(AXI**2)+2.*(AXI**4)-24.*(ETA**2)+48.*(AXI**2)*$
 $1*(ETA**2)-24.*(AXI**4)*(ETA**2)+30.*(ETA**4)-60.*(AXI**2)*$
 $2*(ETA**4)+35.*(AXI**4)*(ETA**4))$
 $P(21) = (-4.*(AXI**4)+8.*(AXI**6)-4.*(AXI**8)+12.*(AXI**4)*(ETA**2)$
 $1-24.*(AXI**6)*(ETA**2)+12.*(AXI**8)*(ETA**2))$
 $P(22) = (12.*(ETA**2)-24.*(AXI**2)*(ETA**2)+12.*(AXI**4)*(ETA**2)$
 $1-60.*(ETA**4)+120.*(AXI**2)*(ETA**4)-60.*(AXI**4)*(ETA**4)+56.*$
 $2*(ETA**6)-112.*(AXI**2)*(ETA**6)+56.*(AXI**4)*(ETA**6))$
 $P(23) = (2.*(AXI**2)-4.*(AXI**4)+2.*(AXI**6)-24.*(AXI**2)*(ETA**2)$
 $1+48.*(AXI**4)*(ETA**2)-24.*(AXI**6)*(ETA**2)+30.*(AXI**2)*$
 $2*(ETA**4)-60.*(AXI**4)*(ETA**4)+30.*(AXI**6)*(ETA**4))$
 $P(24) = (-4.+8.*(AXI**2)-4.*(AXI**4)+12.*(ETA**2)-24.*(AXI**2)$
 $1*(ETA**2)+12.*(AXI**4)*(ETA**2))$
 $P(25) = (1.-3.*(AXI**2)-(ETA**2)+3.*(AXI**2)*(ETA**2))$
 $P(26) = (3.*(AXI**2)-5.*(AXI**4)-3.*(AXI**2)*(ETA**2)+5.*(AXI**4)$
 $1*(ETA**2))$
 $P(27) = ((ETA**2)-3.*(AXI**2)*(ETA**2)-(ETA**4)+3.*(AXI**2)*(ETA$
 $1**4))$
 $P(28) = (5.*(AXI**4)-7.*(AXI**6)-5.*(AXI**4)*(ETA**2)+7.*(AXI**6)$
 $1*(ETA**2))$
 $P(29) = ((ETA**4)-3.*(AXI**2)*(ETA**4)-(ETA**6)+3.*(AXI**2)*$
 $1*(ETA**6))$
 $P(30) = (3.*(AXI**2)*(ETA**2)-5.*(AXI**4)*(ETA**2)-3.*(AXI**2)$
 $1*(ETA**4)+5.*(AXI**4)*(ETA**4))$
 $P(31) = (-2.*AXI*ETA+2.*(AXI**3)*ETA)$
 $P(32) = (-2.*(AXI**3)*ETA+2.*(AXI**5)*ETA)$
 $P(33) = (2.*AXI*ETA-2.*(AXI**3)*ETA-4.*AXI*(ETA**3)+4.*(AXI**3)$
 $1*(ETA**3))$
 $P(34) = (-2.*(AXI**5)*ETA+2.*(AXI**7)*ETA)$
 $P(35) = (4.*AXI*(ETA**3)-4.*(AXI**3)*(ETA**3)-6.*AXI*(ETA**5)$
 $1+6.*(AXI**5)*(ETA**5))$
 $P(36) = (2.*(AXI**3)*ETA-2.*(AXI**5)*ETA-4.*(AXI**3)*(ETA**3)+4.*$
 $1*(AXI**5)*(ETA**3))$
 $P(37) = (-2.*ETA*AXI+2.*AXI*(ETA**3))$
 $P(38) = (-2.*AXI*(ETA**3)+2.*AXI*(ETA**5))$
 $P(39) = (2.*AXI*ETA-4.*(AXI**3)*ETA-2.*AXI*(ETA**3)+4.*(AXI**3)$
 $1*(ETA**3))$
 $P(40) = (-2.*AXI*(ETA**5)+2.*AXI*(ETA**7))$
 $P(41) = (4.*(AXI**3)*ETA-6.*(AXI**5)*ETA-4.*(AXI**3)*(ETA**3)$

```

1*6.*(AXI**5)*(ETA**3)
P(41)=(2.*AXI*(ETA**3)-4.*(AXI**5)*(ETA**3)-2.*AXI*(ETA**1)+6.*
1(AXI**5)*(ETA**5))
P(42)=(1.-(AXI**2)-3.*(ETA**2)+3.*(AXI**2)*(ETA**2))
P(43)=(5.*(ETA**2)-5.*(AXI**2)*(ETA**2)-5.*(ETI**4)+5.*(AXI**2)
1*(ETA**4))
P(44)=((AXI**2)-(AXI**4)-3.*(AXI**2)*(ETA**2)+5.*(AXI**4)+
1(ETA**4))
P(45)=(5.*(ETA**4)-5.*(AXI**2)*(ETA**4)-7.*(ETA**6)+7.*(AXI**2)
1*(ETA**6))
P(46)=((AXI**4)-(AXI**6)-3.*(AXI**4)*(ETA**2)+3.*(AXI**6)
1*(ETA**2))
P(47)=(5.*(AXI**2)*(ETA**2)-3.*(AXI**4)*(ETA**2)-5.*(AXI**2)*
1(ETA**4)+5.*(AXI**4)*(ETA**4))
IF (ETA=0.5) 23,24,24
24 CONTINUE
PUNCH 445
445 FORMAT(3X,56H BENDING STRESS AT MIDDLE OF LONG EDGE)
23 W1XX=C1*P(7)+C2*P(8)+C3*P(9)+C4*P(10)+C5*P(11)+P(12)
W1YY=C1*P(19)+C2*P(20)+C3*P(21)+C4*P(22)+C5*P(23)+P(24)
W2X=-0.5*(R2*W1XX+ANU*W1YY)
W3XX=F1*P(7)+F2*P(8)+F3*P(9)+F4*P(10)+F5*P(11)
W3YY=F1*P(19)+F2*P(20)+F3*P(21)+F4*P(22)+F5*P(23)
W4X=-0.5*(R2*W3XX+ANU*W3YY)
W5XX=Y1*P(7)+Y2*P(8)+Y3*P(9)+Y4*P(10)+Y5*P(11)
W5YY=Y1*P(19)+Y2*P(20)+Y3*P(21)+Y4*P(22)+Y5*P(23)
W6X=-0.5*(R2*W5XX+ANU*W5YY)
PUNCH 446,W2X,W3X,W5X
446 FORMAT(5H W2X=E16.8,5H W3X=E16.8,5H W5X=E16.8)
W2Y=-0.5*(W1YY+ANU*R2*W1XX)
W3Y=-0.5*(W3YY+ANU*R2*W3XX)
W5Y=-0.5*(W5YY+ANU*R2*W5XX)
PUNCH 447,W2Y,W3Y,W5Y
447 FORMAT(5H W2Y=E16.8,5H W3Y=E16.8,5H W5Y=E16.8)
S2X=D1*P(25)+D2*P(26)+D3*P(27)+D4*P(28)+D5*P(29)+D6*P(30)
S4X=G1*P(25)+G2*P(26)+G3*P(27)+G4*P(28)+G5*P(29)+G6*P(30)
W1X=C1*P(1)+C2*P(2)+C3*P(3)+C4*P(4)+C5*P(5)+P(6)
W3X=F1*P(1)+F2*P(2)+F3*P(3)+F4*P(4)+F5*P(5)
T2Y=E1*P(43)+E2*P(44)+E3*P(45)+E4*P(46)+E5*P(47)+E6*P(48)
T4Y=H1*P(43)+H2*P(44)+H3*P(45)+H4*P(46)+H5*P(47)+H6*P(48)
W1Y=C1*P(13)+C2*P(14)+C3*P(15)+C4*P(16)+C5*P(17)+P(18)
W3Y=F1*P(13)+F2*P(14)+F3*P(15)+F4*P(16)+F5*P(17)
IF(ETA=0.5)15,16,16
16 CONTINUE
PUNCH 111
111 FORMAT(3X,39H MEMBRANE STRESS AT MIDDLE OF LONG EDGE)
15 W2X=(R2*S2X+0.5*R2*(W1X*W1X)+ANU*(R*T2Y+0.5*(W1Y*W1Y)))
W4X=(R2*S4X+0.5*R2*(2.*W1X*W3X)+ANU*(R*T4Y+0.5*(2.*W1Y*W3Y)))
W2Y=(R*T2Y+0.5*(W1Y*W1Y)+ANU*(R2*S2X+0.5*R2*(W1X*W1X)))
W4Y=(R*T4Y+0.5*(2.*W1Y*W3Y)+ANU*(R2*S4X+0.5*R2*(2.*W1X*W3X)))
PUNCH 113,W2X,W4X,W2Y,W4Y
113 FORMAT(4X,6H W2X=E16.8,6H W4X=E16.8,6H W2Y=E16.8/6H W4Y=E16.8)
IF (ETA=0.5) 52,51,51
51 CONTINUE

```



```

BR(5,11)=2.*A11-6.*A10
BR(6,1)=12.*A6
BR(6,2)=12.*A44-12.*A6
BR(6,3)=40.*C**R2**R-12.*A8
BR(6,4)=-12.*A44
BR(6,5)=-40.*C**R2**R
BR(6,6)=12.*A8-12.*A44-40.*C**R2**R
BR(6,7)=12.*A11
BR(6,8)=-12.*A11
BR(6,9)=12.*A10-12.*A11
BR(6,11)=-12.*A10
BR(6,12)=12.*A11-12.*A10
BR(7,1)=-2.*A6**R2**C
BR(7,2)=2.*A6**R2**C
BR(7,7)=(-6.*A14+4.*A7**R2**S)-(2.*A7**R2**R)
BR(7,8)=6.*A14
BR(7,9)=2.*A7**R2**R
BR(8,2)=-4.*A6**R2**C
BR(8,4)=4.*A6**R2**C
BR(8,7)=2.*A7**R2**R-8.*A7**R2**S
BR(8,8)=6.*A7**R2**S-20.*A14-2.*A7**R2**R
BR(8,9)=-2.*A7**R2**R
BR(8,10)=20.*A14
BR(8,12)=2.*A7**R2**R
BR(9,1)=6.*A6**R2**C-6.*A6**R**C**S
BR(9,2)=6.*A6**R**C**S-6.*A6**R2**C
BR(9,3)=-6.*A6**R2**C
BR(9,6)=6.*A6**R2**C
BR(9,7)=6.*A14-12.*A7**R2**S
BR(9,8)=-6.*A14
BR(9,9)=12.*A7**R2**S-6.*A14-12.*A7**R2**R
BR(9,11)=12.*A7**R2**R
BR(9,12)=6.*A14
BR(10,4)=-6.*A6**R2**C
BR(10,7)=2.*A7**R2**R-12.*A7**R2**S
BR(10,10)=12.*A7**R2**S-42.*A14-2.*A7**R2**R
BR(11,12)=-2.*A7**R2**R
BR(11,1)=4.*A6**R**C**S
BR(11,2)=-6.*A6**R**C**S
BR(11,3)=-6.*A6**R**C**S+10.*A6**R2**C
BR(11,5)=-10.*A6**R2**C
BR(11,6)=6.*A6**R**C**S-10.*A6**R2**C
BR(11,9)=6.*A14-20.*A7**R2**S
BR(11,11)=20.*A7**R2**S-30.*A7**R2**R-6.*A14
BR(11,12)=-6.*A14
BR(12,2)=12.*A6**R2**C-20.*A6**R**C**S
BR(12,4)=20.*A6**R**C**S-12.*A6**R2**C
BR(12,5)=-12.*A6**R2**C
BR(12,7)=24.*A7**R2**S
BR(12,8)=20.*A14-24.*A7**R2**S
BR(12,9)=12.*A7**R2**R-24.*A7**R2**S
BR(12,10)=-20.*A14
BR(12,11)=-12.*A7**R2**R
201 BR(12,12)=24.*A7**R2**S-12.*A7**R2**R-20.*A14

```

```
CALL LINK(KJPAR3)
END
```

```
****
```

```
*LDISKKJSARE
```

```

SV(1) = -(2.**R2**R*(A16*A16)-2.**R2*S*(-A16)-4.**R2*S*(-A16)+A12
1+A13 *A13*A17-2.**S*(-A17))
SV(2) = -(2.**R2**R*(-A16)-2.**R2*S*(A16*A17)-4.**R2*S+A12*(-A17)
1+A13*(-A17)-2.**S*(A17*A17))
SV(3) = 0.
SV(4) = 0.
SV(5) = 0.
SV(6) = -(2.**R2**R*(A16*A26-A23+A16*A19)-2.**R2*S*(A16*A17+A25-A17
1-A18)-4.**R2*S*(A16*A33-A26-A26)+A12*(-A17+A17*A26-A33)+A13*(A16
2*A22-A16+A17*A26)-2.**S*(-A22+A17*A16+A17*A13))
SV(7) = -(2.**R2**R*(A16*A16-A19+A15*A18)-2.**R2*S*(A16*A20+A15*A17
1-A18)-4.**R2*S*(A16*A30-A33-A18)+A12*(-A20+A17*A33-A30)+A13*(A16
2*A21-A22+A17*A18)-2.**S*(-A21+A17*A22+A17*A20))
SV(8) = -(2.*(A17*A17)-R*A6*S*(-A17)+A15*(-A17)+R2*A6+R2*A7*A16
1*A17)
SV(9) = -(2.*(-A17)-R*A6*S*(A16*A17)+A15+R2*A6*(-A16)+R2*A7*(-A16))
SV(10) = 0.
SV(11) = 0.
SV(12) = 0.
SV(13) = -(2.*(-A21+A17*A22+A17*A20)-R*A6*S*(A16*A21 -A22+A16*A17)
1+A13*(-A20+A33*A17-A30)+R2*A6*(A16*A30-A33-A18) +R2*A7*(A16*A20
2+A17*A19-A16))
SV(14) = -(2.*(-A22+A17*A18+A17*A18)-R*A6*S*(A16*A22-A18+A26*A17)
1+A13*(-A17+A26*A17-A33)+R2*A6*(A16*A33-A26-A26)+R2*A7*(A16*A16
2+A23-A17-A19))
E=UIVALENCE(IH,A)
PUFCH 36,((A(I,J),J=1,N),I=1,N)
PUFCH 36,(SV(J),J=1,N)
36 FORMAT(/(5X,4E16.8))
CALL DIRV77(A,N)
PUFCH 36,((A(I,J),J=1,N),I=1,N)
DO 13 I=1,N
ANS(I)=0.
DO 13 J=1,N
13 ANS(I)=ANS(I)+ A(I,J)*SV(J)
D2=ANS(1)
D3=ANS(2)
D4=ANS(3)
D5=ANS(4)
D6=ANS(5)
D7=ANS(6)
D8=ANS(7)
D9=ANS(8)
E2=ANS(9)
E3=ANS(10)
E4=ANS(11)
E5=ANS(12)
E6=ANS(13)
E7=ANS(14)
PUFCH 36,D2,D3,D4,D5,D6,D7,D8,E2,E3,E4,E5,E6,E7,E8
```

58 FORMAT(4H D2=E16.8,4H D3=E16.8,4H D4=E16.8/4H E5=E16.8,4H E6=E16.8,
 1,4H D7=E16.8/4H E8=E16.8,4H E2=E16.8,4H E3=E16.8/4H E4=E16.8,
 24H E5=E16.8,4H E6=E16.8/4H E7=E16.8,4H E8=E16.8)
 END

 *LDISKKJPAR5

444 U(6)=(R2*R*C*((D2*6.*A39)+(D3-D2)*A23+(3.*D4-3.*D2)*A17
 1+5.*(D7-D3-D4+D2)*A16+(-2.*D2*A19))-2.*R2*C*((D2*(3./2.)*A29
 2*(E3-E2)*A26+(3.*E4-3.*D2)*A30+3.*(D7-E3-D4+D2)*(-1.))+(-2.*R2*
 3A33))+R2*C*S*((D2*6.*A27)+(E3-D2)*A18+5.*(D4-D2)*A21+3.*(E7-E3-
 4-E4+E2)*A17+(-2.*E2*A22))
 U(6)=U(6)-R2*R*C*S*((-D2*A18)+3.*(E2-E3)*A16+2.*(E3-E2)*A16)
 1+2.*R2*C*S*((-D2*A30)+3.*(D2-D3)*(-1.))+2.*(E3-D2)*A33)-R2*C*S*
 2*((-D2*A21)+3.*(D2-D3)*A17+2.*(E3-D2)*A22)+(1./2.)*(R2*2*(E23+
 3(A16*A16*A18)+(2.*A16*A18-2.*A26)*A16+(-2.*A16*A19))-2.*R2*C*S*
 4A26+(A16*A16*A30)+(2.*A16*A18-2.*A26)*(-1.))+(-2.*A16*A33))
 U(6)=U(6)+0.5*(R2*S*((A18+(A16*A16*A21)+(2.*A16*A18-2.*A26)*A17
 2+(-2.*A16*A22))-2.*R2*R*S*((-A17*A23)+(-A16*A18)+(-A18+A20*A16+A17
 3*A26-A18)*A16+(1.+A17*A16)*A19)+4.*R2*S*((-A17*A26)+(-A16*A30)+
 4*(-A18+A20*A16+A17*A26-A18)*(-1.)+(1.+A17*A16)*A33))
 U(6)=U(6)+0.5*(-2.*R*S*((-A17*A18)+(-A16*A21)+(-A18+A20*A16+
 1A17*A26-A18)*A17+(1.+A17*A16)*A22)+R2*S*((A17*A17*A23+A18+(-2.*
 2A20+2.*A17*A18)*A16+(-2.*A17)*A19)-2.*R*S*((A17*A17*A26+A30+(
 3-2.*A20+2.*A17*A18)*(-1.))+(-2.*A17)*A33))+S*((A17*A17*A18+A21+
 4*(-2.*A20+2.*A17*A18)*A17+(-2.*A17)*A22))
 U(6)=U(6)+ANU*(R2*R*C*((E2*6.*A39)+3.*(E3-E2)*A23+(E4-E2)*A18+
 13.*(E7-E3-E4+E2)*A16+(-2.*E2)*A19)-2.*R2*C*((E2*(3./2.)*A29)+
 23.*(E3-E2)*A26+(E4-E2)*A30+3.*(E7-E3-E4+E2)*(-1.))+(-2.*R2*
 3A33)+R2*C*S*((E2*6.*A27)+3.*(E3-E2)*A18+(E4-E2)*A21+3.*(E7-E3-E4+
 4E2)*A17+(-2.*E2)*A22))
 U(6)=U(6)+ANU*(0.5*C*C*R2*((A17*A17*A23)+A18+(-2.*A20+2.*A17*A18)*
 1A16-(1.*A17*A19))-R2*S*((A17*A17*A26)+A30+(-2.*A20+2.*A17*A18)*
 2*(-1.))+(-2.*A17*A33))+0.5*C*C*S*((A17*A17*A18)+A21+(-2.*A20+2.*
 3A17*A18)*A17+(-2.*A17)*A22))
 U(6)=U(6)*12.
 T1=12.*(R2*C*((E2*6.*A27)+3.*(E3-E2)*A18+(E4-E2)*A21+3.*(E7-
 1E3-E4+E2)*A17+(-2.*E2)*A22)+0.5*C*((A17*A17*A18)+A21+(-2.*A20+
 22.*A17*A18)*A17+(-2.*A17)*A22))
 T2=12.*(ANU*(R2*C*((D2*6.*A27)+(D3-D2)*A18+3.*(D4-D2)*A21+3.*(D
 17-D3-D4+D2)*A17+(-2.*D2)*A22)-R2*S*((-D2*A21)+3.*(D2-D3)*A17+
 22.*(E3-E2)*A22)+0.5*C*((R2*((A18)+(A16*A16*A21)+(2.*A16*A18
 3-2.*A26)*A17+(-2.*A16*A22))-2.*R*S*((-A17*A18)+(-A16*A21)+(-A18
 4+A20*A16+A17*A26-A18)*A17+(1.+A17*A16)*A22))))
 T3=T1+12.*ANU*0.5*C*C*(S*((A17*A17*A18)+A21+(-2.*A20+2.*A17*
 1A18)*A17+(-2.*A17)*A22))
 T4=12.*(1.-ANU)*(R2*C*((-D2*A30)+3.*(D2-D3)*(-1.))+2.*(E3-E2)*
 1A33)-R2*S*((-D2*A21)+3.*(D2-D3)*A17+2.*(E3-D2)*A22)+R2*C*((E2*
 2*((-E2*A26)+3.*(E2-E4)*(-1.))+2.*(E4-E2)*A33)-R2*S*((-E2*A18)
 3+3.*(E2-E4)*A17+2.*(E4-E2)*A22)-R2*S*((E2*(3./2.)*A29)+3.*(E3
 4-E2)*A26+(E4-E2)*A30+3.*(E7-E3-E4+E2)*(-1.))+(-2.*E2)*A33))
 T4=12.*(1.-ANU)*(R2*S*((E2*6.*A27)+3.*(E3-E2)*A18+(E4-E2)*
 1A21+3.*(E7-E3-E4+E2)*A17+(-2.*E2)*A22)+R2*C*((-A17*A26)+(-A16*
 2A30)+(-A18+A20*A16+A17*A26-A18)*(-1.)+(1.+A17*A16)*A33)
 3-R2*S*((-A17*A18)+(-A16*A21)+(-A18+A20*A16+A17*A26-A18)*A17

```

4+(1.+A17*A16)*A22))
T5=12.*(1.-A1U)*(-R*S*C*C*((A17*A17*A26)+A30+(-2.*A20+2.*A17*A16)
1*(-1.)+(-2.*A17)*A33)+S*S*C*C*((A17*A17*A18)+A21+(-2.*A20+2.*
2A17*A16)*A17+(-2.*A17)*A22))
U(6)=U(6)+T1+T2+T3+T4+T5
CALL LINK(KJPAR7)
END

```

```

****
*LDISKKJPARG
U(1)=12.*(R2*R2*C*D2*(-4.+2.*C2)+2.*R2*R2*S*C**2+12*C**3*S+26*(-4.+
12.*C1)+A1U*(R2*R2*C*C*(-4.+2.*C2)**2+2.*R2*C*C*S**2+12*C*C*S*S*(-4.
2+2.*C1)**2))+12.*(R*C**4*(-4.+2.*C1)**2+A1U*(R2*C**3*(-4.+2.*C1)
3**2))+12.*(1.-A1U)*(R2*S*C*C*D2+R*S*S*C*C*(-4.+2.*C1)**2)
U(1)=12.*(R2*R2*C*(D2*(12.-24.*C2+12.*C4)+(3.*D4-3.*D2)*(-4.*R.*
1C2))-2.*R2*R2*S*C*((D2*A26)+(-1.)*(3.*D4-3.*D2))+2*C**3*S*(12.*A16
2+(7.*D4-3.*D2)*A17)-R2*A16*C*S*(-D2*A16)+2.*R2*C*S*S*(-D2*(-1.))-
3*C*S*S*(-D2*A17)+1./2.*(R2*R2*(A16**3)-2.*R2*R*S*(A16*A17)*
4*(-1.))-R2*S*S*(A17*A16*A16)-2.*R2*R*S*(A16*(-A16)))
U(2)=U(2)+12.*(1./2.*(4.*R2*S*S*A16-2.*R2*S**3*A17*(-A16)+2*S*S*
1A16-2.*R*S**2*(-1.)+S**4*A17)
2+A1U*(R**3*C*C*((E2*A23)+A16*(E4-E2))-2.*R2*C*C*S*((A24+E2)+(-1.)
3*(E4-E2))+R*C*C*S*S*(A16*E2)+A17*(E4-E2)+(1./2.)*C**2*A16*C
4-R*S*C*C*(-1.)+(1./2.)*C*C*S*S*A17))
U(2)=U(2)+12.*(R*C**4*((A16+E2)+A17*(E4-E2))+1./2.*C**4/17+A1U
1*(R2*C**3*(A16*D2+A17*(3.*D4-3.*D2))-R*S*C**3*(-D2*A17)+1./2.*C*
2C*((R2*A16*A16*A17)-2.*R2*S*A17*(-A16)+S*S*A17))
U(2)=U(2)+12.*(1.-A1U)*(R2*C**3*D2-R*S*C**3*(-D2*A17)-R2*S*C*C*
1(A26*E2-(E4-E2))+R*S*S*C*C*(A16*E2+A17*(E4-E2))+R2*C*C*A16-R*S*C
2*C*(A17*(-A16))-R*S*C*C*(-1.)+S*S*C*C*A17)
CALL LINK(KJPAR5)

```

```

*LDISKKJPARG
N=6
U(3)=12.*(R2*R2*C*(D2*A16+A16*(D3-D2))-2.*R2*R2*S*C*(A30*D2-(D3-
1D2))+R2*C*S*S*(A21*D2+A17*(D3-D2))+0.5*(R2*R2*A16-2.*R2*R*S*(-1.)
2+R2*S*S*A17-2.*R2*R*S*(-A17*A16)+4.*R2*S*S*A17-2.*R*S**3*A17*
3*(-A17)+R2*S*S*A16*A17*A17-2.*R*S**3*(-A17)*A17+S**4/17*A17*A17))
U(3)=U(3)+12.*(A1U*(R2*R2*C*((E2*A17)+(3.*E3-3.*E2)*A16)-2.*R2*
1C*C*S*(E2*A30+(3.*E3-3.*E2)*(-1.))+R*C*C*S*S*(E2*A21+(3.*E3-3.*
2E2)*A17)+1.5*C*C*R2*(A16*A17*A17)-R*S*C*C*(-1.)*A17*A17+0.5*C*C*S*
3S*A17*A17*A17))
U(3)=U(3)+12.*(R*C**4*(E2*A21+(3.*E3-3.*E2)*A17)+0.5*C**4*A17*
1A17*A17+A1U*(R2*C**3*(D2*A21+(D3-D2)*A17)+0.5*C*C*(R2*A17-2.*R*
2S*(-A17)*A17+S*S*A17*A17*A17))
U(3)=U(3)+12.*(1.-A1U)*(R2*R2*C*E2-R2*S*C*C*(-E2)*A17-R2*S*C*C*
1(E2*A21+(3.*E3-3.*E2)*(-1.))+R*S*S*C*C*(E2*A21+(3.*E3-3.*E2)*A17
2)+R2*C*C*A17-R*S*C*C*(-A17)*A17-R*S*C*C*(-1.)*A17*A17+S*S*C*C*
3A17*A17*A17)
U(4)=12.*(R2*R2*C*(D2*A35+3.*(D4-D2)*A25+5.*(D6-D4)*A16)-2.*R2*R*
1S*C*(D2*A35+3.*(D4-D2)*A26+5.*(D6-D4)*(-1.))+R2*C*S*S*(D2*A35+
23.*(D4-D2)*A16+5.*(D6-D4)*A17)-R2*R2*C*S*(-D2*A23+(-D4+D2)*A16)+
32.*R2*C*S*S*(-D2*A26+(-D4+D2)*(-1.))-R*C*S**3*(-D2*A18+(-D4+D2)
4*A17)+0.5*(R2*R2*(A16*A16*A23+(2.*A16*A24)*A16))
U(4)=U(4)+12.*(0.5*(-2.*R2*R*S*(A16*A16*A26+(2.*A16*A24)*(-1.))
1+A26+3*S*(A16*A16*A18+2.*A16*A24*A17)-2.*R2*R*S*(-A16*A23+(-A24

```



```

E+A25*A16)*A16)+G.*R2*S*S*(-A16*A26+(-A24+A25*A16)*(-1.))-2.*A16*
2**5*(-A16*A16+(-A24+A25*A16)*A17)+12*S**4*(A26+(-2.*A25*A17))-2.
4*S**3*(A26+2.*A25)+S**4*(A16+(-2.*A25*A17)))
  U(4)=G(4)+12.*(A16*(R2*R*C*C*(A2*A3+(D4-E2)*A25+(D6-E4)*A17)
1-2.*R2*C*C*S*(A2*A30)+(E4-E2)*A25+(D6-E4)*(-1.))+R*C*C*(A2*(A2*
2*A39)+(D4-E2)*A16+(D6-E4)*A17)+0.*C*C*(A2*(A2*(A22+(-2.*A25*A17)
5-1)*S*C*C*(A26+2.*A25)+0.*S*C*C*S*(A16+(-2.*A25*A17))))
  U(4)=G(4)+12.*(R*C**4*(E2*A39+(D4-E2)*A16+(D6-E4)*A17)+0.*C**4*
1(A16+(-2.*A25*A17))+4*R*(R2*C**5*(D2*A39)+3.*(D4-E2)*A16+1.*(D6
2-E4)*A17)-R*S*C**3*(-D2*A16+(-D4+D2)*A17)+0.*C*C*(D2*(A16+A17)*
3A16+1.*A17*A25*A17)-2.*R*S*(-A16*A16+(-A24+A25*A16)*A17)
4*S*S*(A16+(-2.*A25*A17))))
  U(4)=G(4)+12.*(1.-A16)*(R2*C**5*(-D2*A26+(-D4+D2)*(-1.))-1.*S*
1C**5*(-D2*A16+(-D4+D2)*A17)-R2*S*C*C*(E2*A39)+(D4-E2)*A26+
2*(D6-E4)*(-1.))+R*S*S*C*C*(E2*A39)+(E4-E2)*A16+(D6-E4)*A17)+2*C
5*C*(-A16*A26+(-A24+A25*A16)*(-1.))-S*C*C*(-A16*A16+(-A24+A25*
4A16)*A17)-R*S*C*C*(A26+2.*A25)+S*S*C*C*(A16+(-2.*A25*A17))
  CALL LINK(KJPAR6)
  END

```

14000000701300003200702490240251196361130010200

14000000701300003200702490240251196361130010200
14000000701300003200702490240251196361130010200
14000000701300003200702490240251196361130010200

```
1) SIMUL 10 STRESSES IN CLAMPED SKETCH PLATES  
DIMENSION TETA(2), TAXI(6), P(50)  
COMMON C1,C2,C3,C4,C5,D2,D3,D4,D5,D6,D7,E2,E3,E4,E5,E6,E7,F1,  
1F2,F3,F4,F5, ANU,S,C,TAN,SEC,AXI,ETA,I,J,P  
READ 101,(TETA(I),I=1,2),(TAXI(J),J=1,6)  
PURCH 101,(TETA(I),I=1,2),(TAXI(J),J=1,6)  
101 FORMAT(3F10.5)  
300 READ 10,C1,C2,C3,C4,C5,D2,D3,D4,D5,D6,D7,E2,E3,E4,E5,E6,E7,F1,F2,  
1F3,F4,F5,THETA,R,ANU  
READ 2,Z1,Z2,Z3,Z4  
2 FORMAT(4E10.5)  
PURCH 10,R,THETA,ANU  
18 FORMAT(5F10.5,7H THETA=F10.5,5H ANU=F10.5)  
PURCH 1,C1,C2,C3,C4,C5,D2,D3,D4,D5,D6,D7,E2,E3,E4,E5,E6,E7,F1,F2,  
1F3,F4,F5,THETA,R,ANU  
10 FORMAT(3F10.5)  
1 FORMAT(4E16.8)  
TH1=THETA*0.17453292/10.  
S=SINF(TH1)  
C=COSE(TH1)  
TAN=S/C  
TANZ=SECTF(TAN)  
SEC=1./C  
DO 99 J=1,6  
AXI=TAXI(J)  
DO 99 I=1,2  
ETA=TETA(I)
```

P(1)=-4.*AXI+1.*AXI*ETA*ETA-4.*AXI*(ETA**4)+4.*(1/XI**2)-1.*(AXI**3
 1)*(ETA**2)+4.*(AXI**3)*(ETA**4)-ETA+2.*(ETA**3)-(ETA**5)+1.*Z1
 2*AXI*ETA-12.*(AXI**2)*(ETA**3)+6.*(AXI**2)*(ETA**5)-5.*(1/XI**4)*
 3ETA+10.*(AXI**4)*(ETA**3)-5.*(AXI**4)*(ETA**5)

CALL K01
 CALL K04
 CALL KJ2
 CALL KJ1
 CALL KJ3
 CALL K00
 CALL KJ4

W1XX=P(7)+C1*P(8)+C2*P(9)+C3*P(10)+C4*P(11)+C5*P(12)
 W1YY=P(17)+C1*P(20)+C2*P(21)+C3*P(22)+C4*P(23)+C5*P(24)
 W1XY=P(18)+C1*P(25)+C2*P(27)+C3*P(28)+C4*P(29)+C5*P(30)
 W0X=-0.5*(R**R*W1XX*SEC*SEC-2.*SEC*TAN**R*W1XY+(TAN*TAN+ANU)*W1YY)
 W0Y=-0.5*((1.+ANU*TAN*TAN)**W1YY+ANU*(R**SEC*SEC*W1XX-2.*SEC*TAN
 1**R*W1XY))

W3XX=F1*P(8)+F2*P(9)+F3*P(10)+F4*P(11)+F5*P(12)
 TAU0=R*SEC*W1XY-TAN*W1YY
 W0MAX=(0.5*(W0X+W0Y))+(0.5*SQRT((W0X-W0Y)**2+4.*(TAU0)**2))
 W0MIN=(0.5*(W0X+W0Y))-(0.5*SQRT((W0X-W0Y)**2+4.*(TAU0)**2))
 W3YY=F1*P(20)+F2*P(21)+F3*P(22)+F4*P(23)+F5*P(24)
 W3XY=F1*P(25)+F2*P(27)+F3*P(28)+F4*P(29)+F5*P(30)
 W03X=-0.5*(R**SEC*SEC*W3XX-2.*SEC*TAN**R*W3XY+(TAN*TAN+ANU)*W3YY)
 W03Y=-0.5*((1.+ANU*TAN*TAN)**W3YY+ANU*(R**SEC*SEC*W3XX-2.*SEC
 1*TAN**R*W3XY))

TAU0=R*SEC*W3XY-TAN*W3YY
 W03MAX=(0.5*(W03X+W03Y))+(0.5*SQRT((W03X-W03Y)**2+4.*(TAU0)**2))
 W03MIN=(0.5*(W03X+W03Y))-(0.5*SQRT((W03X-W03Y)**2+4.*(TAU0)**2))
 U1=02*P(31)+03*P(32)+04*P(33)+05*P(34)+06*P(35)+07*P(36)
 UY=02*P(37)+03*P(38)+04*P(39)+05*P(40)+06*P(41)+07*P(42)
 VY=01*P(43)+03*P(44)+04*P(45)+05*P(46)+06*P(47)+07*P(48)
 W1X=P(1)+C1*P(2)+C2*P(3)+C3*P(4)+C4*P(5)+C5*P(6)
 W1Y=P(13)+C1*P(14)+C2*P(15)+C3*P(16)+C4*P(17)+C5*P(18)
 W02X=R**R*SEC*UX-R**TAN*UY+ANU**R*VY+0.5*(R**SEC*SEC*W1X*W1X-2.*R**
 1*SEC*TAN**R*W1Y*W1Y+(ANU+TAN*TAN)*W1Y*W1Y)

W02Y=R**R*VY+0.5*W1Y*W1Y*(1.+ANU*TAN*TAN)+ANU*(R**SEC*UX-R**TAN*UY
 1+0.5*(R**R*W1X*W1X*SEC*SEC-2.*R**SEC*TAN**R*W1X*W1Y))
 W02XY=R**R*W1Y*W1Y*TAN*VY+W1Y*(R**SEC*W1X-TAN*W1Y)
 W2MAX=(0.5*(W02X+W02Y))+(0.5*SQRT((W02X-W02Y)**2+4.*(W02XY)**2))
 W2MIN=(0.5*(W02X+W02Y))-(0.5*SQRT((W02X-W02Y)**2+4.*(W02XY)**2))

IF(AXI-0.005) 25,25,26

25 IF(ETA-0.9) 26,26,27

27 W03Y=0.1*Z1
 W03X=W03X*Z1
 W03MAX=W03MAX*Z1
 W03MIN=W03MIN*0.1*Z1
 W02X=W02X*Z2
 W02Y=W02Y*Z2
 W2MAX=W2MAX*Z2
 W2MIN=W2MIN*Z2
 GO TO 201

20 CONTINUE
 W03Y=W03Y*Z3

MOBX=10.8/6H
 M2MAX=11.8/6H
 M2MIN=11.8/6H
 MOBY=10.8/6H
 M2MAX=11.8/6H
 M2MIN=11.8/6H
 M2XY=10.8/6H

```

101 PUNCH 100
100 FORMAT(10X, 'PERDING STRESSES')
102 PUNCH 102, MOX, MOY, TAUG, M2MAX, M2MIN, MOBX, MOBY, TAUB, M2MAX, M2MIN
103 PUNCH 103, MOX=816.8, 6H MOY=816.8, 6H TAUG=816.8/7H M2MAX=816.8,
17.1 M2MIN=816.8/6H MOBX=816.8, 6H MOBY=816.8, 6H TAUB=816.8/
27H M2MAX=816.8, 7H M2MIN=816.8)
104 PUNCH 104, M2X, M2Y, M2XY, M2MAX, M2MIN, AXI, ETA
105 PUNCH 105, M2X=816.8, 6H M2Y=816.8, 7H M2XY=816.8/7H M2MAX=816.8,
17.1 M2MIN=816.8/6H AXI=86.3, 5H ETA=86.3)
66 TO 68
END

```

BLOCAL, KJ1, KJ2, KJ3, KJ4

0.	-1.	0.	0.25	0.3	0.35	0.4	0.41
0.0283366	1.0821717	-0.031583	0.2871587	0.1638461	1.8056127	-0.108560	-1.9580
3.9687131	0.4884474	-4.040757	1.2635980	-4.084084	5.6228829	1.7503631	-7.738
17.311904	0.3388749	1.1705073	-0.008963	1.7775504	1.2291226	0.	0.3
0.3383							
0.43	0.45	1.	0.513				
-0.041149	0.006814	-0.001683	-0.027448	0.3244454	1.8628599	-1.021573	-3.327
-3.081146	-1.340746	-5.017219	1.5374749	-4.176846	10.840732	2.9471995	-2.249
25.128278	0.319018	1.7693852	-0.086921	3.1558596	1.2253061	15.	0.
3.3333							
0.4	0.47	0.4	-0.6235				
-0.070919	0.6404040	-0.005818	-0.398525	0.8643556	0.6454937	-4.594001	-3.380
-4.582424	-3.248934	-15.06079	2.0952549	-4.530145	19.005327	3.590871	1.9676
39.586915	0.2736639	2.3966780	-0.057855	4.9104088	0.0219636	30.	0.
0.3333							
0.4	0.3	0.38	-1.54				
-0.084847	0.3446099	-0.025627	-0.712415	1.5062099	0.1375416	-3.601022	-4.971
-0.372049	-3.384006	-25.92181	2.9104908	-5.981934	32.506423	3.2738428	-6.337
36.537413	0.1925858	2.6887051	0.1503837	6.4493865	-2.490413	45.	0.
0.3333							
0.46	0.59	0.5	0.148				
-0.083358	0.3193961	-0.034448	-0.772948	1.6643584	0.1309978	-2.601147	-10.48
1.5113085	-2.616377	-28.94166	3.2794362	-6.790375	37.990865	3.0500532	-13.20
65.473939	0.2023443	2.5343719	0.2528271	6.2652200	-3.042813	50.	0.
0.3333							
0.46	0.5	0.5	0.0915				
-0.081819	0.7385456	-0.051260	-0.824604	1.8684829	-0.288222	0.2920520	-14.28
3.4980980	-0.944880	-36.51766	4.3117554	-8.920896	49.123947	2.6110637	-40.43
32.681437	0.3190798	1.6915845	0.4800764	4.5664996	-3.236667	60.	0.3
0.3333							
0.4	0.37	0.4	0.5				

*JUL 5
*MAY 5
*PAC. N1610
*LDISK

SUBROUTINE KJ1

```

P(2)=-4.*AXI*(ETA**2)+6.*AXI*(ETA**4)-4.*AXI*(ETA**6)+4.*(AXI**2)
1*(ETA**2)-3.*(AXI**3)*(ETA**4)+4.*(AXI**3)*(ETA**6)-(ETA**3)+2.*(
2ETA**5)-(ETA**7)+6.*(AXI**2)*(ETA**3)-12.*(AXI**2)*(ETA**5)
3+4.*(AXI**2)*(ETA**7)-5.*(AXI**4)*(ETA**3)+10.*(AXI**4)*(ETA**5)
4-5.*(AXI**4)*(ETA**7)
P(3)=2.*AXI-6.*AXI*(ETA**2)+2.*AXI*(ETA**4)-8.*(AXI**3)+16.*(
1AXI**3)*(ETA**2)-3.*(AXI**3)*(ETA**4)+6.*(AXI**5)-12.*(AXI**5)*
2(ETA**2)+8.*(AXI**5)*(ETA**4)-3.*(AXI**2)*ETA+6.*(AXI**2)*
3(ETA**5)-3.*(AXI**2)*(ETA**5)+10.*(AXI**4)*ETA-20.*(AXI**4)*(ETA**
45)+10.*(AXI**4)*(ETA**5)-7.*(AXI**6)*ETA+14.*(AXI**6)*(ETA**3)
P(3)=P(3)-7.*(AXI**6)*(ETA**5)
P(4)=-1*(ETA**5)+6.*(AXI**2)*(ETA**5)-5.*(AXI**4)*(ETA**5)-4.*
1AXI*(ETA**4)+4.*(AXI**3)*(ETA**4)+2.*(ETA**7)-12.*(AXI**2)*
2(ETA**7)+10.*(AXI**4)*(ETA**7)+8.*AXI*(ETA**6)-8.*(AXI**3)*
3(ETA**6)-(ETA**9)+6.*(AXI**2)*(ETA**9)-5.*(AXI**4)*(ETA**9)
4-4.*AXI*(ETA**8)+4.*(AXI**3)*(ETA**8)
P(5)=4.*(AXI**3)-5.*(AXI**4)*ETA-12.*(AXI**5)+14.*(AXI**6)*ETA+3.*
1(AXI**7)-9.*(AXI**8)*ETA-8.*(AXI**5)*(ETA**2)+10.*(AXI**4)*
2(ETA**5)+24.*(AXI**5)*(ETA**2)-20.*(AXI**6)*(ETA**5)-16.*
3(AXI**7)*(ETA**2)+16.*(AXI**6)*(ETA**5)+4.*(AXI**3)*(ETA**4)-5.*
4(AXI**4)*(ETA**5)-12.*(AXI**5)*(ETA**4)+14.*(AXI**6)*(ETA**5)
P(5)=P(5)+1.*(AXI**7)*(ETA**4)-9.*(AXI**4)*(ETA**5)
P(6)=2.*AXI*(ETA**2)-3.*(AXI**2)*(ETA**3)-6.*(AXI**3)*(ETA**2)
1+10.*(AXI**4)*(ETA**3)+6.*(AXI**5)*(ETA**2)-7.*(AXI**6)*(ETA**3)
2-4.*AXI*(ETA**4)+6.*(AXI**2)*(ETA**5)+13.*(AXI**3)*(ETA**4)
3-20.*(AXI**4)*(ETA**5)-12.*(AXI**5)*(ETA**4)+14.*(AXI**6)*(
4ETA**5)+8.*AXI*(ETA**6)-3.*(AXI**2)*(ETA**7)-6.*(AXI**3)*(ETA**6)
P(6)=P(6)+10.*(AXI**4)*(ETA**7)+6.*(AXI**5)*(ETA**6)-7.*(AXI**6)
1*(ETA**7)
RETURN
END

```

SUBROUTINE KJA

```

P(7)=-4.*6.*(ETA**2)-4.*(ETA**4)+12.*(AXI**2)-24.*(AXI**2)*(ETA**2
1)+12.*(AXI**2)*(ETA**4)+12.*AXI*ETA-24.*AXI*(ETA**3)+12.*AXI*
2(ETA**5)-20.*(AXI**3)*ETA+40.*(AXI**3)*(ETA**3)-20.*(AXI**3)*
3(ETA**5)
P(8)=-4.*(ETA**2)+6.*(ETA**4)-4.*(ETA**6)+12.*(AXI**2)*(ETA**2)
1-24.*(AXI**2)*(ETA**4)+12.*(AXI**2)*(ETA**6)+12.*AXI*(ETA**3)
2-24.*AXI*(ETA**5)+12.*AXI*(ETA**7)-20.*(AXI**3)*(ETA**3)+40.*
3(AXI**5)*(ETA**5)-20.*(AXI**3)*(ETA**7)
P(9)=2.-4.*(ETA**2)+2.*(ETA**4)-24.*(AXI**2)+45.*(AXI**2)*(ETA**2)
1-24.*(AXI**2)*(ETA**4)+30.*(AXI**4)-60.*(AXI**4)*(ETA**2)+30.*
2(AXI**4)*(ETA**4)-6.*AXI*ETA+12.*AXI*(ETA**3)-6.*AXI*(ETA**5)
P(10)=12.*AXI*(ETA**5)-20.*(AXI**3)*(ETA**5)-4.*(ETA**4)+12.*(
P(11)=12.*(AXI**2)-20.*(AXI**3)*ETA-60.*(AXI**4)+84.*(AXI**5)*ETA+
P(11)=P(11)+4.*(AXI**5)*(ETA**5)+56.*(AXI**6)*(ETA**4)
P(12)=2.*(ETA**2)-6.*AXI*(ETA**3)-24.*(AXI**2)*(ETA**2)+40.*
P(12)=P(12)+40.*(AXI**3)*(ETA**7)+30.*(AXI**4)*(ETA**6)-42.*

```

RETURN
END

SUBROUTINE K02

```

P(13)=-4.*ETA+4.*(ETA**3)+8.*(AXI**2)*ETA-8.*(AXI**2)*(ETA**3)
1-4.*(AXI**4)*ETA+4.*(AXI**4)*(ETA**3)-AXI+6.*AXI*(ETA**2)-5.*
2AXI*(ETA**4)+2.*(AXI**5)-12.*(AXI**3)*(ETA**2)+10.*(AXI**3)*
3(ETA**4)-(AXI**5)+6.*(AXI**5)*(ETA**2)-5.*(AXI**5)*(ETA**4)
P(14)=1.*ETA-4.*(ETA**3)+6.*(ETA**5)-4.*(AXI**2)*ETA+16.*(
1AXI**2)*(ETA**3)-12.*(AXI**2)*(ETA**5)+2.*(AXI**4)*ETA-8.*(AXI
2**4)*(ETA**3)+6.*(AXI**4)*(ETA**5)-3.*AXI*(ETA**2)+10.*AXI*(
3ETA**4)-7.*AXI*(ETA**6)+6.*(AXI**3)*(ETA**2)-20.*(AXI**3)*(ETA**4)
4+14.*(AXI**3)*(ETA**6)-3.*(AXI**5)*(ETA**2)+10.*(AXI**5)*(ETA**4)
P(14)=P(14)-7.*(AXI**5)*(ETA**6)

```

```

P(15)=-4.*(AXI**2)*ETA+4.*(AXI**2)*(ETA**3)+8.*(AXI**4)*ETA
1-6.*(AXI**4)*(ETA**3)-4.*(AXI**6)*ETA+4.*(AXI**6)*(ETA**3)-
2(AXI**3)+6.*(AXI**3)*(ETA**2)-5.*(AXI**3)*(ETA**4)+2.*(AXI**5)
3-12.*(AXI**5)*(ETA**2)+10.*(AXI**5)*(ETA**4)-(AXI**7)+6.*(AXI**7)
4*(ETA**2)-5.*(AXI**7)*(ETA**4)
P(16)=4.*(ETA**3)-5.*AXI*(ETA**4)-12.*(ETA**5)+14.*AXI*(ETA**6)
1-9.*AXI*(ETA**8)+8.*(ETA**7)-8.*(AXI**2)*(ETA**3)+10.*(AXI**3)*
2(ETA**4)+24.*(AXI**2)*(ETA**5)-28.*(AXI**3)*(ETA**6)-16.*(AXI**2)
3*(ETA**7)+16.*(AXI**3)*(ETA**8)+4.*(AXI**4)*(ETA**3)-5.*(AXI**5)*
4(ETA**4)-12.*(AXI**4)*(ETA**5)+14.*(AXI**5)*(ETA**6)

```

```

P(16)=P(16)+8.*(AXI**4)*(ETA**7)-9.*(AXI**5)*(ETA**8)
P(17)=-*(AXI**5)+6.*(AXI**5)*(ETA**2)-5.*(AXI**5)*(ETA**4)-4.*
1(AXI**4)*ETA+4.*(AXI**4)*(ETA**3)+2.*(AXI**7)-12.*(AXI**7)*(ETA**2
2)+10.*(AXI**7)*(ETA**4)+6.*(AXI**6)*ETA-8.*(AXI**6)*(ETA**3)
3-(AXI**9)+6.*(AXI**9)*(ETA**2)-5.*(AXI**9)*(ETA**4)-4.*(AXI**8)*
4ETA+4.*(AXI**8)*(ETA**3)

```

SUBROUTINE K05

```

P(18)=2.*(AXI**2)*ETA-3.*(AXI**5)*(ETA**2)-8.*(AXI**2)*(ETA**3)
1+10.*(AXI**3)*(ETA**4)+6.*(AXI**2)*(ETA**5)-7.*(AXI**3)*(ETA**6)
2-6.*(AXI**4)*ETA+6.*(AXI**5)*(ETA**2)+16.*(AXI**4)*(ETA**3)
3-20.*(AXI**5)*(ETA**4)-12.*(AXI**4)*(ETA**5)+14.*(AXI**5)*(ETA
4**6)+2.*(AXI**6)*ETA-3.*(AXI**7)*(ETA**2)-8.*(AXI**6)*(ETA**3)

```

```

P(18)=P(18)+10.*(AXI**7)*(ETA**4)+6.*(AXI**6)*(ETA**5)-7.*(AXI**7)
1*(ETA**6)
P(19)=-4.+12.*(ETA**2)+8.*(AXI**2)-24.*(AXI**2)*(ETA**2)-4.*
P(20)=2.-24.*(ETA**2)+30.*(ETA**4)-4.*(AXI**2)+48.*(AXI**2)*
P(20)=P(20)-42.*(AXI**5)*(ETA**5)
P(21)=-4.*(AXI**2)+12.*(AXI**2)*(ETA**2)+8.*(AXI**4)-24.*(AXI**4)
P(22)=12.*(ETA**2)-20.*AXI*(ETA**3)-60.*(ETA**4)+84.*AXI*(ETA**5)-
P(22)=P(22)+56.*(AXI**4)*(ETA**6)-72.*(AXI**5)*(ETA**7)
P(23)=12.*(AXI**5)*ETA-20.*(AXI**5)*(ETA**3)-4.*(AXI**4)+12.*
P(24)=2.*(AXI**2)-6.*(AXI**3)*ETA-24.*(AXI**2)*(ETA**2)+40.*
P(24)=P(24)+30.*(AXI**6)*(ETA**4)-42.*(AXI**7)*(ETA**5)

```

RETURN
END

340003200701300003200702490240251196361130010200

***JOL 5
***FOR 5
***FANCK 1610

*LDISK

SUBROUTINE KJB

COMMON C1,C2,C3,C4,C5,D2,D3,D4,D5,D6,D7,E2,E3,E4,E5,E6,E7,F1,
IF2,F3,F4,F5,G,ANU,S,C,TAM,SEC,AXI,ETA,I,J,P

P(25)=16.*AXI*ETA-16.*AXI*(ETA**3)-16.*(AXI**2)*ETA+16.*(AXI**3)*

P(26)=-9.*AXI*ETA+32.*AXI*(ETA**3)-24.*AXI*(ETA**5)+8.*(AXI**3)

P(27)=-6.*AXI*ETA+8.*AXI*(ETA**3)+32.*(AXI**3)*ETA-32.*(AXI**3)

P(28)=-5.*(ETA**4)+30.*(AXI**2)*(ETA**4)-25.*(AXI**4)*(ETA**4)

P(29)=-5.*(AXI**4)+14.*(AXI**6)-9.*(AXI**8)-16.*(AXI**3)*ETA

P(30)=4.*AXI*ETA-9.*(AXI**2)*(ETA**2)-16.*(AXI**3)*ETA+30.*

P(30)=P(30)+70.*(AXI**4)*(ETA**6)+36.*(AXI**5)*(ETA**5)

RETURN

END

SUBROUTINE KJC

P(31)=1.-2.*AXI*ETA-3.*(AXI**2)+4.*(AXI**3)*ETA-(ETA**2)+2.*AXI*(
1ETA**3)+3.*(AXI**2)*(ETA**2)-4.*(AXI**3)*(ETA**3)

P(32)=(ETA**2)-2.*AXI*(ETA**3)-3.*(AXI**2)*(ETA**2)+4.*(AXI**3)

1*(ETA**3)-(ETA**4)+2.*AXI*(ETA**5)+3.*(AXI**2)*(ETA**4)

2-4.*(AXI**3)*(ETA**5)

P(33)=3.*(AXI**2)-4.*(AXI**3)*ETA-5.*(AXI**4)+6.*(AXI**5)*ETA

1-5.*(AXI**2)*(ETA**2)+4.*(AXI**3)*(ETA**3)+5.*(AXI**4)*(ETA**2)

2-6.*(AXI**5)*(ETA**3)

P(34)=(ETA**4)-2.*AXI*(ETA**5)-3.*(AXI**2)*(ETA**4)+4.*(AXI**3)*

1(ETA**5)-(ETA**6)+2.*AXI*(ETA**7)+3.*(AXI**2)*(ETA**6)-4.*(AXI**3)

2*(ETA**7)

P(35)=5.*(AXI**4)-6.*(AXI**5)*ETA-7.*(AXI**6)+8.*(AXI**7)*ETA-5.

1*(AXI**4)*(ETA**2)+6.*(AXI**5)*(ETA**3)+7.*(AXI**6)*(ETA**2)

2-8.*(AXI**7)*(ETA**3)

P(36)=3.*(AXI**2)*(ETA**2)-4.*(AXI**3)*(ETA**3)-5.*(AXI**4)*

1(ETA**2)+3.*(AXI**5)*(ETA**3)-3.*(AXI**2)*(ETA**4)+4.*(AXI**3)

2*(ETA**3)+5.*(AXI**4)*(ETA**4)-6.*(AXI**5)*(ETA**5)

P(37)=-1*(AXI**2)+1*(AXI**4)-2.*AXI*ETA+3.*(AXI**2)*(ETA**2)+2.*(AXI

1**3)*ETA-3.*(AXI**4)*(ETA**2)

P(38)=2.*AXI*ETA-3.*(AXI**2)*(ETA**2)-2.*(AXI**3)*ETA+3.*(AXI**4)

1*(ETA**2)-4.*AXI*(ETA**3)+5.*(AXI**2)*(ETA**4)+4.*(AXI**3)*(ETA**3

2)-5.*(AXI**4)*(ETA**4)

P(39)=-1*(AXI**4)+1*(AXI**6)-2.*(AXI**3)*ETA+3.*(AXI**4)*(ETA**2)

1+2.*(AXI**5)*ETA-3.*(AXI**6)*(ETA**2)

P(40)=4.*AXI*(ETA**3)-5.*(AXI**2)*(ETA**4)-4.*(AXI**3)*(ETA**3)

1+5.*(AXI**4)*(ETA**4)-6.*AXI*(ETA**5)+7.*(AXI**2)*(ETA**6)+6.

2*(AXI**3)*(ETA**5)-7.*(AXI**4)*(ETA**6)

P(41)=-1*(AXI**5)+1*(AXI**8)-2.*(AXI**5)*ETA+3.*(AXI**6)*(ETA**2)+

22.*(AXI**7)*ETA-3.*(AXI**8)*(ETA**2)

RETURN

END

34003200701360303200702490240251196361150010200

**JOB 5

**FOR 5

**PAPR1616

*LDISK

SUBROUTINE KJ4

COMMON C1,C2,C3,C4,C5,D2,D3,D4,D5,D6,D7,E2,E3,E4,E5,E6,E7,F1,

IF2,F3,F4,F5,G,ANU,S,C,TAM,SEC,AXI,ETA,I,J,P

```

IFR, F5, F4, F3, , ANU, S, C, TAN, SEC, AXI, ETA, I, J, P
P(42)=2.*(AXI**5)*ETA-3.*(AXI**4)*(ETA**2)-2.*(AXI**3)*ETA+5.
1*(AXI**6)*(ETA**2)-4.*(AXI**5)*(ETA**3)+5.*(AXI**4)*(ETA**4)
2+4.*(AXI**5)*(ETA**5)-1.*(AXI**6)*(ETA**4)
P(43)=1.-1.*AXI*ETA-(AXI**2)+2.*(AXI**3)*ETA-3.*(ETA**2)+4.*AXI
1*(ETA**4)+7.*(AXI**2)*(ETA**2)-4.*(AXI**5)*(ETA**3)
P(44)=3.*(ETA**4)-4.*AXI*(ETA**3)-3.*(AXI**2)*(ETA**2)+4.*(AXI
1**5)*(ETA**3)-5.*(ETA**4)+6.*AXI*(ETA**5)+5.*(AXI**2)*(ETA**4)-6.
2*(AXI**5)*(ETA**5)
P(45)=(AXI**2)-2.*(AXI**3)*ETA-(AXI**4)+2.*(AXI**5)*ETA-3.*(AXI
1**2)*(ETA**2)+4.*(AXI**3)*(ETA**3)+3.*(AXI**4)*(ETA**2)-4.*
2*(AXI**5)*(ETA**5)
P(46)=5.*(ETA**4)-6.*AXI*(ETA**5)-5.*(AXI**2)*(ETA**4)+6.*(
1AXI**5)*(ETA**5)-7.*(ETA**6)+8.*AXI*(ETA**7)+7.*(AXI**2)*(ETA**5)
2-8.*(AXI**5)*(ETA**7)
P(47)=(AXI**4)-2.*(AXI**5)*ETA-(AXI**6)+2.*(AXI**7)*ETA-3.*(
1AXI**4)*(ETA**2)+4.*(AXI**5)*(ETA**3)+3.*(AXI**6)*(ETA**2)
2-4.*(AXI**7)*(ETA**5)
P(48)=3.*(AXI**2)*(ETA**2)-4.*(AXI**3)*(ETA**3)-3.*(AXI**4)*(ETA**
12)+4.*(AXI**5)*(ETA**3)-5.*(AXI**2)*(ETA**4)+6.*(AXI**3)*(
2ETA**5)+5.*(AXI**4)*(ETA**4)-6.*(AXI**5)*(ETA**5)
RETURN
END

```

340008E00701330003200702490240251126361130010200

***JOB B

***FORX B

***FALOKI 10

C EXPERIMENTAL RESULTS FOR SKETCHED PLATE

100 READ 10, SA, SB, SC

10 FORMAT(DF10.5)

PUNCH 11, SA, SB, SC

11 FORMAT(4H SA=E16.8, 4H SB=E16.8, 4H SC=E16.8)

EZ=5000000.

AMU=0.5555

AMINS=E16*((SA+SC)/(1.-AMU)+(1./(1.+AMU))*SQRT((SA-SC)**2
1+(2.*SB-(SA+SC))**2))

AMINS=E2*((SA+SC)/(1.-AMU)-(1./(1.+AMU))*SQRT((SA-SC)**2+
1+(2.*SB-(SA+SC))**2))

TAU=E2/(1.+AMU)*SQRT((SA-SC)**2+(2.*SB-(SA+SC))**2)

ANGLE=0.5*ATANF(2.*SB-(SA+SC)/(SA-SC))

DEGRE=ANGLE/0.017453292

PUNCH 13, AMINS, AMINS, DEGRE

13 FORMAT(7H AMINS=E16.8, 7H AMINS=E16.8, 7H DEGRE=F10.5)

GO TO 100

END

APPENDIX B

EXPERIMENTAL DATA FOR LATERAL DEFLECTIONS

AND UNIT STRAINS

Table 5. Lateral Deflection Results for Plate 1, Test 1.

(inches)

	p.s.i.	qb^4 / Dh	Loading	Unloading	Average	w/h
Dial Gauge No. 1	0.375	46.79	0.042	0.044	0.043	0.344
	0.5	62.40	0.057	-	0.057	0.456
	0.625	78.00	0.067	0.066	0.066	0.532
	0.750	93.6	0.084	0.090	0.087	0.696
	1.000	124.8	0.102	0.107	0.104	0.836
	1.250	156.0	0.117	0.121	0.119	0.952
	1.500	187.2	0.145	0.145	0.145	1.160
	1.750	218.4	0.159	0.160	0.160	1.276
	2.000	245.0	0.174	0.179	0.177	1.412
	2.250	280.8	0.194	0.191	0.193	1.540
	2.500	312.0	0.205	-	0.205	1.640
Dial Gauges Nos. 2 and 3	0.375	46.79	0.035	0.036	0.035	0.284
	0.500	62.4	0.049	-	0.049	0.392
	0.625	78.0	0.057	0.056	0.056	0.452
	0.750	93.6	0.074	0.076	0.075	0.600
	1.000	124.8	0.090	0.093	0.091	0.732
	1.250	156.0	0.103	0.105	0.104	0.832
	1.500	187.3	0.116	0.120	0.118	0.944
	1.750	218.4	0.130	0.131	0.131	1.044
	2.000	245.0	0.142	0.143	0.142	1.140
	2.250	280.8	0.156	0.154	0.155	1.240
	2.500	312.0	0.169	-	0.169	1.352
Dial Gauge No. 4	0.375	46.79	0.021	0.025	0.023	0.184
	0.500	62.4	0.029	-	0.029	0.232
	0.625	78.0	0.035	0.038	0.036	0.292
	0.750	93.6	0.046	0.051	0.049	0.388
	1.000	124.8	0.056	0.060	0.058	0.464
	1.250	156.0	0.065	0.072	0.068	0.548
	1.500	187.2	0.075	0.078	0.077	0.612
	1.750	218.4	0.083	0.087	0.085	0.680
	2.000	245.0	0.092	0.097	0.095	0.756
	2.250	280.8	0.101	0.101	0.101	0.808
	2.500	312.0	0.111	-	0.111	0.888

Table 6. Lateral Deflection Results for Plate 1, Test 2.

(inches)

	p.s.i.	qb^4 / Dh	Loading	Unloading	Average	w/h
Dial Gauge No. 1	0.375	46.79	0.045	0.048	0.047	0.372
	0.500	62.4	--	-	-	-
	0.625	78.0	0.064	0.071	0.067	0.54
	0.75	93.6	0.084	0.089	0.085	0.69
	1.000	124.8	0.101	0.107	0.104	0.832
	1.250	156.0	0.119	0.121	0.120	0.96
	1.500	187.2	0.141	0.147	0.144	1.152
	1.750	218.4	0.157	0.161	0.159	1.272
	2.000	245.0	0.177	0.177	0.177	1.416
	2.250	280.8	0.193	0.193	0.193	1.544
	2.500	312.0	0.206	-	0.206	1.648
Dial Gauges Nos. 2 and 3	0.375	46.79	0.037	0.039	0.038	0.304
	0.500	62.4	-	-	-	-
	0.625	78.0	0.055	0.059	0.057	0.456
	0.750	93.6	0.073	0.075	0.074	0.592
	1.000	124.8	0.089	0.091	0.090	0.720
	1.250	156.0	0.104	0.106	0.105	0.840
	1.500	187.2	0.116	0.120	0.118	0.944
	1.750	218.4	0.129	0.131	0.130	1.040
	2.000	245.0	0.143	0.143	0.143	1.144
	2.250	280.8	0.155	0.155	0.155	1.240
	2.500	312.0	0.165	-	0.165	1.320
Dial Gauge No. 4	0.375	46.79	0.023	0.026	0.024	0.196
	0.500	62.4	-	-	-	-
	0.625	78.0	0.035	0.036	0.036	0.284
	0.750	93.6	0.046	0.048	0.047	0.376
	1.000	124.8	0.056	0.061	0.059	0.468
	1.250	156.0	0.066	0.072	0.069	0.552
	1.500	187.2	0.076	0.081	0.079	0.628
	1.750	218.4	0.084	0.088	0.086	0.688
	2.000	245.0	0.092	0.096	0.094	0.752
	2.250	280.8	0.102	0.102	0.102	0.816
	2.500	312.0	0.109	-	0.109	0.872

Table 7. Lateral Deflection Results for Plate 1, Test 3.

(inches)

	p.s.i.	qb^4 / Dh	Loading	Unloading	Average	w/h
Dial Gauge 1	0.625	78.0	0.065	0.079	0.072	0.576
	1.000	124.8	0.101	0.104	0.102	0.82
	1.500	187.3	0.143	0.145	0.144	1.152
	2.000	245.0	0.169	0.170	0.169	1.352
	2.500	312.0	0.204	-	0.204	1.632
Dial Gauges Nos. 2 and 3	0.625	78.0	0.056	0.057	0.057	0.452
	1.000	124.8	0.089	0.089	0.089	0.712
	1.500	187.2	0.117	0.117	0.117	0.936
	2.000	245.0	0.143	0.140	0.142	1.132
	2.500	312.0	0.164	0.162	0.163	1.304
Dial Gauge 1	0.625	78.0	0.034	0.037	0.036	0.284
	1.000	124.8	0.055	0.059	0.057	0.456
	1.500	187.2	0.075	0.080	0.078	0.620
	2.000	245.0	0.092	0.095	0.094	0.748
	2.500	312.0	0.108	0.107	0.108	0.860

Table 8. Lateral Deflection Results for Plate 2, Test 1.

(inches)

	Height of water (in.)	qb^4 / Dh	Loading	Unloading	Average	w/h
Dial Gauge No. 1	0.5	36.05	0.018	0.020	0.019	0.304
	1.0	72.10	0.036	0.039	0.038	0.60
	1.5	108.15	0.050	0.051	0.050	0.808
	2.0	144.20	0.060	0.064	0.062	0.902
	2.5	180.25	0.070	0.073	0.071	1.14
	3.0	216.30	0.078	0.083	0.080	1.28
	3.5	252.35	0.090	0.094	0.092	1.47
	4.0	288.41	0.096	0.099	0.98	1.56
Dial Gauges No. 2 and 3	0.5	36.05	0.013	0.013	0.013	0.208
	1.0	72.10	0.021	0.022	0.021	0.344
	1.5	108.15	0.032	0.033	0.032	0.520
	2.0	144.2	0.036	0.039	0.038	0.608
	2.5	180.25	0.042	0.045	0.044	0.696
	3.0	216.3	0.044	0.051	0.048	0.760
	3.5	252.35	0.052	0.058	0.055	0.880
	4.0	288.41	0.055	0.057	0.056	0.896
Dial Gauge No. 4	0.5	36.05	0.006	0.005	0.006	0.088
	1.0	72.10	0.014	0.013	0.014	0.216
	1.5	108.15	0.020	0.021	0.020	0.328
	2.0	144.20	0.025	0.027	0.026	0.416
	2.5	180.25	0.029	0.034	0.032	0.504
	3.0	216.30	0.035	0.035	0.035	0.560
	3.5	252.35	0.042	0.041	0.041	0.664
	4.0	288.41	0.044	-	0.044	0.704

Table 9. Lateral Deflection Results for Plate 2, Test 2.

(inches)

	Height of water (in)	qb^4 / Dh	Loading	Unloading	Average	w/h
Dial Gauge No. 1	0.5	36.05	0.019	0.021	0.020	0.320
	1.00	72.10	0.029	0.035	0.032	0.512
	1.5	108.15	0.046	0.046	0.046	0.736
	2.0	144.20	0.061	0.062	0.062	0.954
	2.5	180.24	0.069	0.070	0.070	1.112
	3.0	216.30	0.082	0.084	0.083	1.328
	3.5	252.35	0.086	0.090	0.088	1.408
	4.0	288.41	0.096	0.102	0.099	1.584
Dial Gauges No. 2 and 3	0.5	36.05	0.014	0.010	0.012	0.184
	1.0	72.10	0.025	0.021	0.023	0.368
	1.5	108.15	0.030	0.032	0.031	0.496
	2.0	144.20	0.038	0.038	0.038	0.608
	2.5	180.25	0.043	0.045	0.044	0.704
	3.0	216.30	0.050	0.047	0.049	0.776
	3.5	252.35	0.058	0.056	0.057	0.912
	4.0	288.41	0.058	0.060	0.059	0.944
Dial Gauge No. 4	0.5	36.05	0.005	0.006	0.005	0.088
	1.0	72.10	0.011	0.013	0.012	0.192
	1.5	108.15	0.018	0.019	0.019	0.296
	2.0	144.20	0.023	0.023	0.023	0.368
	2.5	180.24	0.028	0.032	0.030	0.480
	3.0	216.30	0.031	0.033	0.032	0.512
	3.5	252.35	0.038	0.040	0.039	0.624
	4.0	288.41	0.041	0.042	0.042	0.664

Table 10. Lateral Deflection Results for Plate 2, Test 3.

(inches)

Height of water(in.)	qb^4 / Dh	Loading	Unloading	Average	w/n	
Dial Gauge No. 1	0.5	36.05	0.018	0.019	0.018	0.296
	1.00	72.10	0.033	0.034	0.034	0.536
	1.50	108.15	0.045	0.046	0.046	0.728
	2.00	144.20	0.061	0.062	0.062	0.984
	2.50	180.25	0.065	0.066	0.066	1.506
	3.0	216.30	0.075	0.076	0.076	1.208
	3.5	252.35	0.087	0.088	0.087	1.400
	4.0	288.41	0.096	0.097	0.097	1.544
Dial Gauges No. 2 and 3	0.5	36.05	0.013	0.014	0.014	0.216
	1.00	72.10	0.022	0.022	0.022	0.352
	1.50	108.15	0.030	0.031	0.031	0.488
	2.00	144.20	0.037	0.038	0.038	0.600
	2.50	180.25	0.044	0.044	0.044	0.704
	3.00	216.30	0.046	0.049	0.047	0.760
	3.50	252.35	0.053	0.057	0.055	0.880
	4.00	288.41	0.059	0.059	0.059	0.944
Dial Gauge No. 4	0.5	36.05	0.005	0.007	0.006	0.096
	1.0	72.10	0.013	0.013	0.013	0.208
	1.5	108.15	0.017	0.019	0.018	0.288
	2.0	144.20	0.025	0.025	0.025	0.400
	2.5	180.25	0.030	0.032	0.031	0.406
	3.0	216.30	0.034	0.033	0.034	0.536
	3.5	252.35	0.041	0.040	0.040	0.648
	4.0	288.41	0.043	0.044	0.044	0.696

Table 11. Lateral Deflection Results for Plate 3, Test 1.

(inches)

Height of water (in)	qb^4 / Dh	Loading	Unloading	Average	w/h	
Dial Gauge No. 1	1.0	25.24	0.030	0.032	0.031	0.496
	2.0	50.49	0.051	0.051	0.051	0.816
	3.0	75.73	0.066	0.069	0.067	1.072
	4.0	100.98	0.079	0.080	0.079	1.264
	5.0	126.22	0.090	0.094	0.092	1.472
	6.0	151.46	0.099	0.101	0.100	1.600
	7.0	176.71	0.106	0.108	0.107	1.712
	8.0	201.95	0.112	-	0.112	1.792
Dial Gauges No. 2 and 3	1.0	25.24	0.018	0.022	0.020	0.320
	2.0	50.49	0.030	0.034	0.032	0.512
	3.0	75.73	0.040	0.042	0.041	0.656
	4.0	100.98	0.048	0.049	0.048	0.768
	5.0	126.22	0.056	0.058	0.057	0.912
	6.0	151.46	0.060	0.061	0.061	0.976
	7.0	176.71	0.065	0.066	0.066	1.056
	8.0	201.95	0.069	-	0.069	1.104
Dial Gauge No. 4	1.0	25.24	0.012	0.012	0.012	0.192
	2.0	50.49	0.019	0.021	0.020	0.320
	3.0	75.73	0.024	0.027	0.026	0.416
	4.0	100.98	0.029	0.031	0.030	0.480
	5.0	126.22	0.034	0.034	0.034	0.544
	6.0	151.46	0.038	0.038	0.038	0.608
	7.0	176.71	0.040	0.040	0.040	0.640
	8.0	201.95	0.042	-	0.042	0.673

Table 12. Lateral Deflection Results for Plate 3, Test 2.

(inches)

Height of water (in.)	qb^4 / Dh	Loading	Unloading	Average	w/h	
Dial Gauge No. 1	1.0	25.244	0.028	0.032	0.030	0.48
	2.0	50.49	0.047	0.050	0.049	0.78
	3.0	75.73	0.062	0.066	0.064	1.024
	4.0	100.98	0.075	0.079	0.077	1.232
	5.0	126.22	0.089	0.089	0.089	1.424
	6.0	151.46	0.095	0.097	0.096	1.536
	7.0	176.71	0.103	0.106	0.104	1.664
	8.0	201.95	0.109	-	0.109	1.744
Dial Gauge No. 2	1.0	25.24	0.018	0.022	0.020	0.032
	2.0	50.49	0.032	0.031	0.031	0.496
	3.0	75.73	0.038	0.042	0.040	0.640
	4.0	100.98	0.045	0.051	0.048	0.768
	5.0	126.22	0.054	0.060	0.057	0.912
	6.0	151.46	0.059	0.061	0.060	0.960
	7.0	176.71	0.065	0.065	0.065	1.040
	8.0	201.95	0.068	-	0.068	1.088
Dial Gauge No. 3	1.0	25.24	0.019	0.022	0.020	0.320
	2.0	50.49	0.028	0.031	0.030	0.480
	3.0	75.73	0.037	0.041	0.039	0.624
	4.0	100.98	0.045	0.048	0.047	0.752
	5.0	126.22	0.052	0.054	0.053	0.848
	6.0	151.46	0.056	0.060	0.058	0.928
	7.0	176.71	0.062	0.063	0.062	0.992
	8.0	201.95	0.065	-	0.065	1.040

Table 13. Lateral Deflection Results for Plate 3, Test 3.

(inches)

Height of water(in)	q_b^4 / Dh	Loading	Unloading	Average	w/h	
Dial Gauge No. 1	1.0	25.24	0.028	0.033	0.030	0.48
	2.0	50.49	0.045	0.050	0.048	0.768
	3.0	75.73	0.059	0.063	0.061	0.976
	4.0	100.98	0.075	0.077	0.076	1.216
	5.0	126.22	0.088	0.090	0.089	1.424
	6.0	151.46	0.093	0.098	0.095	1.520
	7.0	176.71	0.100	0.103	0.102	1.632
	8.0	201.95	0.109	-	0.109	1.744
Dial Gauges No. 2 & 3	1.0	25.24	0.018	0.022	0.020	0.320
	2.0	50.49	0.028	0.033	0.030	0.480
	3.0	75.73	0.039	0.040	0.039	0.624
	4.0	100.98	0.046	0.053	0.049	0.784
	5.0	126.22	0.054	0.059	0.056	0.896
	6.0	151.46	0.059	0.061	0.060	0.960
	7.0	176.71	0.063	0.065	0.064	1.024
	8.0	201.95	0.068	-	0.068	1.088
Dial Gauge No. 4	1.0	25.24	0.009	0.013	0.011	0.176
	2.0	50.49	0.018	0.020	0.019	0.304
	3.0	75.73	0.022	0.027	0.024	0.384
	4.0	100.98	0.027	0.032	0.030	0.480
	5.0	126.22	0.030	0.036	0.033	0.528
	6.0	151.464	0.034	0.037	0.036	0.576
	7.0	176.71	0.038	0.040	0.039	0.624
	8.0	201.96	0.041	-	0.041	0.656

Table 14. Lateral Deflection Results for Plate 4, Test 1.
(inches)

	p.s.i.	qb^4 / Dh	Loading	Unloading	Average	w/h
Dial Gauge No. 1	0.5	21.85	0.050	0.054	0.052	0.416
	1.0	43.69	0.086	0.091	0.088	0.704
	1.5	65.54	0.115	0.119	0.117	0.936
	2.0	87.38	0.147	0.153	0.150	1.200
	2.5	109.23	0.162	0.167	0.165	1.320
	3.0	131.08	0.182	0.187	0.184	1.472
	3.5	152.92	0.200	0.203	0.201	1.606
	4.0	174.77	0.208	0.214	0.211	1.688
	4.5	196.61	0.218	0.222	0.220	1.760
	5.0	218.46	0.228	0.233	0.231	1.848
	5.5	240.31	0.235	0.239	0.237	1.896
	6.0	262.15	0.243	-	0.243	1.944
Dial Gauges Nos. 2 and 3	0.5	21.85	0.027	0.029	0.028	0.232
	1.0	43.69	0.049	0.052	0.051	0.408
	1.5	65.54	0.069	0.071	0.070	0.056
	2.0	87.38	0.086	0.088	0.087	0.696
	2.5	109.23	0.099	0.102	0.100	0.800
	3.0	131.08	0.110	0.115	0.113	0.904
	3.5	152.92	0.121	0.125	0.123	0.984
	4.0	174.77	0.131	0.133	0.131	1.048
	4.5	196.61	0.132	0.139	0.136	1.008
	5.0	218.46	0.141	0.147	0.144	1.152
	5.5	240.31	0.147	0.151	0.149	1.192
	6.0	262.15	0.153	-	0.153	1.224
Dial Gauge No. 4	0.5	21.85	0.018	0.022	0.020	0.160
	1.0	43.69	0.037	0.039	0.038	0.304
	1.5	65.54	0.051	0.057	0.054	0.432
	2.0	87.38	0.064	0.068	0.066	0.528
	2.5	109.23	0.075	0.079	0.077	0.616
	3.0	131.08	0.089	0.089	0.089	0.712
	3.5	152.92	0.100	0.104	0.102	0.816
	4.0	174.77	0.108	0.110	0.109	0.872
	4.5	196.61	0.114	0.114	0.114	0.912
	5.0	218.46	0.122	0.122	0.122	0.976
	5.5	240.31	0.126	0.127	0.126	1.008
	6.0	262.15	0.131	-	0.131	1.048

Table 15. Lateral Deflection Results for Plate 4, Test 2.
(inches)

	p.s.i.	qb^4 / Dh	Loading	Unloading	Average	w/h
Dial Gauge No. 1	0.5	21.85	0.046	0.054	0.050	0.400
	1.0	43.69	0.086	0.083	0.085	0.681
	1.5	65.54	0.116	0.114	0.115	0.920
	2.0	87.38	0.145	0.149	0.147	1.180
	2.5	109.23	0.162	0.166	0.164	1.131
	3.0	131.08	0.180	0.185	0.182	1.460
	3.5	152.92	0.201	0.200	0.200	1.605
	4.0	174.77	0.216	0.210	0.208	1.660
	4.5	196.61	0.220	0.222	0.221	1.770
	5.0	218.46	0.230	0.231	0.230	1.830
	5.5	240.31	0.234	0.235	0.234	1.870
	6.0	262.15	0.243	-	0.243	1.940
Dial Gauges Nos. 2 and 3	0.5	21.85	0.026	0.029	0.027	0.216
	1.0	43.69	0.046	0.052	0.049	0.392
	1.5	65.54	0.068	0.071	0.069	0.551
	2.0	87.38	0.086	0.088	0.087	0.796
	2.5	109.23	0.098	0.098	0.098	0.784
	3.0	131.08	0.110	0.110	0.110	0.880
	3.5	152.92	0.119	0.123	0.121	0.969
	4.0	174.77	0.130	0.129	0.129	1.030
	4.5	196.61	0.130	0.138	0.134	1.070
	5.0	218.46	0.141	0.146	0.143	1.140
	5.5	240.31	0.148	0.149	0.148	1.180
	6.0	262.15	0.153	-	0.153	1.220
Dial Gauge No. 4	0.5	21.85	0.019	0.020	0.019	0.157
	1.0	43.69	0.037	0.038	0.037	0.296
	1.5	65.54	0.054	0.054	0.054	0.432
	2.0	87.38	0.065	0.067	0.066	0.528
	2.5	109.23	0.077	0.077	0.077	0.616
	3.0	131.08	0.092	0.089	0.090	0.671
	3.5	152.92	0.101	0.101	0.101	0.810
	4.0	174.77	0.109	0.107	0.108	0.865
	4.5	196.61	0.113	0.114	0.114	0.912
	5.0	218.46	0.122	0.122	0.122	0.977
	5.5	240.31	0.126	0.126	0.126	1.010
	6.0	262.15	0.131	-	0.131	1.040

Table 16. Lateral Deflection Results for Plate 4, Test 3.
(inches)

	p.s.i.	$\frac{4}{qb / Dh}$	Loading	Unloading	Average	w/h
Dial Gauge No. 1	0.5	21.85	0.049	0.055	0.052	0.416
	1.0	43.69	0.083	0.091	0.087	0.696
	1.5	65.54	0.113	0.123	0.116	0.944
	2.0	87.38	0.140	0.150	0.145	1.160
	2.5	109.23	0.160	0.166	0.163	1.310
	3.0	131.08	0.178	0.186	0.182	1.450
	3.5	152.92	0.195	0.205	0.200	1.600
	4.0	174.77	0.206	0.216	0.211	1.690
	4.5	196.61	0.215	0.225	0.220	1.760
	5.0	218.46	0.229	0.231	0.230	1.840
	5.5	240.31	0.232	0.242	0.237	1.890
	6.0	262.15	0.243	-	0.243	1.940
Dial Gauges No. 2 and 3	0.5	21.85	0.026	0.032	0.029	0.232
	1.0	43.69	0.049	0.053	0.051	0.408
	1.5	65.54	0.068	0.072	0.070	0.560
	2.0	87.38	0.085	0.089	0.087	0.696
	2.5	109.23	0.097	0.101	0.099	0.791
	3.0	131.08	0.112	0.114	0.113	0.903
	3.5	152.92	0.120	0.126	0.123	0.983
	4.0	174.77	0.125	0.137	0.131	1.040
	4.5	196.61	0.133	0.139	0.136	1.090
	5.0	218.46	0.140	0.148	0.144	1.150
	5.5	240.31	0.146	0.152	0.149	1.190
	6.0	262.15	0.153	-	0.153	1.220
Dial Gauge No. 4	0.5	21.85	0.017	0.023	0.020	0.160
	1.0	43.69	0.034	0.037	0.036	0.296
	1.5	65.54	0.050	0.056	0.053	0.424
	2.0	87.38	0.063	0.069	0.066	0.527
	2.5	109.23	0.075	0.077	0.076	0.615
	3.0	131.08	0.086	0.092	0.089	0.712
	3.5	152.92	0.099	0.104	0.101	0.808
	4.0	174.77	0.110	0.108	0.109	0.863
	4.5	196.61	0.111	0.117	0.114	0.911
	5.0	218.46	0.120	0.124	0.122	0.975
	5.5	240.31	0.127	0.128	0.126	1.010
	6.0	262.15	0.131	-	0.131	1.040

Table 17. Lateral Deflection Results for Plate 3, Yield Test.

(inches)

Dial Gauge No. 1

p.s.i.	$\frac{4}{qb} / Dh$	Deflection	w/h
1.0	699	0.217	3.48
1.5	1047	0.235	3.76
2.0	1400	0.248	3.97
2.5	1750	0.275	4.40
3.0	2100	0.285	4.57
3.5	2450	0.292	4.67
4.0	2800	0.312	5.00
4.5	3150	0.330	5.28
5.0	3500	0.346	5.54
5.5	3850	0.365	5.84
6.0	4200	0.380	6.09
7.0	4900	0.395	6.32
7.5	5200	0.415	6.65
8.0	5600	0.440	7.05
9.0	6300	0.470	7.52
10.0	7000	0.500	8.00

Table 18. Lateral Deflection Results for Plate 4, Yield Test.

(inches)

Dial Gauge No. 1

p.s.i.	qb / Dh	Deflection	w/h
10	436.92	0.275	2.20
15	655.38	0.345	2.76
20	873.84	0.412	3.29
25	1092.3	0.47	3.76
30	1280.76	0.535	4.28
35	1499.22	0.585	4.68
40	1747.68	0.645	5.16
45	1966.14	0.690	5.52
50	2183.60	0.775	6.20
55	2402.06	0.815	6.52
60	2621.52	0.865	6.92
65	2839.98	0.912	7.29
70	3058.44	0.945	7.56
75	3276.90	1.025	8.20
80	3495.36	1.056	8.43
85	3713.82	1.085	8.68
90	3932.28	1.125	9.00
95	4150.74	1.195	9.55

EXPERIMENTAL DATA

FROM DIGITAL STRAIN INDICATOR

Plate 1 Test 2 27 psi. Loading	Plate 1 Test 2 2.25 p.s.i. Unloading	Plate 1 Test 2 1.75 p.s.i. Unloading	Plate 1 Test 2 1.5 p.s.i. Unloading	Plate 1 Test 2 1.25 p.s.i. Unloading	Plate 1 Test 2 1 p.s.i. Unloading	Plate 1 Test 2 0.75 p.s.i. Unloading	Plate 1 Test 2 0.5 p.s.i. Unloading	Plate 1 Test 2 0.375 p.s.i. Unloading	Plate 1 Test 3 Zero Loading	Plate 1 Test 3 0.375 p.s.i. Loading	Plate 1 Test 3 0.5 p.s.i. Loading
01	01	01	01	01	01	01	01	01	01	01	01
02	02	02	02	02	02	02	02	02	02	02	02
03	03	03	03	03	03	03	03	03	03	03	03
04	04	04	04	04	04	04	04	04	04	04	04
05	05	05	05	05	05	05	05	05	05	05	05
06	06	06	06	06	06	06	06	06	06	06	06
07	07	07	07	07	07	07	07	07	07	07	07
08	08	08	08	08	08	08	08	08	08	08	08
09	09	09	09	09	09	09	09	09	09	09	09
10	10	10	10	10	10	10	10	10	10	10	10
11	11	11	11	11	11	11	11	11	11	11	11
12	12	12	12	12	12	12	12	12	12	12	12
13	13	13	13	13	13	13	13	13	13	13	13
14	14	14	14	14	14	14	14	14	14	14	14
15	15	15	15	15	15	15	15	15	15	15	15
16	16	16	16	16	16	16	16	16	16	16	16
17	17	17	17	17	17	17	17	17	17	17	17
18	18	18	18	18	18	18	18	18	18	18	18
19	19	19	19	19	19	19	19	19	19	19	19
20	20	20	20	20	20	20	20	20	20	20	20
21	21	21	21	21	21	21	21	21	21	21	21
22	22	22	22	22	22	22	22	22	22	22	22
23	23	23	23	23	23	23	23	23	23	23	23
24	24	24	24	24	24	24	24	24	24	24	24
25	25	25	25	25	25	25	25	25	25	25	25
26	26	26	26	26	26	26	26	26	26	26	26
27	27	27	27	27	27	27	27	27	27	27	27
28	28	28	28	28	28	28	28	28	28	28	28
29	29	29	29	29	29	29	29	29	29	29	29
30	30	30	30	30	30	30	30	30	30	30	30
31	31	31	31	31	31	31	31	31	31	31	31
32	32	32	32	32	32	32	32	32	32	32	32
33	33	33	33	33	33	33	33	33	33	33	33
34	34	34	34	34	34	34	34	34	34	34	34
35	35	35	35	35	35	35	35	35	35	35	35
36	36	36	36	36	36	36	36	36	36	36	36
37	37	37	37	37	37	37	37	37	37	37	37
38	38	38	38	38	38	38	38	38	38	38	38
39	39	39	39	39	39	39	39	39	39	39	39
40	40	40	40	40	40	40	40	40	40	40	40
41	41	41	41	41	41	41	41	41	41	41	41
42	42	42	42	42	42	42	42	42	42	42	42
43	43	43	43	43	43	43	43	43	43	43	43
44	44	44	44	44	44	44	44	44	44	44	44
45	45	45	45	45	45	45	45	45	45	45	45
46	46	46	46	46	46	46	46	46	46	46	46
47	47	47	47	47	47	47	47	47	47	47	47
48	48	48	48	48	48	48	48	48	48	48	48
49	49	49	49	49	49	49	49	49	49	49	49
50	50	50	50	50	50	50	50	50	50	50	50
51	51	51	51	51	51	51	51	51	51	51	51
52	52	52	52	52	52	52	52	52	52	52	52
53	53	53	53	53	53	53	53	53	53	53	53
54	54	54	54	54	54	54	54	54	54	54	54
55	55	55	55	55	55	55	55	55	55	55	55

Plate IV Test 2 Loading 3.5 p.s.i.	Plate IV Test 2 Loading 4 p.s.i.	Plate IV Test 2 Loading 5 p.s.i.	Plate IV Test 2 Loading 5 p.s.i.	Plate IV Test 2 Unloading 4 p.s.i.	Plate IV Test 2 Unloading 4 p.s.i.	Plate IV Test 2 Unloading 3.5 p.s.i.
001	001	001	001	001	001	001
002	002	002	002	002	002	002
003	003	003	003	003	003	003
004	004	004	004	004	004	004
005	005	005	005	005	005	005
006	006	006	006	006	006	006
007	007	007	007	007	007	007
008	008	008	008	008	008	008
009	009	009	009	009	009	009
010	010	010	010	010	010	010
011	011	011	011	011	011	011
012	012	012	012	012	012	012
013	013	013	013	013	013	013
014	014	014	014	014	014	014
015	015	015	015	015	015	015
016	016	016	016	016	016	016
017	017	017	017	017	017	017
018	018	018	018	018	018	018
019	019	019	019	019	019	019
020	020	020	020	020	020	020
021	021	021	021	021	021	021
022	022	022	022	022	022	022
023	023	023	023	023	023	023
024	024	024	024	024	024	024
025	025	025	025	025	025	025
026	026	026	026	026	026	026
027	027	027	027	027	027	027
028	028	028	028	028	028	028
029	029	029	029	029	029	029
030	030	030	030	030	030	030
031	031	031	031	031	031	031
032	032	032	032	032	032	032
033	033	033	033	033	033	033
034	034	034	034	034	034	034
035	035	035	035	035	035	035
036	036	036	036	036	036	036
037	037	037	037	037	037	037
038	038	038	038	038	038	038
039	039	039	039	039	039	039
040	040	040	040	040	040	040
041	041	041	041	041	041	041
042	042	042	042	042	042	042
043	043	043	043	043	043	043
044	044	044	044	044	044	044
045	045	045	045	045	045	045
046	046	046	046	046	046	046
047	047	047	047	047	047	047
048	048	048	048	048	048	048
049	049	049	049	049	049	049
050	050	050	050	050	050	050

Plate 3 Yield 22 p.s.i.	Plate 3 Yield 24 p.s.i.	Plate 3 Yield 26 p.s.i.	Plate 3 Yield 28 p.s.i.	Plate 3 Yield 30 p.s.i.	Plate 4 Yield 10 p.s.i.	Plate 4 Yield 15 p.s.i.	Plate 4 Yield 20 p.s.i.	Plate 4 Yield 25 p.s.i.	Plate 4 Yield 30 p.s.i.	Plated Yield 35 p.s.i.
0012345678901011121314151617181920212223242526272829303132333435363738394041424344454647484950	0012345678901011121314151617181920212223242526272829303132333435363738394041424344454647484950	0012345678901011121314151617181920212223242526272829303132333435363738394041424344454647484950	0012345678901011121314151617181920212223242526272829303132333435363738394041424344454647484950	0012345678901011121314151617181920212223242526272829303132333435363738394041424344454647484950	0012345678901011121314151617181920212223242526272829303132333435363738394041424344454647484950	0012345678901011121314151617181920212223242526272829303132333435363738394041424344454647484950	0012345678901011121314151617181920212223242526272829303132333435363738394041424344454647484950	0012345678901011121314151617181920212223242526272829303132333435363738394041424344454647484950	0012345678901011121314151617181920212223242526272829303132333435363738394041424344454647484950	0012345678901011121314151617181920212223242526272829303132333435363738394041424344454647484950

REFERENCES

- (1) S. P. Timoshenko and S. Woinowski-Krieger, Theory of Plates and Shells, 2nd Edition, (McGraw Hill, 1959).
- (2) S. Way, Uniformly Loaded Rectangular Plates With Large Deflections, Proceedings of the Fifth International Congress for Applied Mechanics, Cambridge, Mass., 1938.
- (3) S. Levy, Square Plates With Clamped Edges Under Normal Pressure Producing Large Deflections, NACA TR 740, 1942.
- (4) L. S. D. Morley, Skew Plates and Structures, Pergamon Press, 1963, p.119.
- (5) J. B. Kennedy, On the Bending of Clamped Skewed Plates Under Uniform Pressure, Journal of the Royal Aeronautical Society, May 1965.
- (6) J. B. Kennedy and S. Ng, Analysis of Skewed Plate Structures With Fixed Edges, Transactions of the Engineering Institute of Canada, October, 1965.
- (7) S. F. Ng, Analysis of Clamped Skewed Plates Subjected to Lateral Uniform Loading, thesis, submitted to the University of Windsor in partial fulfilment for the degree of Master of Applied Science in Civil Engineering, 1964.
- (8) Van Dyke, Perturbation Methods in Fluid Mechanics, Academic Press, 1964.
- (9) E. H. Mansfield, The Bending and Stretching of Plates, Pergamon Press, 1964.

- (10) C. V. Brigatti, Applicazione del metodo di H. Marcus al calcolo della piastra parallelogrammica, Ricerche di Ingegneria, Vol. XVI, No. 2, Mar-Apr. 1938, p.42.
- (11) A. Anzelius, Uber die dlastische Deformation Parallelogrammformiger Platten, Der Bauingenieur, Vol. 20, No. 35-36, Sept. 1939, p. 478.
- (12) V. P. Jensen, Analysis of Skew Slabs, Bulletin No. 332, University of Illinois Eng. Experimental Station, Urbana, Ill., Sept. 1941.
- (13) F. H. Dorman, The Thin Clamped Parallelogram Plate Under Uniform Normal Pressure, Dept. of Supply, Australia, Aeronautical Research Laboratories, Report SM 214, 1953.
- (14) I. Mirsky, The Deflection of a Thin Flat Clamped Parallelogram Plate Subjected to Uniform Normal Loading, Dept. of Supply, Australia, Aeronautical Research Laboratories, Report SM 175, 1951.
- (15) P. D. Jones, Small Deflection Theory of Flat Plates Using Complex Variables, Dept. of Supply, Australia, Aeronautical Research Laboratories, Report SM 260, 1958.
- (16) J. B. Kennedy and M. W. Huggins, Series Solution of Skewed Stiffened Plates, Proceedings of the American Society of Civil Engineers, Feb. 1964.
- (17) J. B. Kennedy and I. C. Martens, Stresses Near Corners of Skewed Stiffened Plates, The Structural Engineer, Nov. 1965.

- (18) W. Z. Chien, Large Deflection of A Circular Plate Under Uniform Pressure, Chinese Journal of Physics, Vol. 7, 1947, pp. 102-113.
- (19) C. T. Wang, Nonlinear Large-Deformation Boundary-Value Problems of Rectangular Plates, NACA TN 1425, 1948.
- (20) N.A. Weil and N. M. Newmark, Large Deflections of Elliptical Plates, Journal of Applied Mechanics, Trans. A.S.M.E., March 1956.
- (21) S. N. Sinha, Large Deflections of Plates on Elastic Foundations, Proceedings of the ASCE, Vol. 89, No. EM1, February 1963.
- (22) S. F. Ng and J. B. Kennedy, Linear and Nonlinear Analyses of Rectangular Plates on Elastic Foundations, presented to the 80th Annual General and Professional Meeting of the EIC, June, 1966.
- (23) A. M. Freudenthal, The Inelastic Behaviour of Engineering Materials and Structures, John Wiley and Sons, 1950, pp.249-263.
- (24) Aluminum Company of America Handbook, Pittsburgh, Pennsylvania, 1960 Edition.
- (25) T. Kato, On the Convergence of the Perturbation Method, Progress in Theoretical Physics, Vol. 4, 1949, and Vol. 5, 1950.
- (26) M. Van Dyke, Perturbation Methods in Fluid Mechanics, Academic Press, 1964, pp. 30-32.

NOMENCLATURE

D	= flexural rigidity of plate
E	= modulus of elasticity of plate material
G	= shear modulus
Q	= dimensionless uniformly distributed load
R	= aspect ratio, b/a
U, V, W	= dimensionless displacement components parallel to $x, y,$ and z directions respectively.
W_o	= dimensionless lateral displacement at center of plate
$C_i, D_j, E_k,$	= unknown constants
F_l, G_m, H_n	
$2a, 2b$	= sides of plates along α and β axes respectively
$c, s.$	= $\cos \theta$ and $\sin \theta$
h	= thickness of plate
n	= outwardly drawn normal
q	= intensity of uniformly distributed load
u, v, w	= displacement of point on the middle plane of plate parallel to $x, y,$ and z axes respectively
x, y, z	= rectangular cartesian coordinates
θ	= skew angle
α, β	= oblique coordinates
γ_i	= undetermined constants
ζ, η	= dimensionless oblique coordinates
ν	= Poisson's ratio
$\sigma_x'', \sigma_y'', \tau_{xy}''$	= extreme fibre bending and shearing stresses

$\sigma_x', \sigma_y', \tau_{xy}'$ = membrane stresses in the middle surface of plate

S_x'', S_y'', S_{xy}'' = nondimensional bending stresses

S_x', S_y', S_{xy}' = nondimensional membrane stresses

∇^2 = Laplacian operator

VITA AUCTORIS

- 1937 Simon Shung Fun Ng was born in Canton, China, on March 6, 1937.
- 1945 In September, 1945, he entered Pui Ying School, Canton, China, where he obtained his elementary Education.
- 1950 In September, 1950, he enrolled at Wah Yan College, Hong Kong, where he obtained his secondary education.
- 1957 In September, 1957, he enrolled in first year Science at McGill University, Montreal, Canada.
- 1958 In September, 1958, he entered the University of British Columbia, Vancouver, Canada to study Civil Engineering.
- 1962 In May, 1962, he was graduated from the University of British Columbia with a Bachelor of Applied Science Degree. In June, he was employed as junior engineer in the hydro-electric design division of the International Power and Engineering Consultants, Ltd., Vancouver, British Columbia.
- 1963 In September, 1963, he enrolled at the University of Windsor for graduate studies.
- 1964 In October, 1964, he graduated from the University of Windsor with a Master's Degree in Applied Science. In the same year, he enrolled as a Ph. D. student in the Department of Civil Engineering.
- 1967 In January, 1967, He was employed as an engineer in the IBM datacentre, Toronto, Ontario.